NIGERIAN MINING JOURNAL

ISSN 1117 - 4307

Volume 20 Number 1 November 2022

A Publication of

NIGERIAN SOCIETY OF MINING ENGINEERS

NIGERIAN MINING JOURNAL

Volume 20 Number 1 November 2022

Table of Contents

NIGERIAN
MINING JOURNAL
ISSN 1117-4307

Volume 20 | Number 1 | November 2022

A PUBLICATION OF THE NIGERIAN SOCIETY OF MINING ENGINEERS

Publisher
Nigerian Society of Mining Engineers (NSME)
NSME Secretariat, Bukuru,
P.M.B. 2036,Jos, Plateau State, Nigeria

Editorial Address
Department of Mineral and Petroleum Resources
College of Engineering,
Kaduna Polytechnic, Kaduna.
Tel: 08030495371, 08023636689
Email: nigerianminingjournal@gmail.com
Website: www.nsme.org.ng

NIGERIAN
MINING JOURNAL

ISSN 11174307

A Publication of
Nigerian Society of Mining Engineers

INFORMATION FOR AUTHORS

Scope: NIGERIAN MINING JOURNAL is the technical publication of Nigerian Society of Mining Engineers. The Journal publishes peer-reviewed papers covering various fields of mining, mineral processing and extractive metallurgy. The papers provide in-depth information on research findings from various aspects of actual exploitation of minerals and related engineering practice. Researches based on local technology are particularly welcome.

Manuscripts: Manuscripts submitted for publication must represent original contributions and should not have been proposed for publication elsewhere. The papers should be based on original research, innovations and field experience in mineral exploration, mining, mineral processing, extractive metallurgy and equipment maintenance, relevant to the minerals industry. The manuscript must be prepared preferably in Microsoft Word environment, and should be submitted by email to *nigerianminingjournal@gmail.com*

Abstract: The manuscript must include an abstract summarizing the main aspects of the paper in not more than 200 words. The main results/findings must be stated clearly.

Keywords: A minimum of 5 and maximum of 7 keywords should be included.

Text: Papers should be typewritten with double-line spacing and margins of 25 mm on all sides. Each page should be numbered. The first page should include a concise title of the paper and the author(s) full name(s), affiliation(s) and address(es). In order to maintain consistency, titles such as Mr, Mall, Mrs, Miss, Engr, Dr, Prof, etc., should be avoided, as they frequently change. The author(s) should secure the right of reproduction of any material that has already been published elsewhere.

Units: The S.I. unit is mandatory. However, in isolated accepted cases, authors should insert conversion factors or nomographs for units other than S.I.

Mathematical symbols and formulae: All characters available on a normal typewriter must be typewritten in the text as well as in the equations. Subscripts and superscripts should all be clear. Equations referred to in the text should be placed between parentheses at the right hand margin.

Figures: All illustrations should be drawn using black ink, or suitable computer software, on good quality paper. The originals or good quality photographic prints (maximum 210 x 297mm) should be submitted together with the manuscript. Each figure should carry a brief title *under* it. Figures must be referred to in the text with the number clearly written on the back of the photograph or drawing. Lettering of figures should be large enough to ensure clarity of reproduction after reduction.

Tables: Each table should be typed on a separate sheet as the authors expect it to appear in print. Tables should carry a brief title on top, and should be numbered and referred to in the text.

References: References should be in APA system and must be listed at the end of the article, in alphabetical order of the first author's surname. Citation of papers in the reference list should be as follows:

***Books**:*

Hartman, H.L. & Mutmansky, J.M. (2002). *Introductory Mining Engineering* (2nd Ed.). New Jersey: John Wiley & Sons.

***Journals**:*

Zimbovsky, I.G., Ivanova, T.A., & Chanturia, V.A. (2015). Complexing collecting agent for selective flotation of chalcopyrite. *Journal of Mining Science*. 51(3), 562-567.

Unpublished work:

Arubisan, A.P. (2013). *Amelioration of grain size and its effect on iron ore concentrate in Itakpe, West Central Nigeria*. Unpublished M.Tech. Thesis, Federal University of Technology, Minna.

***Proceedings**:*

Oyeladun, O.A.W, Abubakar, S. & Adewuyi, E.A.A. (2012). Application of Igoli mercury-free gold extraction for recovery of Wamba gold. *Proceedings of Nigerian Society of Mining Engineers,* Ilorin, 2012, 67-70.

Assignment of Copyright Ownership: Submission of a manuscript for possible publication in the Nigerian Mining Journal carries with it the understanding that the manuscript has not been published nor is being simultaneously considered for publication elsewhere. On submission of a manuscript, the author(s) agree that the copyright to their articles is assigned to the Nigerian Society of Mining Engineers (NSME) if and when the articles are accepted for publication.

Sikiru and Idris (2022) Nigerian Mining Journal, (20) 1 - 8

Analysis of Drilling and Blasting Techniques for Cost Optimization: Case Study of Ashaka Cement Plc, Gombe State, Nigeria

Sikiru, M. H[1a] and Idris, M.A[2]
[1]*Lafarge Africa PLC, AshakaCEM, Gombe State, Nigeria.*
[2]*Department of Mining Engineering, Federal University of Technology, P.M.B 704, Akure, Ondo State, Nigeria.*
[a] *Corresponding Author: sikiru.haruna@lafargeholcim.com*[1]

Abstract
Drilling and blasting are major mining and quarrying operations, accounting for more than 50% of the overall capital cost of the mining/quarrying operations. Therefore, optimizing the cost of the drilling and blasting operations will reduce the capital cost and increase the net profit. In this study, the current cost trends associated with the drilling and blasting operations of Ashaka Cement Plc, a limestone quarry in Gombe, were analyzed, and suitable, cost-effective drill and blast geometric parameters for the mine were developed. The study was conducted on three operational pits of the mine, namely South-West, North-West and North-North pits. The current and three proposed sets of blast geometric parameters for each active Pit for ore zones were assessed with the Kuz-Ram fragmentation model. The blast performance was measured in terms of the Powder Factor, the mean fragment size and the volume of blasted material per blast hole in three operational pits of the mine. Proposal 2 showed optimum properties for the three quarries. At the southwest pit, the proposed blast geometric parameter shows a 54% reduction in drilling and blasting cost per volume, while the powder factor reduces from 0.22 kg/m^3 to 0.09 kg/m^3 with a corresponding fragmentation size increment from 51.5% to 73.1%. At the northwest pit, the proposed blast geometric parameter shows a drilling and blasting cost reduction of 54%. At the same time, the powder factor reduces from 0.21 kg/m^3 to 0.1 kg/m^3, with a corresponding increase in fragmentation size from 48.5% to 72.1%. At the north-north pit, cost reduction of 56% and powder factor reduces from 0.24 kg/m^3 to 0.12 kg/m^3, with a corresponding increase in fragmentation size from 45% to 71.9%. Therefore, the study concluded that by applying this proposed model to drilling and blasting operations, the cost of the operation could be optimized with improved fragmentation.
Keywords: Drilling, Blasting, Cost optimization, Powder factor, Fragmentation size, Kuz-Ram model

1 Introduction

Mining operation involves four main processes; drilling, blasting, loading and hauling. These processes require careful planning to achieve maximum effectiveness in operating costs and environmental sustainability. On a global scale, mining companies seek cost-effective operation techniques to maximize profitability by reducing overall operation costs (ICMM, 2012). Most of the operational costs are incurred during the drilling and blasting operations, but with appropriate design, the cost-effectiveness of the overall operation is maximized (Anon., 2014; Palangio and Palangio, 2005; Bozic, 1998). Good blasting design results in more efficient loading and drilling operations (Brahma *et al.,* 2007). Observations have shown that more attention is being placed on the blast operation, not the drilling operation. However, it is paramount to note that any efficient blasting operation must be preceded by an accurately optimized design (Vasileios, 2008; Siddiqui *et al*., 2009; Engin, 2010). Appropriate blast design parameters could reduce the drill and blast costs of a mine (Leng *et al.,* 2018; Anon., 2014).

The blast pattern is among the significant factors to be considered during the blasting design. The blast pattern can be square, rectangular or staggered. The efficiency of the blasting design is measured by the level of rock fragmentation, which depends on the end use

of the fragmented rock.
Rock fragmentation depends on two factors - controllable and uncontrollable factors. The blast design must consider these factors to achieve the desired fragmentation.

The controllable factors are blast geometric parameters and pattern, which are bench height, hole diameter, spacing, burden, hole length, bottom charge, specific charge, explosives costs, density and type of explosive, while the uncontrollable factors are the geological nature of the formation which comprise the rock strength, discontinuity spacing and orientation, rock density (Siddiqui *et al*., 2009). The hole diameter controls the choice of burden, spacing and stemming length. There is a direct relationship between the blast hole, the fragment size and the blasting cost in open pit mining (Leng *et al.,* 2020).

There are many proposed methods for evaluating or predicting rock fragmentation, such as visual analysis, image processing techniques and empirical methods. In the empirical method, the size distribution of the fragmented rock is predicted using various proposed models. The most commonly used models include Rosin-Rammler, Kuz-Ram, and Swebrec functions.

The Kuz-Ram model (Kuznetsov and Rosin-Rammler) proposed by Cunningham (1983) has been used extensively in the mining industries for the empirical prediction of rock fragmentation size distribution (Cunningham, 1983, 1987). This theory, first proposed by Kuznetsov (1973), describes the blasted rock fragmentation. Using this approach, the rock factor that describes the nature and geology of the rock is calculated. The uniformity index is also obtained and characterizes the explosive loading and blast pattern type and dimensions. This allows the characteristic size and distribution to be calculated according to the Rosin-Rammler procedure. Too many input parameters that are not precise may result in an unsatisfactory rock factor, adversely affecting fragmentation prediction. Cunningham (1983, 1987) helped improve the efficiency of that approach.

Technological advancement has changed the level of effectiveness and requirements of the drill and blast operations. The innovations include new explosives, electronic delay detonators, initiation of shock tubes, air-deck system, blast performance monitoring, cost-effective explosive formulations, etc. Even with the current levels of innovation with optimum blasting patterns and scientifically selected explosives, to attain maximum effectiveness, a lot of research is needed in the area of management and control.
To analyze the drilling and blasting technique for cost saving, information on the drill and blast geometric parameters was gathered from three locations within a quarry in Ashaka, Gombe State, Nigeria. The results were analyzed and compared to serve as a basis for suggesting the cost-effective geometric parameters.

2 Materials and Methods

2.1 Study Area

This study was carried out at Ashaka Cement Limestone Quarry, Jalingo, Gombe State (Figure 1) in the Northern Region of Nigeria with the coordinates 10° 56' 10″N and 11^{0}27' 20″ E. This quarry was selected for research because, presently, it is the only active quarry in the Northern region of Nigeria.

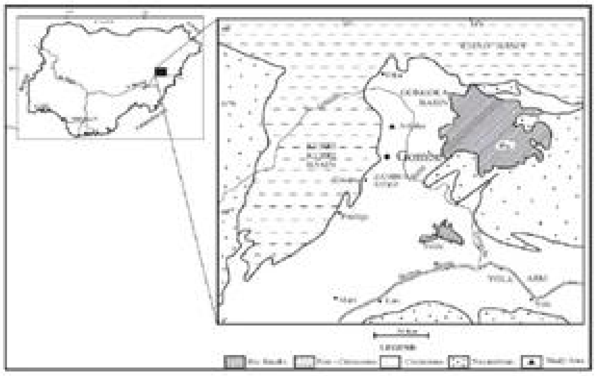

Figure 1: Map of Nigeria Showing the Geological Map of the Study Area (Ashaka, Gombe State, North-Eastern Nigeria) (Usman *et al.,* 2016).

2.2 Data Collection

In this research, data were obtained through analysis of the geometric parameters.

2.2.1 Data

The data obtained from Ashaka Cement Limestone Quarry were categorized into two sets – drill and explosives parameters and shown in Tables 1 and 2, respectively. The geological nature of the rock formation and the nature of the rock mass were observed to determine the rock factor. The rock factor was determined based on the guideline proposed by Hustrulid (1999). The nature of rock mass observed at the quarry is medium soft, and the corresponding rock factor is 7 (Hustrulid, 1999).

Table 1: Drill Parameters from the Quarry

S/N	Parameter
1	Burden (*B*), m
2	Spacing (*S*), m
3	Hole Diameter (*d*), mm
4	Bench Height (*H*), m
5	Sub-drill (*U*), m
6	Stemming (*T*), m
7	Drilling Cost per meter (Dcpm), ₦/m
8	Charge Length (*L*), m

Table 2: Explosive Data used for this study

S/N	Parameter
1	Explosive Type
2	Explosive density (kg/m^3)
3	Relative Explosives Energy, REE
4	Explosive Cost (₦/t)
5	Loading Density, Mc (kg/m)
6	Actual Powder Factor (*K*), kg/m^3
7	Explosive cost per meter (₦/t)

2.3 Methods and Tools of Analysis

The Kuz-Ram fragmentation Model was adopted to analyze the drilling and blasting performance quantitatively. This aided in generating appropriate sets of geometric parameters for drilling and blasting in the quarry and how the different parameters affect the blast performance. The total cost per cubic meter blasted, and the fragmentation size determines the level of effectiveness of a drill-blast operation. The Kuz-Ram was used to estimate the mean fragment size and predict the mass fraction retained on the screen. The terminologies and formulas used for the analysis are presented in Table 3.

3 Results and Discussion

The study is limited to the drilling and blasting operations in the factory's ore section; the parameters used are stated in Table 4. The current research parameters quantitatively developed by the Kuz-Ram fragmentation model aimed at optimizing the cost of the overall blasting operation were analyzed. The three equations of the Kuz-Ram Model, Kuznetsov and uniformity equation were used for the analysis. The approach eliminates unnecessary costs while improving productivity and maintaining the desired rock fragmentation.

3.1 Current Drill and Blast Geometric Parameter

The current geometric parameters for the drilling and blasting at the three operational pits at the quarry are summarized in Table 4.

3.2 Drill and Blast Cost Evaluation

The performance of drilling and blasting operations in the quarry was compared with the Kuz-Ram fragmentation model. Three proposed sets were developed using the Kuz-Ram fragmentation model named proposals 1, 2 and 3. A comparative analysis of the parameters for the current operation and the proposed Kuz-Ram fragmentation models was performed and presented in Tables 5, 6, 7 and 8.

3.3 South-West Pit Drill and Blast Cost Evaluation and Performance

Proposal 2 is the optimum alternative for ore zones in the southwest from the numerical analysis in Tables 5 and 6 and Figures 2 and 3. It shows the highest reduction in Powder Factor from 0.22 to 0.09 kg/m^3, and the highest mean fragment size increases slightly from 21 cm to 40 cm. It also shows the lowest total cost per volume of 349.9 N/m^3 compared to the other proposals. Table 6 shows the comparison between the data obtained for the percent passing of fragments from blasting using current data, proposal 1, proposal 2, and proposal 3, respectively. The predicted fragmentation size in the range (0.2 m to 1.5 m) increases from 51.5% to 73.1%, and the percent undersize decreases from 48.5% to 24.7%, as shown in Table 6. The total cost per volume (BCM) of drilling and blasting reduces efficiently by 54%. The Volume fragmented per blast hole would considerably increase to twice the current trend, an added advantage for the quarry.

Table 4: Current Geometric Parameter for Drilling and Blasting at the Quarry

Parameter	South-West Pit	North-West Pit	North-North Pit
Burden (m)	3.7	3.7	3.5
Spacing (M)	4.5	4.5	4.5
Hole Diameter (Mm)	120	120	120
Bench Height (M)	8	5	6
Sub-Drill (M)	0.6	0.5	1
Stemming (M)	1.8	1.4	1.8
Explosive Type	Blend	Blend	Blend
Explosive Final Density (Kg/M^3)	0.0012	0.0012	0.0012
Relative Explosives Energy	95.38	95.38	95.38
Drilling Cost (₦/M)	3500	3500	3500
Explosive Cost (₦/Kg)	1033.5	1033.5	1033.5
Loading Density (Kg/M)	10	10	10
Charge Length (M)	6.8	4.1	5.2

3.4 North-West Pit Drill and Blast Cost Evaluation

Proposal 2 is the optimum alternative for ore zones in North-West from the numerical analysis in Tables 7 and 8 and Figures 4 and 5. It shows the highest reduction in Powder Factor is from 0.21 to 0.1 kg/m^3, and the highest mean fragment size increases slightly from 21cm to 40 cm. It also shows the lowest total cost per volume of 344.6 N/m^3 compared to the other proposals. Table 8 shows the comparative analysis of the percent passing of fragments from blasting operations using current data, proposal 1, proposal 2, and proposal 3, respectively. The predicted fragmentation size in the range (0.2 m to 1.5 m) increases from 48.3% to 72.1%, and the percent undersize decreases from 51.7% to 27.0%, as shown in Table 8. This would result in a 54% reduction in drilling and blasting costs per volume (BCM). The volume fragmented per blast hole would increase by 116% compared to the current trend, an added advantage for the quarry.

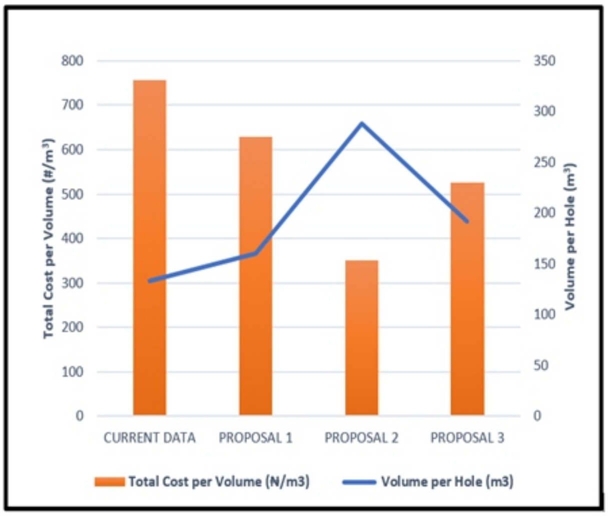

Figure 2: South-West Pit Drill and Blast Cost and Volume Evaluation

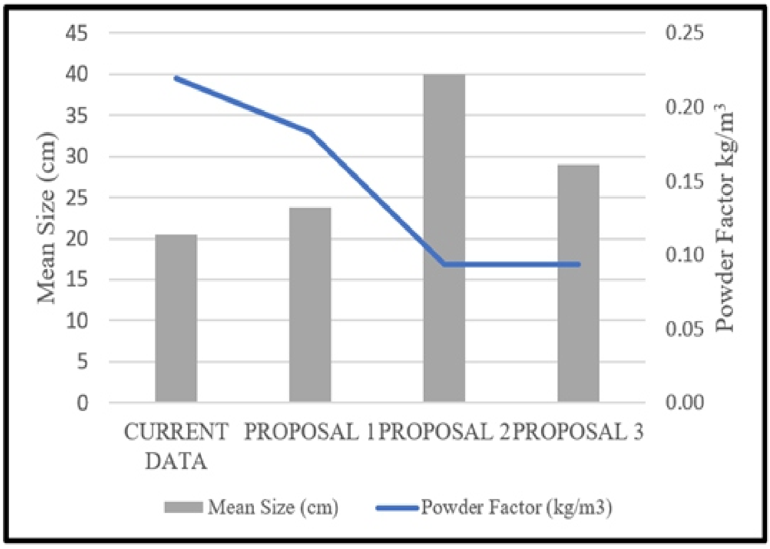

Figure 3: Change in Mean Size and powder Factor as Parameters in S-W pit are altered.

Table 5: Evaluation of Drilling and Blasting for South-West Pit

Parameter	**Value**			
	Current data	Proposal 1	Proposal 2	Proposal 3
Burden (m)	3.7	5	6	4
Spacing (m)	4.5	4	6	6
Hole Diameter (mm)	120	120	120	120
Bench Height (m)	8	8	8	8
Sub-drill (m)	0.6	0.6	0.6	0.6
Stemming (m)	1.8	1.8	1.8	1.8
Explosive Type	Blend	Blend	Blend	Blend
Explosive Final Density (kg/m^3)	0.0012	0.0012	0.0012	0.0012
Relative Explosives Energy	95.38	95.38	95.38	95.38
Drilling Cost (₦/m)	3500	3500	3500	3500
Explosive Cost (₦/kg)	1033.5	1033.5	1033.5	1033.5
Loading Density (kg/m)	10	10	10	10
Charge Length (m)	6.8	6.8	6.8	6.8
Mass per Hole (kg)	68	68	68	68
Mass above Grade (kg)	62	62	62	62
Powder Factor (kg/m^3)	0.22	0.18	0.09	0.09
Uniformity index	1.7	1.4	1.3	1.7
Mean size (cm)	21	24	40	29
Volume per Hole (m^3)	133.2	160	288	192
Explosives Cost per Hole (₦)	70278	70278	70278	70278
Initiation Cost per Hole (₦)	400	400	400	400
Drilling Cost per Hole (₦)	30100	30100	30100	30100
Total Cost per Hole (₦)	100778	100778	100778	100778
Explosives Cost per Volume (₦/m^3)	527.6	439.2	244.0	366.0
Initiation Cost per Volume (₦/m^3)	3.0	2.5	1.4	2.1
Drilling Cost per Volume (₦/m^3)	226.0	188.1	104.5	156.8
Total Cost per Volume (₦/m^3)	756.6	629.9	349.9	524.9

Table 6: Predicted Fragmentation by Size distribution for South-West.

Fragmentation sizing	Current data	Proposal 1	Proposal 2	Proposal 3
Oversize	0.0 %	0.0%	2.2%	0.0%
In range	51.5 %	58.1%	73.1%	69.6%
Undersize	48.5%	41.9%	24.7%	30.4%

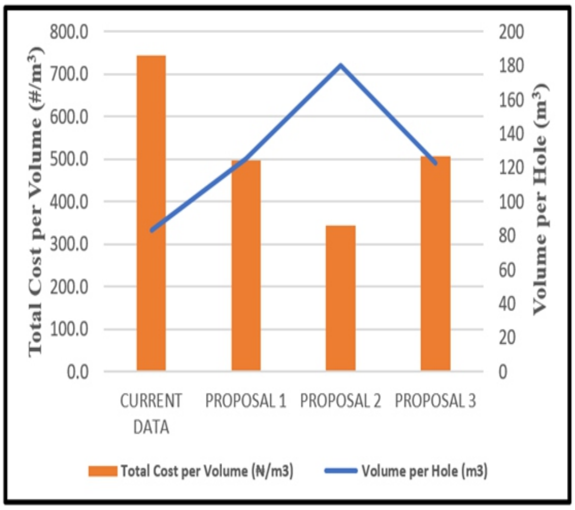

Figure 4: North-West Pit Drill and Blast Cost and Volume Evaluation

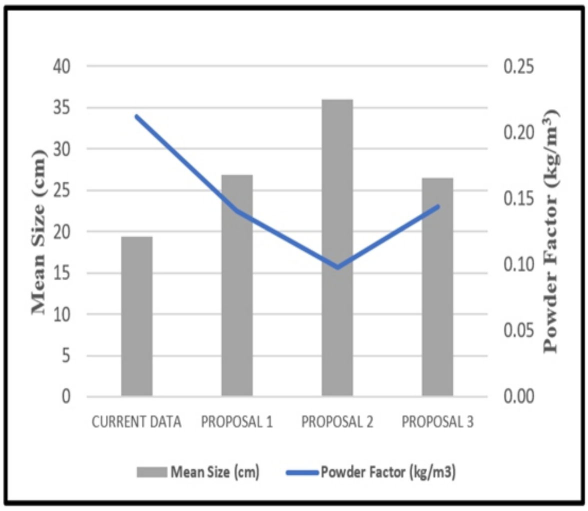

Figure 5: Change in Mean Size and Powder Factor as Parameters in S-W pit are altered.

Table 7: Evaluation of Drilling and Blasting for North-West Pit

Parameter	Value			
	Current data	Proposal 1	Proposal 2	Proposal 3
Burden (m)	3.7	5	6	7
Spacing (m)	4.5	5	6	3.5
Hole Diameter (mm)	120	120	120	120
Bench Height (m)	5	5	5	5
Sub-drill (m)	0.5	0.5	0.5	0.5
Stemming (m)	1.4	1.4	1.4	1.4
Explosive Type	Blend	Blend	Blend	Blend
Explosive Final Density (kg/m³)	0.0012	0.0012	0.0012	0.0012
Relative Explosives Energy	95.38	95.38	95.38	95.38
Drilling Cost (₦/m)	3500	3500	3500	3500
Explosive Cost (₦/kg)	1033.5	1033.5	1033.5	1033.5
Loading Density (kg/m)	10	10	10	10
Charge Length (m)	4.1	4.1	4.1	4.1
Mass per Hole (kg)	41	41	41	41
Mass above Grade (kg)	36	36	36	36
Powder Factor (kg/m³)	0.21	0.14	0.10	0.14
Uniformity index	1.6	1.4	1.3	1.1
Mean size (cm)	19	27	36	26
Volume per Hole (m³)	83.25	125	180	122.5
Explosives Cost per Hole (₦)	42373.5	42373.5	42373.5	42373.5
Initiation Cost per Hole (₦)	400	400	400	400
Drilling Cost per Hole (₦)	19250	19250	19250	19250
Total Cost per Hole (₦)	62023.5	62023.5	62023.5	62023.5
Explosives Cost per BCM (₦/m³)	509.0	339.0	235.4	345.9
Initiation Cost per BCM (₦/m³)	4.8	3.2	2.2	3.3
Drilling Cost per BCM (₦/m³)	231.2	154.0	106.9	157.1
Total Cost per Volume (₦/m³)	745.0	496.2	344.6	506.3

Table 8: Predicted Fragmentation by Size distribution for North-West.

Fragmentation sizing	Current data	Proposal 1	Proposal 2	Proposal 3
Oversize	0.0%	0.0%	0.9%	1.1%
In Range	48.3%	63.6%	72.1%	58.7%
Undersize	51.7%	36.4%	27.0%	40.1%

5. Conclusion

This research used the Kuz-Ram method to develop three fragmentation model proposals (proposal 1, proposal 2 and proposal 3). The model was numerically analyzed in the southwest and northwest mines of the company within four weeks. The geometric parameters analyzed include the powder factor, mean fragment size, volume of blasted material per blast hole and the total cost per volume. The three proposals displayed significant improvement for all the geometric parameters analyzed. Proposal 2 of the model showed optimum and efficient characteristics for the geometric parameters. From the numerical analysis, it is therefore concluded that Proposal 2 would give the optimum model.

Acknowledgements

The authors are grateful to the Department of Mining Engineering, School Engineering and Engineering Technology, The Federal University of Technology, Akure, Ondo State, Nigeria, for providing their support and guidance during the research. The authors are also grateful to the staff of Lafarge Africa PLC, AshakaCEM, Gombe State, Nigeria, for their support regarding information, materials and equipment during the research.

References

Anon., (2014). Reducing the Cost of Drill and Blast through Blast Design Optimization, North Parkes Open Cut Mine, Australia, Orica Mining Services.

Bozic B. (1998). Control of Fragmentation by Blasting", Rudarsko-geoloiko-nafinizbornik, Vol. 10, str. 49-57, *Zagreb.*

Brahma, K C, Pal, B K and Das C. (2007). A Study on Application of Markovian Decision Process in Drilling and Blasting Operation of Opencast Mines. *Journal of Mines, Metals and Fuels*, 55(1): 24–29

Cunningham, C.V.B. (1983). The Kuz–Ram Model for Prediction of Fragmentation from Blasting, R. Holmberg & A. Rustan (Eds), *Proceedings of First International Symposium on Rock Fragmentation by Blasting*, (pp. 439– 454). Luleå.

Cunningham, C.V.B. (1987). Fragmentation estimations and the Kuz–Ram model – four years on, W. Fourney (ed.) *Proceedings of Second International Symposium on Rock Fragmentation by Blasting, Keystone*, (pp. 475–487), Colorado.

Engin, I. C. (2010) A Practical Method of Bench Blasting for Desired Fragmentation based on Digital Image Processing Technique and the Kuz-Ram Model, *AfyonKocatape University, Iscehisar Vocational School, Iscehisar, Afyonkarahisar.*

Hustrulid, W. A. (1999). *Blasting principles for open pit mining: general design concepts*. Balkema.

ICMM, (2012).Trends in the Mining and Metals Industry, Mining's Contribution to Sustainable Development, *International Council on Mining and Metals (ICMM)*, October 2012.

Kuznetsov V. M. (1973). The mean diameter of the fragments formed by blasting rock. *Soviet Mining Science,* pp.144-148

Leng, Z., Fan, Y., Gao, Q. and Hu, Y., (2020). Evaluation and optimization of blasting approaches to reducing oversize boulders and toes in open-pit mine, International Journal of Mining Science and Technology, 30(1): 373–380

Leng. Z. D., Zhao, M. S. and Lu, W. B. (2018). Explosive-Rock Interactions Based on Non-Ideal Detonation Model. *Engineering Blast,* 24(6): 1–9.

Palangio, T.W and Palangio T.C. (2005). Advanced Automatic Optical Blast Fragmentation Sizing and Tracking", Brighton Conference Proceedings 2005, R. Holmberg et al, European Federation of Explosives Engineers.

Siddiqui, F. I., Shah, S. M. A. and Behan, M. Y.

(2009). Measurement of Size Distribution of Blasted Rock Using Digital Image Processing, *JKAU: Eng. Sci.*, 20(2): 81 – 93.

Usman, U. A., Kumar, P., Abdulkadir, A. B., Kamale, H. I., Sadiq, H. M., Muhammed, D. D., Ibrahim, Y and Wulo, I. B. (2016). Geochemical assessment of toxic metals stocking in top-soil within the area of limestone quarry in Gombe of North-eastern Nigeria. *African Journal of Environmental Science and Technology*, *10*(9), 283-291.

Vasileios, D. (2008): Fragmentation Analysis of Optimized Blasting Rounds in the Aitik Mine – Effect of Specific Charge", Unpublished Master's Thesis Report, Luleå University of Technology, Sweden, p. 108.

Chemical Characterisation and Upgrading of Adudu/Obi Lead-Zinc Complex Ore using Froth Flotation Method

Tolu, S., Oyeladun, O. A. W. and Salawu A. O.

Department of Mineral and Petroleum Resources Engineering, Kaduna Polytechnic, Kaduna

Corresponding author: oawoyeladun@gmail.com

Abstract

Flotation is one of the ways of upgrading of sulphide ore. Hence, to upgrade Adudu/Obi lead – zinc complex ore, froth flotation was employed. The lead – zinc complex ore was sourced from Adudu in Obi Local Government Area of Nasarawa State, Nigeria using grab method. The ore was crushed using laboratory jaw crusher and ground using ball mill. Then chemical characterised using XRF: it was revealed that ore contained 18.203%Pb, 17.802%Zn and 24.65%Si. The mineralogical analysis showed the presence of 28% galena (PbS), 22% sphalerite (ZnS), 19% siderite ($FeCO_3$) and 31% Quartz (SiO_2). The size fraction using froth flotation was – 90 + 50μm. The concentration of ore using bulk froth flotation process was carried out and it was revealed that 24.60% of lead concentrate and 28.4% of zinc concentrate at 83.06% and 87.29% recoveries respectively were obtained. The concentration of ore using differential froth flotation process was further employed to upgrade the concentrate from bulk froth flotation concentrate and the following concentrate was obtained: 56.25% of lead concentrate and 45.09% of zinc concentrate at 80.9% and 88.6% recoveries respectively.

Keywords: concentration, bulk froth flotation, differential froth flotation, recoveries.

1.0. Introduction

The characterization of the ore was carried out to establish the parameters required for the design of the ore process flowsheet, alongside the determination of the material balance, metallurgical recoveries and quality of the products. Hence, it is absolutely necessary to perform the mineralogical and physico – chemical analysis of the ore (Oyeladun *et al.*, 2016). This is because mineral processing of ores essentially depends on the chemical composition of the valuable and non-valuable elements of the matrix of the ore. The laboratory test carried out provides information on the operating parameters for design purposes and also used to determine capital and operating costs estimates. In developing the flow-sheet, the mineral engineer must necessarily consider overall economics when choosing a process or combination of process routes (Oyeladun *et al.*, 2016).

Bulk of the world's lead and zinc is supplied from their sulphide ore deposit which generally occurred as finely disseminated bands of galena and sphalerite with varying amount of pyrite. In Nigeria, lead – zinc complex ore plays an important role in the exportation of non – ferrous metals. The numinous advantage of the lead – zinc ore had made it necessary to encourage private and joint venture partners to develop and exploit the various lead – zinc deposits all over the nation (MMSD, 2014). Adudu/Obi lead – zinc complex ore lies within latitude 8°21'43” and longitude 8°20'40”.

Moreover, froth flotation is widely used for concentration of low-grade lead – zinc complex ore for meeting the required specifications of the concentrates for the extraction of its metals (Singh *et al.*, 2004). Froth Flotation is a process for making a solid – solid separation based on differences in the physico-chemical properties of minerals (composition and electrical charge). A froth is formed by introducing air into a fine particle slurry (pulp) containing a frothing (foaming) agent and other reagent inside the flotation cell. Particles with air affinity for air bubble (hydrophobic) are carried by the bubbles to the surface where they are removed by scrapping (Wills and Napier-Munn, 2006).

Moreover, reagent used to coat the desired mineral with a hydrophobic coating and allows bubble to attach to the surface of the mineral are called collector. They are organic chemicals which make the surface hydrophobic and hence the mineral is capable of being collected in the process. Each collector molecule contains a polar and non – polar group. When attached to the mineral particle, these molecules are so orientated that the non – polar or hydrocarbon group is extended outward. Such orientation results in the formation of a hydrophobic hydrocarbon film on the mineral surface. A selective collector may be used at the head of the circuit, to float the highly hydrophobic minerals, after which a more powerful, but less selective one is added to promote recovery of the slower floating minerals (Weiss, 1985). The sulphide minerals collectors can be grouped as shown in Table 1. **Table 1: Collector Classification**

Table 1: The Group of Sulphide Minerals Collectors

Anionic for Sulphide Minerals	Anionic for Non - Sulphide Minerals	Cationic for Non - Sulphide Minerals
Xanthates, Thionocarbonates, Dithiophosphate, Xanthogen formats	Fatty acids	Alky amines, Quaternary ammonium compounds

Source: (Weiss, 1985)

Also, the frother is the reagent used to create a stable froth, stiff enough to facilitate mineral separation, but not break so as to facilitate subsequent handling. This objective is accomplished by imparting temporary toughness to covering film of the bubble. The life of the individual bubble is thus prolonged until it can be further stabilized by adherence of mineral particles and joined with other bubbles of the pulp surface to form a froth. Once it is withdrawn from the flotation machine, however, the froth should break down rapidly, to prevent interference with subsequent processing operations. The choice of froth depends on the cost, readily available, effective in low concentrations and essentially free of collector properties, only a few materials have been found suitable. Examples of frothers are Dowfroth 250, alcohol, pine oil and cresylic acid (Weiss, 1985).

Furthermore, Modifiers are reagent used to ensure that the desired mineral float and the undesired mineral sink These are organic or inorganic chemicals used to modify the slurry conditions to enhance the difference in surface chemistry between the valuable and gangue minerals. The regulators can be classed as activators, depressant or pH modifiers. Other reagents that may be used in specific cases include dispersants for removing clay slimes from mineral surfaces for removing interfering ions from solution. The main use of these modifying agents is in the differential flotation of a mixed ore. That is the successive removal of two or more valuable minerals from each other by flotation. For example, the separation of copper, lead, zinc and iron sulphides from a single ore is selective flotation whereas the flotation of the combined sulphides from the gangue is referred to as bulk flotation (Wills and Napier-Munn, 2006). These include activator, depressant, pH modifying agents, blocking agents, etc. (Moore, 1990; Wills and Napier-Munn, 2006).

Flotation machines are apparatus usually used to carry out flotation process. They are classified on the basis of inventors rather than principle of operation which are Denver and Wenco Fragergren cells. The functions of flotation machines are:

a. to produce the separating interface
b. to lead selected and rejected particles out of the machine by different path.

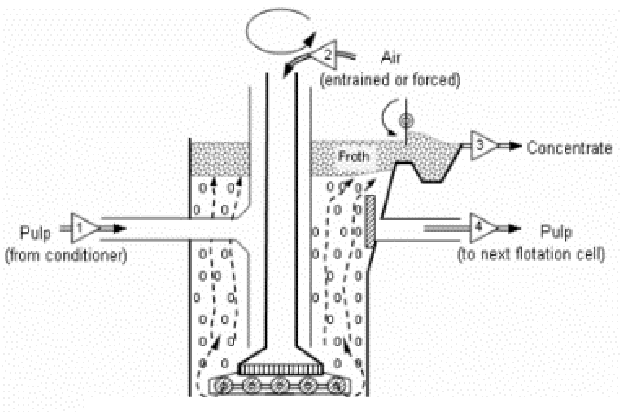

Figure 1: Flotation Cell (Weiss, 1985)

This research work is targeted at beneficiation of Adudu/Obi lead-zinc complex ore using froth flotation method. The objectives include determination of chemical composition, mineralogical composition, particle size analysis, metallurgical accounting of bulk and differential flotation as well as material balance of Adudu/Obi Lead-Zinc Complex ore.

2.0. Materials and Methods

2.1 Equipment and Materials

The equipment used in the course of this research were: jaw crushing machine, pulverizing machine, ball milling machine, sieve shaking machine, froth flotation machine, weighing machine, pH meter, Stopwatch, X-ray fluorescence spectroscopy (XRF) Model Mini PAL 4 and X-ray diffractometer (XRD) by PAN Analytical BV of Netherland.

The materials used include: Sodium ethyl xanthate, Copper sulphate, MIBC Frother, 1 M NaOH solution,1M HCl solution and Adudu/Obi Lead-Zinc Complex ore.

2.2 Methods

2.2.1 Sample collection and preparation of the Adudu/Obi Lead-Zinc Complex ore

50kg was collected from various locations of the Adudu/Obi Lead-Zinc Complex ore deposit at Obi village of Obi Local Government Area of Nasarawa State, Nigeria and these samples were collected from 3 different locations using grab method.

2.2.2. Chemical characterization of the Adudu/Obi Lead-Zinc Complex ore

The head sample collected from the various locations within latitude 8°19´25˝ to 8°19´71˝ and longitude 9°0´22˝ to 9°06´77˝ and depth of about 10meters of the Adudu/Obi Lead-Zinc Complex ore using grab method. The sample was subject to chemical analysis using XRF Machine.

2.2.3. Mineralogical characterization of the Adudu/Obi Lead-Zinc Complex ore

The head sample collected from the various locations and depths of the Adudu/Obi Lead-Zinc Complex ore was subject to mineralogical analysis using XRD Machine.

2.2.4. Sample Preparation

Sample collected was first crushed utilizing the Denver Jaw crusher in order to reduce the samples to reasonable size for further grinding. The sample was further ground using ball mill.

2.2.5. Sieve Analysis

The ore was broken using sledge hammer and pulverized. This was later ground using laboratory ball mill and sieved using various sieve size ranging from +250µm to – 50 µm using a nest of sieves based on √2 scheme with the coarsest on top and the finest sieve used at the bottom. The nominal apertures of the sieves used were 250µm, 180µm, 125µm, 90µm and 50µm. The chemical composition of each sieve size was determined by using XRF machine. This provided information concerning the liberation size.

2.2.6. Concentration using Froth Flotation Method

a. Bulk Flotation of Adudu/Obi Lead-Zinc Complex ore

Concentration of Adudu/Obi Lead-Zinc Complex ore was done using froth flotation method. -125 + 90µm sieve size fraction was used for the concentration process.200g of the sample was fed into flotation cell. The frother (pine oil) and collector (Sodium ethyl xanthate) dosages were 2ml each. The conditioning time was 5 minutes at pH of 9. After conditioning, air was introduced into the pulp. The float was skimmed and dried. The weight of products collected were: 123.89g concentrate and 76.10g tailing. The products were analysed using XRF machine. The ratio of concentration and recovery were calculated using the formula and Table 2.

Table 2: Metallurgical Accounting for Bulk Flotation

Product	Weight (%)	Sample Assay (%)	Calculated
Feed	F	f	
Concentrate	C	c	
Tailing	T	t	
Ratio of Concentration			$\bar{K}$
Recovery (%)			R

$$\bar{K} = \frac{F}{C} \text{ and } R = \frac{c(f-t)}{f(c-t)} \times 100$$

b. Differential Flotation of the Concentrate

i. The concentrate was reground to -90µm sieve size fraction. 100g of concentrate of the bulk flotation was charge into the flotation cell with pH at 9. Conditioning for 5 minutes with zinc suphate, then collector sodium isobutyl xanthate was added and conditioned for another 5 minutes. Air was introduced into the flotation cell and the float was skimmed until the float became barren. The concentrate was dried and weighed.

ii. The tailings of the above froth flotation test served as the feed for the concentration of zinc. The frother (pine oil) and collector (Sodium ethyl xanthate) dosages were 2ml each. The conditioning time was 5 minutes at pH of 9. After conditioning, air was introduced into the pulp. The float was skimmed.

The products collected were dried and weighed. The products were analysed using XRF machine. The ratio of concentration and recovery were calculated using the formula and Table 3.

Table 3: Differential Flotation of the Concentrate of Two Products

Product	Weight (%)	% Pb Assay	% Zn Assay	Calculated
Feed	F	l_1	z_1	
Pb Concentrate	L	l_2	z_2	
Zn Concentrate	Z	l_3	z_3	
Tailing	T	l_4	z_4	
Ratio of Concentration				$\bar{K}_{Pb} and\ \bar{K}_{Zn}$
Recovery (%)				$R_{Pb} and\ R_{Zn}$

The ratios of concentration, $\bar{K}_{Pb} and\ \bar{K}_{Zn}$ are those for the lead and zinc concentrates, respectively, with $R_{Pb} and\ R_{Zn}$ the percentage recoveries of the lead and zinc concentrates. As follows:

$$L = \frac{F\,(l_1 - l_4)(\,z_3 - z_4) - (z_1 - z_4)(l_3 - l_4)}{(l_2 - l_4))(\,z_3 - z_4) - (z_2 - z_4)(\,l_3 - l_4)} = \text{tons Pb concentrate}$$

$$Z = \frac{F(l_2 - l_4)(\,z_1 - z_4) - (l_1 - l_4)(\,z_2 - z_4)}{(l_2 - l_4)(\,z_3 - z_4) - (z_2 - z_4)(\,l_3 - l_4)} = \text{tons Zn concentrate}$$

$$R_{Pb} = \frac{100L \times l_2}{F \times l_1} = \text{ lead recovery \%}$$

$$R_{zn} = \frac{100Z \times z_2}{F \times z_1} = \text{ zinc recovery \%}$$

$$\bar{K}_{Pb} = \frac{F}{L} \text{ and } \bar{K}_{Zn} = \frac{F}{Z} = \text{ ratio of concentration}$$

The three-products solution can be achieved by taking an intermediate tailings sample between the two stages of concentration; i.e., a lead tail (zinc feed) sample.

Then, adding the notations:
Lead tail (zinc feed) = CT with lead and zinc assays = l_5 and z_5
From mill feed, F, as Unity 1
Then, L + LT = 1
(L x l_2) + (LT x l_5) = l_1
(L x l_5) + (LT x l_5) = l_5
Subtracting both above,

$$L(l_2 - l_5) = (l_1 - l_5)$$

Then,

$$\text{L} = \text{F}\,\frac{l_1 - l_5}{(l_2 - l_5)} = \text{ tons lead concentrate}$$

and similarly,

$$Z = \frac{(F - C)(z_5 - z_4)}{(z_3 - z_4)} = \text{tons zinc concentrate.}$$

3.0. Result and Discussion

3.1. Chemical Composition of Head Sample

Table 4: Chemical Analysis of the Adudu/Obi Lead-Zinc Complex ore

Element	Mg	Al	Si	S	Cl	K	Ca	Ti	As
%	4.930	5.420	**24.650**	15.420	0.200	0.620	0.180	0.150	0.763
Element	**Cr**	**Mn**	**Fe**	**Sn**	**Cu**	**Zn**	**Pb**	**P**	**Ba**
%	0.020	0.830	10.150	1.550	0.370	**17.802**	**18.203**	0.130	0.070

Table 2 presents the chemical analysis of the head sample using XRF. It reveals that the ore contains 18.203%Pb, 17.802%Zn and 24.65%Si. From the result in Table 2, it could be observed that silica, iron, lead, zinc and sulphur are predominant, while other associated elements are minor in the matrix of the ore. This phenomenon could be attributed to the mineralization of the deposit created by the geochemical formation of the ore deposit. Damisa (2008), reported that lead-zinc-copper complex ore situated within the Benue trough of which Nasarawa state is located contains copper; Jatau et al, (2014) also in their findings, reported that the chemical analysis of the ore sample obtained from similar geological formation in Nasarawa state contains appreciable amount of lead and zinc. Hence, the similarity in the result obtained for Adudu/Obi lead-zinc complex ore deposit with those reported in the literatures. Therefore, Adudu/Obi lead-zinc complex ore deposit could serve as another potential source for lead and zinc minerals since it contains 18.203%Pb and 17.802% (Weiss, 1985).

3.2. Mineralogical Composition of Head Sample

Table 3: Mineralogical Composition of the Adudu/Obi Lead-Zinc Complex ore

Mineral Name	Chemical Name	Chemical Formula	Percentage
Galena	Lead Sulphide	PbS	28
Sphalerite	Zinc Sulphide	ZnS	22
Siderite	Iron carbonate	$FeCO_3$	19
Quartz	Silica	SiO_2	31

Table 3 presents the result of XRD analysis of the ore sample. The result revealed the presents of galena, sphalerite, siderite and quartz. From the result it could be observed that the minerals present have the following estimations: galena (28%), sphalerite (22%), siderite (19%) and quartz (31%) with galena, sphalerite, siderite as the major minerals. These findings compared favorably with similar works done by Jatau et al, (2014) and Damisa, (2008) where they stated that the lead and zinc ore minerals within the Nasarawa schist are predominantly galena and sphalerite in association with iron, titanium and aluminum as gangues. Hence, the need for the beneficiation of the ore in order to upgrade its lead and zinc content.

3.3 Particle Size Distribution

Table 4: Chemical Analysis of various sieve size fractions

Sieve Size/ Element (%wt)	$+250\mu m$	-250 $+180\mu m$	-180 $+125\mu m$	-125 $+90\mu m$	-90 $+50\mu m$	$-50\mu m$
Fe	12.120	10.880	10.195	10.199	8.875	8.700
Cu	0.274	0.243	0.305	0.380	0.372	0.367
Pb	**6.778**	**8.371**	**12.330**	**12.976**	**18.284**	**12.78**
Mg	3.748	3.823	3.028	5.235	4.235	4.110
Al	4.667	4.816	4.235	5..545	4.50	4.550
Mn	0.342	0.826	0.892	0.915	0.950	0.726
Zn	**9.979**	**10.979**	**12.297**	**11.530**	**12.880**	**10.292**
Zr			0.02	0.09	0.04	0.04
Ti				1.88	0.52	
Nb				0.04	0.05	0.03
Ag	0.005		0.008	0.008	0.008	0.012
As					0.23	
Si	40.46	39.29	31.37	29.61	26.38	35.66
S	11.06	12.20	10.59	13.65	14.907	12.51

Table 4 presents chemical analysis of the various particle sizes. The result reveals that at 250μm contains 12.12%Fe, 6.78%Pb, 9.98%Zn, at 180μm contains 10.88%Fe, 8.37%Pb, 10.98%Zn, at 125μm contains 10.195%Fe, 12.33%Pb, 12.297%Zn, at 90μm contains 10.199%Fe, 12.976%Pb, 11.53%Zn, at 50μm contains 8.88%Fe, 18.28%Pb, 12.88%Zn and pan 8.7%Fe, 12.78%Pb, 10.29%Zn.

Table 5: Particle Size Analysis of Adudu/Obi Lead-Zinc Ore

Sieve Size μm	Weight (g)	Weight (%)	Nominal Aperture (μm)	Cumulative	
				Undersize	Oversize
$+250$	12.63	12.63	250	87.37	12.63
– 250 + 180	15.93	15.93	180	71.44	28.56
– 180 + 125	21.76	21.76	125	49,68	50.32
– 125 + 90	12.08	12.08	90	37.6	62.40
– 90 + 50	23.80	23.80	50	13.80	86.20
– 50	13.80	13.80	–		100.00

From Table 5, the iron and silica minerals distributed itself normally. This trend compared favourably with works done by Weiss, (1985) and Wills, (2006) where they also observed similar trends. Furthermore, the liberation size of the lead – zinc complex ore is found to be 50μm being the sieve size with the highest assay value of the total iron content of 18.28%Pb and 12.88%Zn and distribution of 23.80% as defined (Wills, 2006; Mills, 2014).

3.4. Metallurgical Balance Accounting for Bulk Flotation

Table 6: Metallurgical Accounting for Bulk Flotation of Lead Concentrate

Product	Weight (%)	Sample Assay (%)	Calculated
Feed	100	18.203	
Concentrate	61.95	24.60	
Tailing	38.05	8.00	
Ratio of Concentration			1.61
Recovery (%)			83.06

Table 6 present the metallurgical accounting of bulk flotation of lead concentrate showing the concentrate and tailings in their percentage. It can be deduced that ratio of concentration and recovery are 1.61 and 83.06% respectively. This shows appreciable increase in the lead assay in the concentrate and it is line other literatures

Table 7: Metallurgical Accounting for Bulk Flotation of Zinc Concentrate

Product	Weight (%)	Sample Assay (%)	Calculated
Feed	100	17.802	
Concentrate	61.95	28.40	
Tailing	38.05	5.00	
Ratio of Concentration			1.61
Recovery (%)			87.29

Table 7 present the metallurgical accounting of bulk flotation of zinc concentrate showing the concentrate and tailings in their percentage. It can be deduced that ratio of concentration and recovery are 1.61 and 87.29% respectively. This shows appreciable increase in the lead assay in the concentrate and it is line other literatures.

Tables 6 and 7 present lead and zinc concentration ratios and recoveries which is in line with roughing (ie. Bulk) stage of flotation.

3.5. Metallurgical Accounting for Differential Flotation

Table 8: Metallurgical Accounting for Differential Flotation of the Adudu/Obi Lead-Zinc Complex ore

Product	Weight (%)	% Pb Assay	% Zn Assay	Calculated
Feed	100	24.60	28.40	
Pb Concentrate	35.3	56.25	8.40	
Zn Concentrate	55.8	8.20	45.09	
Tailing	8.9	1.50	3.09	
Ratio of Concentration				2.8 and 1.8
Recovery (%)				80.9 and 88.6

Table 7 present the metallurgical accounting of differential flotation of lead – zinc complex ore from the bulk flotation product showing the concentrate and tailings in various percentages. It can be deduced that ratio of concentration is 2.8 and 1.8 for lead zinc respectively, while recovery 80.9 and 88.6% for lead zinc respectively. This shows appreciable increase in the lead and zinc assays in the concentrate and it is line other literatures.

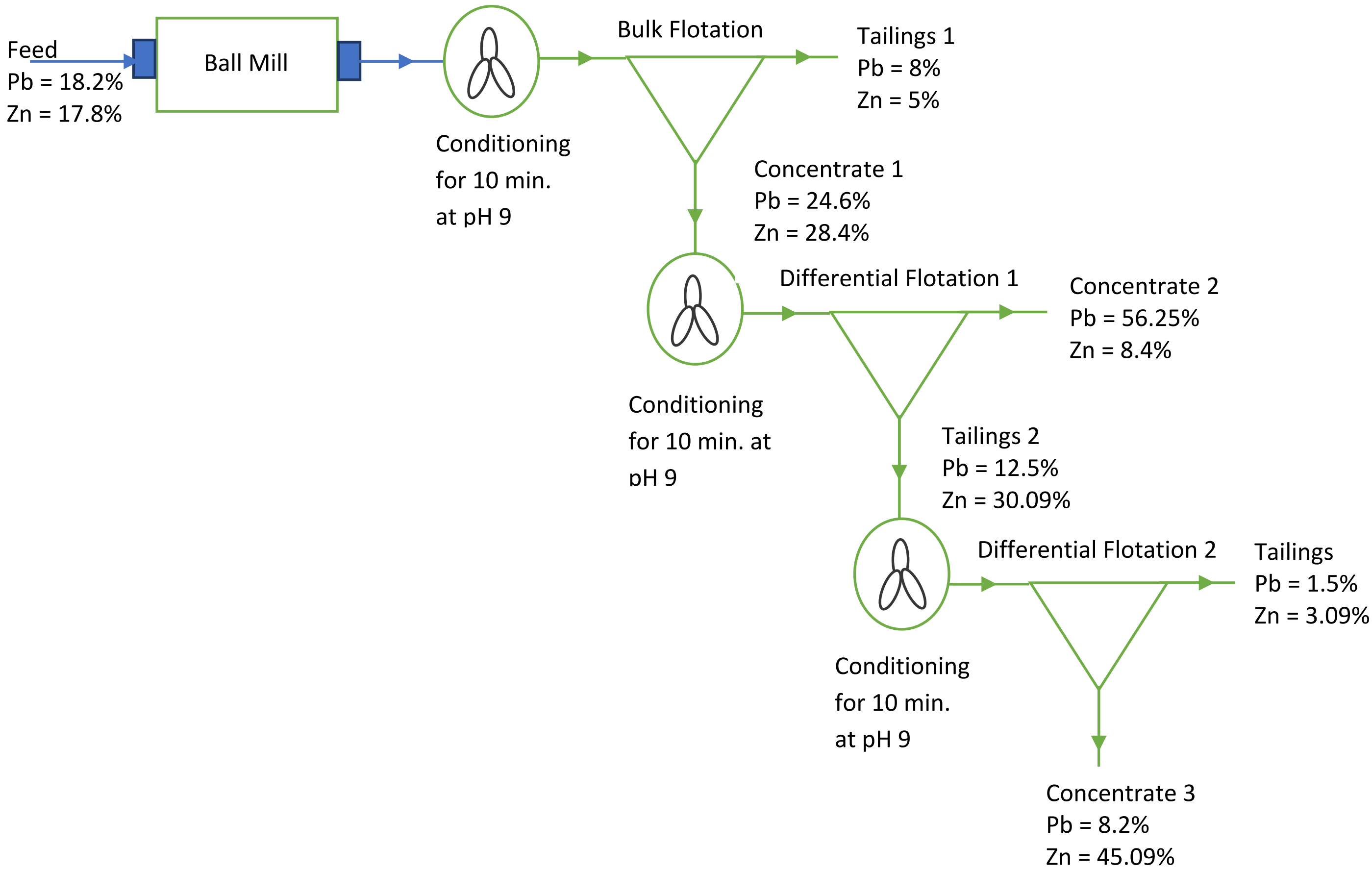

Figure 2: Flowchart of froth flotation of Adudu/Obi Lead-Zinc Complex

3.6. Material Balance

Table 8: Material Balance for Differential Froth Flotation of the Adudu/Obi Lead-Zinc Complex ore

	Model Input	
Milling of ore, tonnes/day	1000	
	% Lead	% Zinc
Feed	24.60	28.40
Lead Concentrate	56.25	8.40
Zinc Concentrate	8.20	45.09
Tailings	1.50	3.09

Model Output	
353	Tonne Lead Concentrate
558	Tonne Zinc Concentrate
80.9	Lead Recovery
88.6	Zinc Recovery
2.8	Lead Concentration ratio
1.8	Zinc Concentration ratio

From Table 8, it was revealed that when 1000 tonnes/day of product from the bulk froth flotation process was introduced into the differential froth flotation production sections, the output of model will be 353 tonnes of lead concentrate and 558 tonnes of zinc concentrate at 80.9% and 88.6% recoveries respectively was achieved.

4.0. Conclusion

The froth flotation of Adudu/Obi lead – zinc complex ore was carried out and the following conclusions were drawn that:

i. the characterization of the Adudu/Obi Lead-Zinc Complex ore using XRF revealed that ore contained 18.203%Pb, 17.802%Zn and 24.65%Si;

ii. the concentration of ore using bulk froth flotation process, 24.60% of lead concentrate and 28.4% of zinc concentrate at 83.06% and 87.29% recoveries respectively were achieved;
iii. the concentration of ore using differential froth flotation process, 56.25% of lead concentrate and 45.09% of zinc concentrate at 80.9% and 88.6% recoveries respectively were achieved.

5.0. References

Gupta, A. and Yan, D.S. (2006) Mineral Processing Design and Operation - An Introduction Amsterdam, Elsevier B.V., P693

Ministry of Mines and Steel Development (MMSD) (2014): Occurrence of Lead – Zinc Ore in Nigeria.

Moore J. J. (1990): Chemical Metallurgy, Buttworth – Heinemann

Oyeladun, O. A. W., Tolu, S. and Salawu A. O. (2021): Beneficiation of Kudaru Iron Ore Using Magnetic Separator, Nigerian Metallurgical Society Conference, Jos Hybrid 2021.

Oyeladun, O. A. W., Thomas D. G. and Yaro S. A. (2016): Physico - chemical and Mineralogical Analysis of Azara Complex Ore, Nigerian Mining Journal Vol. 14 No. 2

Singh, R. Banerjee, B and Srivastava J. P. (2004): Effects of Process Parameters on Selective Flotation of Lead – Zinc Ore, International Seminar on Mineral Processing Technology, Orissa.

Weiss, N. L., (1985): Mineral Processing Handbook by American Institute of Mining Metallurgical and Petroleum Engineering Incorporated in the United States of America by Kings Port Press.

Wills, B. A. and Napier-Munn, T. (2006): Mineral Processing Technology-An Introduction to the Practical Aspects of Ore Treatment and Mineral Recovery, Seventh Edition, Amsterdam: Elsevier Science and Technology Books, P450

Umar *et al* (2022) Nigerian Mining Journal, (20) 18 - 33

Integrated Methods for Exploration of Dimension Stones in Part of the Basement Complex Rocks of Southwest, Nigeria

Umar, N. D.[1], Aliyu A. I.[2*], Omonona, O. V.[3] and Abdullahi, A. M.[1]
[1]*Department of Geology, Federal University of Lafia*
[2]*Department of Geology, University of Nigeria*
[3]*Department of Geology/Geophysics, Alex Ekwueme Federal University, Ndufu-Alike*
[*]*Corresponding author:* aliyu.itari@gmail.com

Abstract

Geological, geophysical and geotechnical surveys were employed to ascertain the suitability of Basement Complex rocks for dimension stones in part of Abeokuta, southwest Nigeria. The area is underlain by Porphyroblastic gneiss, granite gneiss, and migmatite gneiss characterized by low density shallow-seated, NW- SE trending lineaments underlay the study area. Thin section analysis revealed quartz (35 - 49%), orthoclase (25 - 37%), plagioclase (14 - 28%), biotite (5 -20%) and hornblende (1–14%). Joints dimension range from 0.2m - 1.2m, while Rock Quality Designation (RQD) range from 54% - 65%. The compressive strength (135 – 205 Mpa), water absorption (0.44 – 1.35 %), porosity (2.69 – 2.84 g/cm^3) and density (0.35 – 0.88 %) meet the specification requirements for dimension stones. Recovered cores show textural and colour consistency which indicates that the colour variation resulted from physical weathering and not mineral segregation. The porphyroblastic gneiss and granite gneiss have the potential to produce larger blocks, thus suitable for use as dimension stone.

Keywords: Dimension stone; Gneiss; Slab; Block volume; Abeokuta

Introduction

Nigeria's construction industry is growing in an unprecedented manner, hence the need to meet the increasing demand for industrial rocks (dimension stones and aggregates). Abeokuta and environs located in southwest Nigeria is underlain by Basement Complex rocks which offers a collection of rocks with varying textures and colours with a good prospect for use as dimension stones.

Dimension stone also referred to as ornamental stone is a collective term for various natural stones (granite, marble, limestone, gneiss, sandstone, quartzite, or slate) which are used for structural and decorative purposes in construction and monumental applications such as floors and pavements, memorial arts, external and internal wall claddings (Arora, 2004). Rocks used for dimension stone are first quarried into suitable blocks, slabs, and sheets, cut into specific sizes, and finally shaped and polished. The desirable criteria for potential dimension stone prospects are: substantial exposure, lithological uniformity, low density of joints and fractures, rock durability, attractiveness, and absence of deleterious materials (Arora, 2004). These qualities will result in low cost of excavations, enhance aesthetic appearance when polished, recovery of rectangular blocks of suitable sizes relative to aggregate and a good compressive strength.

The economic value of a dimension stone depends largely on its appearance, the possibility of producing rectangular blocks larger than 1m^2 and the accessibility of the resource location (Deere, 1989). The appearance of a dimension stone is determined by the rock's physical properties (colour, mineralogy, and texture). These properties also control the workability, ability to take polish as well as resistance to physical and chemical weathering and abrasion. Structural discontinuities such as fractures, joints, faults, veins, and intrusions serve as weaknesses along which rocks are quarried into blocks for dimension stones (Yarahmadi *et al.,* 2015). However, joints are the most important discontinuities in dimension stones as they are a major weakness along which the formation of different blocks occurs in the rock mass (Yarahmadi *et al.,* 2015) as a profusely jointed rock will not be economically viable for dimension stone.

Exploring for dimension stone is a very complex task that requires careful evaluation of the various factors involved in the decision-making. Yarahmadi *et al.* (2015) evaluated the various techniques used in assessing the geometry of discontinuities on rocks to be used as dimension stones and concluded that the window and imaging survey techniques are best suited for an open quarry while the coring and Ground Penetrating Radar (GPR) surveys are best suited for rocks covered by soils areas. Nasir *et al.* (2015) employed geotechnical tests such as porosity, water absorption, compressive strength and density to ascertain the suitability of a rock for dimension stone.

The aim of this research is to determine the overburden thickness/depth to bedrock, geotechnical properties of rocks and identify the geometry of the discontinuities (Joints, fractures, faults, and veins) and ascertain the suitability of the rocks for use as dimension stones.

The area under investigation lies between longitudes 3°5'24" to 3°7'00"N and latitudes 7°27'00" to 7°31'30"E. It is located in Obafemi-Owode local government area of Ogun State (Figure 1). Accessibility is by the Abeokuta – Kajola – Ibadan road and further improved by minor routes and footpaths linking villages, farmlands, and streams. The major stream flows in a NE – SW direction which corresponds to the strike direction of most structures generally found in the area indicating a structurally controlled stream.

Geology of The Area

Regionally, the area lies within the Precambrian Basement Complex of southwest Nigeria which is underlain by crystalline igneous and metamorphic rocks mostly undifferentiated migmatite-granite gneiss, quartzite and quartz-schist complex as well as localized pegmatite and quartz veins intrusions (Rahaman, 1989).

The main rock types found in the study area are porphyroblastic gneiss, migmatite gneiss, and granite gneiss (Figure 2). Large outcrops of granitic rocks occur within the area and there is also the presence of low-lying outcrops of granite and granite gneiss which are highly indurated and contain quartz inclusions. The rocks are generally light in colour while the weathered surface is brownish in colour based on field observations.

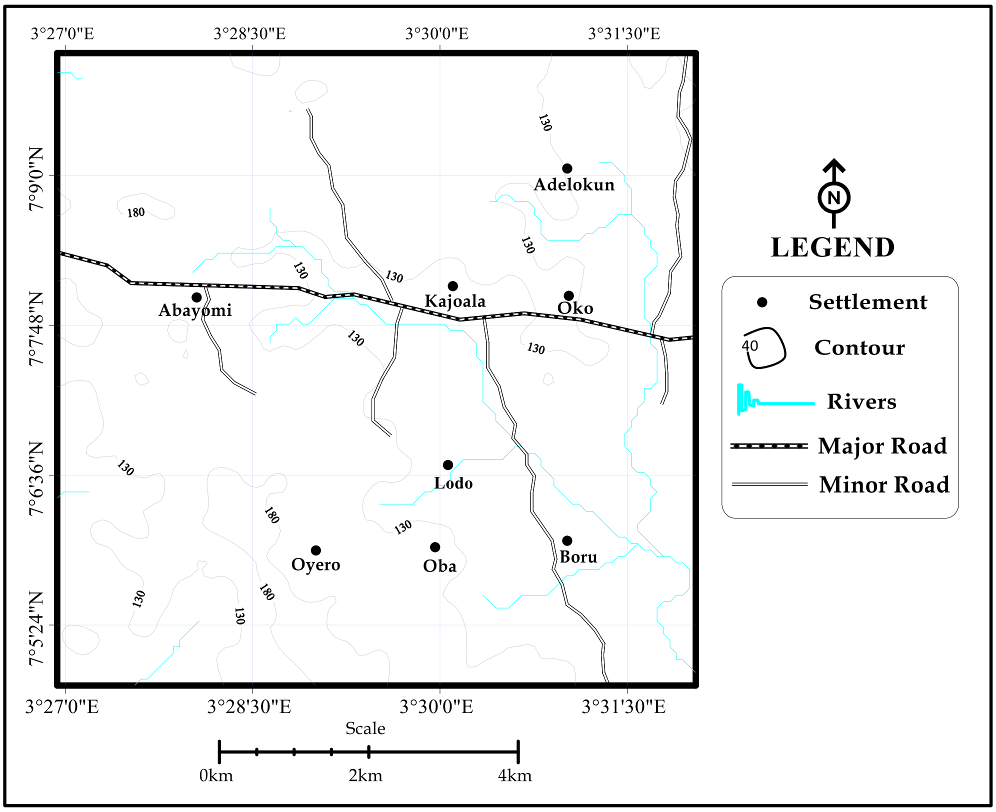

Figure 1: Topographic map of the study area

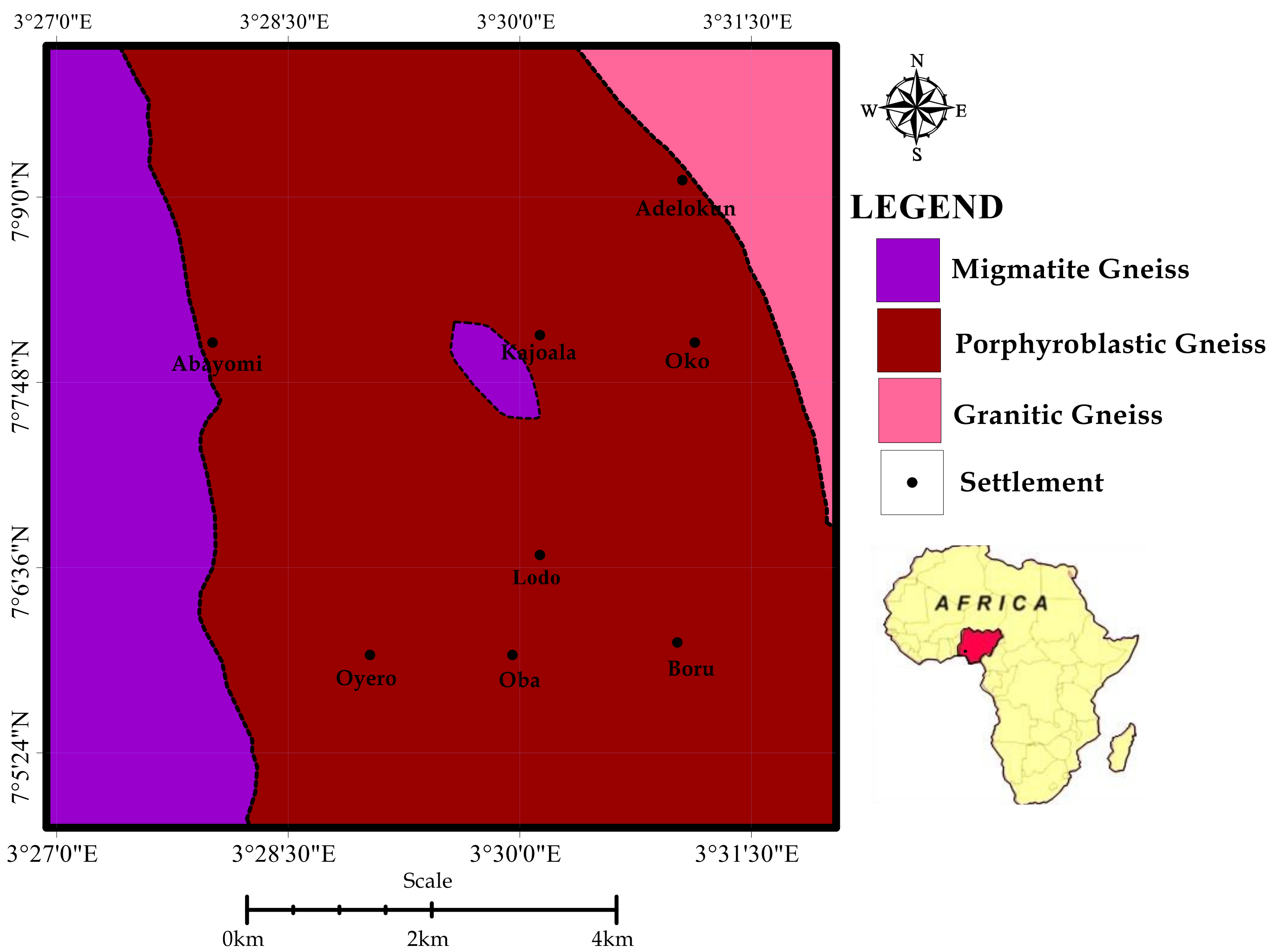

Figure 2: Geologic Map of the Study Area

Methodology

The geological mapping was preceded by an initial study of topographic maps on a scale of 1:100,000 The study area was gridded into four quadrants for easy geologic mapping which consisted of reconnaissance and detailed mapping of outcrops along streams, rivers, and road cuts. The geographic position (longitude and latitude) and elevation above the mean sea level of each outcrop were determined using Geographic Positioning System (e-Tress 20 Garmin model). The features of an outcrop that were studied and described include rock type, colour, and texture.

Mineral compositions of the rocks were determined using thin section analysis of a polished surface of the rock sample under plane-polarized and cross-polarized lights. State the results in modal composition and thin sections with magnifications).

A 2-dimensional mapping method where a rock mass was gridded into 3-meter square and the properties of all the discontinuities within the gridded portion are measured (Jing & Stephansson, 2007; Bonnet *et al.,* 2001; Yarahmadi *et al.,* 2015). Three sets of joints were measured in a specific region of the rock mass for each rock type. The frequency of the joints measurement was used in calculating the volumetric joint count (Jv) while the joints spacing were used to calculate the block volume (Vb) according to Palmstrom (2005).

Volumetric joint count;

$$Jv = \sum \text{frequencies} \quad (1)$$

Block volume;

Vb = S1 x S2 x S3 x S4 x S5 x... Sn………(2)

Where S = joint set.

This involves image processing and interpretation of remotely acquired (aeromagnetic) data using ArcGIS. This aided in mapping deep-seated discontinuities, their densities and dominant trend (Lato *et al.,* 2010; Mah *et al.,* 2011).

Investigation was conducted into the subsurface using ABEM SAS 1000 Terrameter. VES techniques employing the Schlumberger electrode configuration were used for data acquisition. It involves the injection of measured low-frequency direct current (DC) into the subsurface via a pair of current electrodes (AB) and measuring the corresponding voltage drop via another pair of potential electrodes (MN). The depth of penetration is proportional to the separation between the current electrodes inhomogeneous subsurface and varying the separation of the electrode, provides information about the stratification of the subsurface (Umar & Igwe, 2019; Umar *et al.,* 2019). Current electrode spacing (AB/2) varied from 1 to 100m, while potential electrode separation varied between 0.5 and 20m. The apparent resistivity was computed using (Umar *et al.,* 2019).

Three vertical holes were drilled using diamond core drilling on exposed rock surfaces to the depth of 20m in order to ascertain the rock's structural, textural, and colour uniformity with depth as well as its degree of fracturing and weathering by calculating the rock quality designation (RQD) expressed as a percentage (Deere, 1989; Arora, 2004). Borehole 1 was drilled on porphyroblastic gneiss, borehole 2 on granitic gneiss, and borehole 3 on migmatite gneiss.

$$\mathrm{RQD} = \frac{ength\ of\ recovered\ cores\ >\ 10cm}{total\ depth\ of\ drilled\ hole} \quad \ldots (3)$$

Geotechnical tests such as compressive shear strength (CS), water absorption ratio, density and porosity were conducted on six core samples and three surface rocks samples sizing 60 mm in dimension following the American Society for Testing Materials (ASTM, 2005) procedures. These will determine the strength and resistance of the rocks to abrasion; water retention capacity and susceptibility to weathering; void spaces and degree of compact (denseness).

Result and Discussions

Geological Analysis

Rocks in the study area are affected by high-grade regional metamorphism. From the geological mapping, a massive low laying, light coloured porphyroblastic- gneiss (Plate 1), moderately jointed and intruded by quartzo-feldspathic veins (0.6 – 1.3m) covers most part of the study area. The phenocryst which is 0.5 – 1.2cm thick and made up of k-feldspars will give a good aesthetic when polished. Other parts of the study area are covered by a compact, laminated and foliated migmatite-gneiss (Plate 2) and granitic-gneiss (Plate 3). These rocks are highly indurated, multicoloured (light/dark/grey) with quartz intrusions and a shiny appearance suitable for dimension stones.

Plate 1: Porphyroblastic gneiss

Plate 2: Migmatite Gneiss

Plate 3: Granite Gneiss

Rock Elemental Composition

Whole rock analysis using X-Ray Fluorescence was conducted on the three rock samples (Table 1). Quartz-forming elements such as silicon, aluminium and potassium constitute 75% of the rock samples. Quartz is known to be highly resistive to abrasion thereby making it suitable for use as a dimension stone. Mineralogical composition significantly influences the weathering resistance of the rock.

Table 1: Average Rock Elemental Composition

Elements	CY1	CY2	CY3
Mg	0.482	0.618	0.804
Al	1.507	2.716	3.033
Si	75.458	75.447	74.14
Na	18.416	14.321	16.498
S	< LOD	0.03	< LOD
K	1.724	2.216	2.385
Ca	0.281	0.285	0.11
Ti	0.423	0.304	0.125
V	0.027	0.01	0.008
Cr	0.003	0.01	0.007
Mn	0.212	0.01	0.009
Fe	0.540	3.932	2.815
Zn	< LOD	0.002	0.002
Rb	0.010	0.003	0.004
Sr	0.002	0.003	0.003
Zr	0.075	0.046	0.011
Nb	0.082	< LOD	< LOD
Ba	0.036	0.042	0.044
Pb	< LOD	< LOD	< LOD
Total	99.998	99.995	99.998

Thin Section Analysis

Thin section analysis was conducted on three (3) gneisses (porphyroblastic, granitic, and migmatite), samples showed that the dominant minerals are quartz, orthoclase, and plagioclase feldspars (Plates 4, 5, and 6), having modal composition ranging from 35 to 49%, 25 to 37%, and 14 to 28% respectively. Other associated minerals were biotite (5 - 20%) and hornblende (1 – 14%), with the granitic gneiss having no presence of hornblende (Plate 1). Quartz as the dominant mineral is highly resistant to weathering and abrasion and also has the ability to take polish giving dimension stone a shining appearance. Based on these, the porphyroblastic and granitic gneisses with higher content of quartz and feldspars are more suitable compared to migmatite gneiss which recorded the least amount of quartz and high biotite and hornblende contents. The suitability of a dimension stone depends on its weathering properties along with the petrology and petrophysical properties (Stuck *et al.*, 2011).

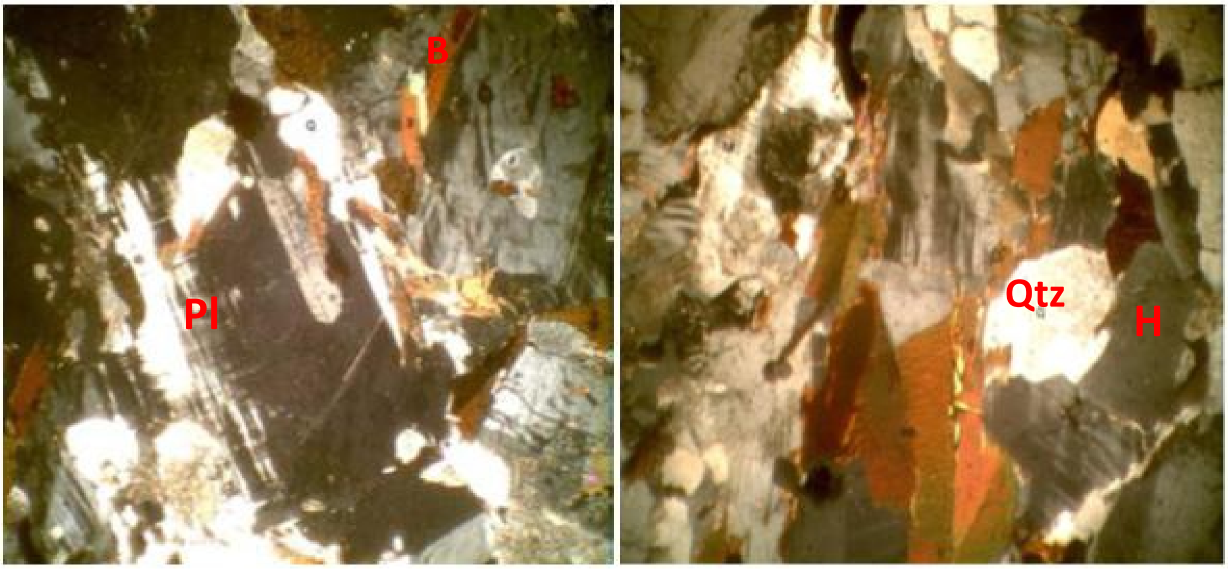

Plate 4: Photomicrographs (a) and (b) of a Porphyroblastic gneiss under cross-polarized light (PPL) showing mineral constituents; hornblende (H), quartz (Qtz), biotite (B) and plagioclase (Pl). Magnification = X 40.

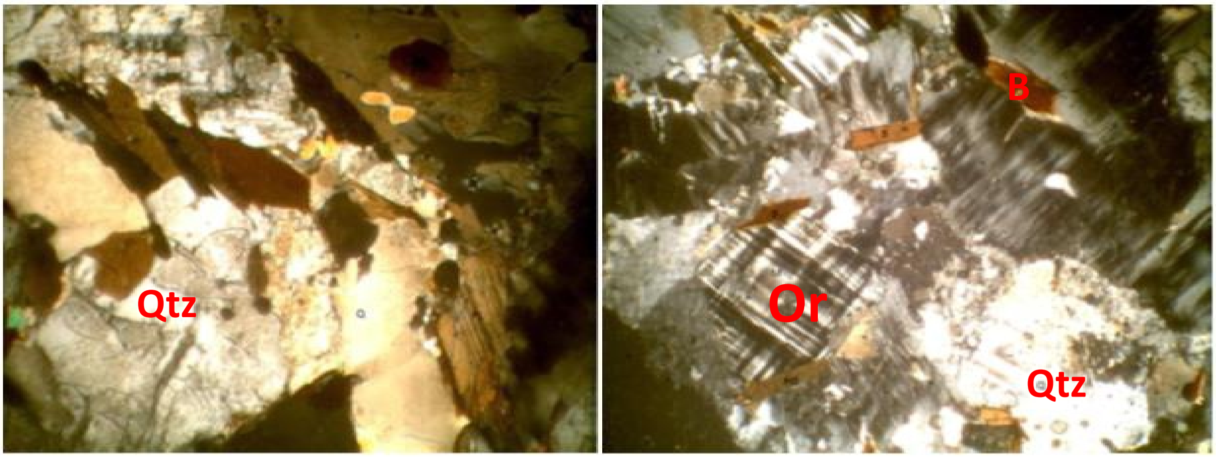

Plate 5: Photomicrograph of a Granite gneiss under cross-polarized (XPL) light showing mineral constituents quartz (Qtz), orthoclase (Or), and biotite (B). Magnification = X 40.

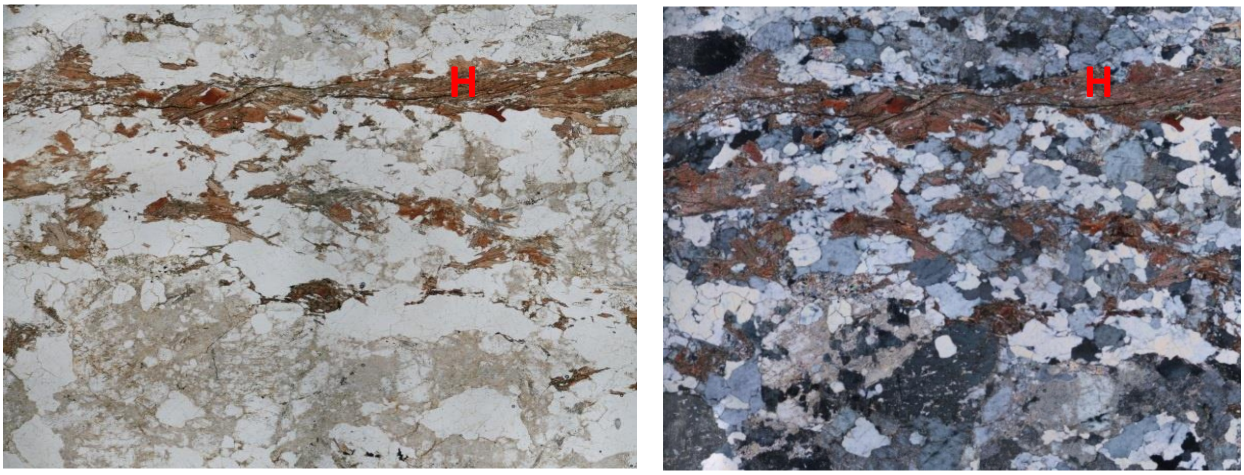

Plate 6: Photomicrographs (a) and (b) of a Migmatite gneiss under plane polarized light (PPL) showing mineral constituent hornblende (H). Magnification = X 40.

Structural Analysis

From the measurement of the discontinuities summarized in Table 3, the joints rose plot showed a dominant northeast-southwest trend (Fig. 3). These joints are moderately close (0.2 – 0.7m) to widely spaced (1.1 – 1.2m), (Arora, 2004) described this jointing system as having blocky and massive rock quality respectively. The maximum, minimum, and average volumetric joint count (Jv) ranges from 7.3-8.9; 4.9-6.2; and 6.1-7.88 respectively (Table 3), the jointing is of moderate to a high degree in migmatite gneiss while porphyroblastic and granitic gneisses exhibit a moderate degree of jointing (Palmstrom, 1985). Generally, joints are zones of weakness while the spacing between them determines the degree of weakness or strength.

It is widely accepted that spacing of joints is of great importance in appraising a rock mass structure (Bieniawski, 1973; Palmstrom, 1985). Granitic and porphyroblastic gneisses will recover moderate (0.14 and 0.15m^3) to large (1.44m^3 and 1.49m^3) block volume (Vb) respectively (Table 3), while small (0.18m^3) to moderate (0.78m^3) blocks would be recovered from migmatite gneiss (Palmstrom, 1985) due to the high degree of jointing (Table 2).

Table 2: Volumetric Joint Count (Jv) And Block Volume (Vb) Classification (Palmstrom, 1995)

Degree of jointing	Jv	Block Size	Vb
Very low	<1	Very small	10 – 200cm3
Low	1 – 3	Small	0.2 - 10dm3
Moderate	3 – 10	Moderate	10 – 200dm3
High	10 – 30	Large	0.2 – 10m3
Very high	30 – 60	Very large	>10m3
Crushed	>60		

Table 3: Calculation of Volumetric Joint Count (Jv) and Block Volume (Vb) From Sets of Joint Measurements for Porphyroblastic, Granitic and Migmatite Gneisses.

Joint Set	Minimum Spacing (m)	Maximum Spacing (m)	Average Spacing	Maximum Frequency	Minimum Frequency	Average frequency
Set 1	0.6	1.1	0.85	3.3	1.2	2.25
Set 2	0.5	1.5	0.60	3.4	2.5	2.95
Set 3	0.5	0.9	0.40	2.2	1.3	1.75
Volumetric Joint count Jv = ∑frequencies				Jv = 8.9 Max Jv	Jv = 5 Min Jv	Jv = 6.95 Ave. Jv
Block volume = Vb	0.15m^3 Min Vb	1.49m^3 Max Vb	0.204m^3 Ave. Vb			
Granitic Gneiss						
Set 1	0.7	1.2	0.95	2.0	1.6	1.80
Set 2	0.5	1.0	0.40	2.1	1.8	1.95
Set 3	0.4	1.2	0.56	3.2	1.5	2.35
Volumetric Joint count Jv = ∑frequencies				Max. Jv 7.3	Min. Jv 4.9	Ave. Jv 6.1
Block volume = Vb	Min Vb 0.14 m^3	Max Vb 1.44 m^3	Ave. Vb 0.213 m^3			
Migmatite Gneiss						
Set 1	0.2	1.4	0.8	5.0	2.5	3.3
Set 2	0.3	0.7	0.5	2.5	1.7	2.0
Set 3	0.3	0.8	0.6	3.3	2.0	2.5
Volumetric Joint count Jv = ∑frequencies				Max. Jv 10.8	Min. Jv 6.2	Ave. Jv 7.8
Block volume = Vb	Min. Vb 0.18 m^3	Max. Vb 0.78 m^3	Ave. Vb 0.24 m^3			

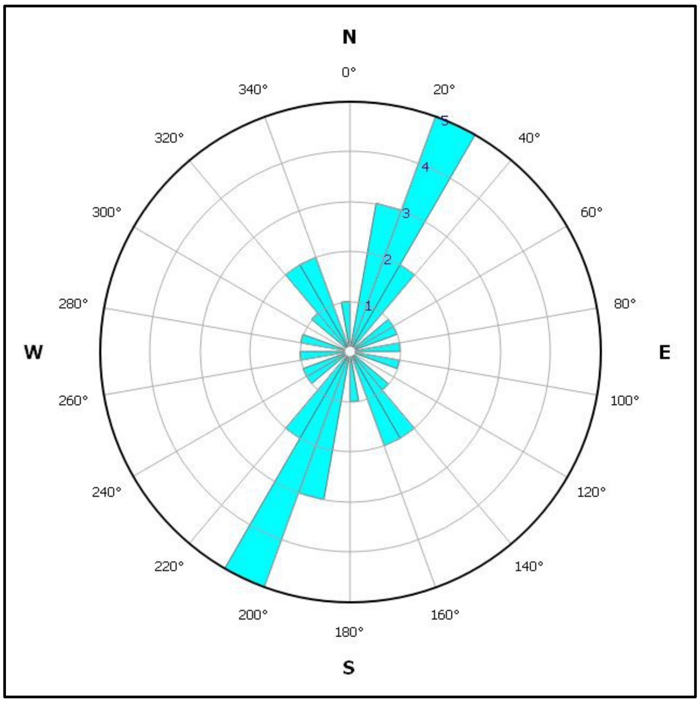

Figure 3: Structural Orientation of joints and fractures measured on the field

Remote Sensing & Geographic Information System (GIS)

Analysis of the aeromagnetic data revealed the area to be underlain by undifferentiated basement complex rocks which were later identified as porphyroblastic gneiss, migmatite gneiss, and granitic gneiss through field survey and thin section analysis. Low densities of deep-seated lineaments trending in different directions were concentrated in the area with the dominant trend being northwest-southeast (Fig. 4). These lineaments are generally short in length (0.01 – 0.3m) and serve as weak zones along which rocks can be easily extracted into blocks or slabs. However, it is noteworthy that smaller blocks are recoverable given their densities which may not be economical as dimension stone.

Geophysical survey

The VES results (Table 4) revealed thin topsoil cover (0.34 – 1.31m thick) while the weathered regolith and partly fractured layer ranges 1.04 to 6.73m and 4.24 to 33.04m respectively. Both the regolith and the fractured layers overlie the highly resistive and compact crystalline basement rock with high compressive strength and low abrasive potentials. The shallow overburden indicates a low degree of weathering, a high proportion of slabs to deleterious materials, and low cost of excavation hence, preferred for dimension stone. The ratio of overburden to bedrock is 3:22 in VES location 1, 4:21 in VES location 2, 22:78 in VES location 3 and 42:58 in VES location 5. Expectedly, these should translate into a high proportion of slabs to aggregate.

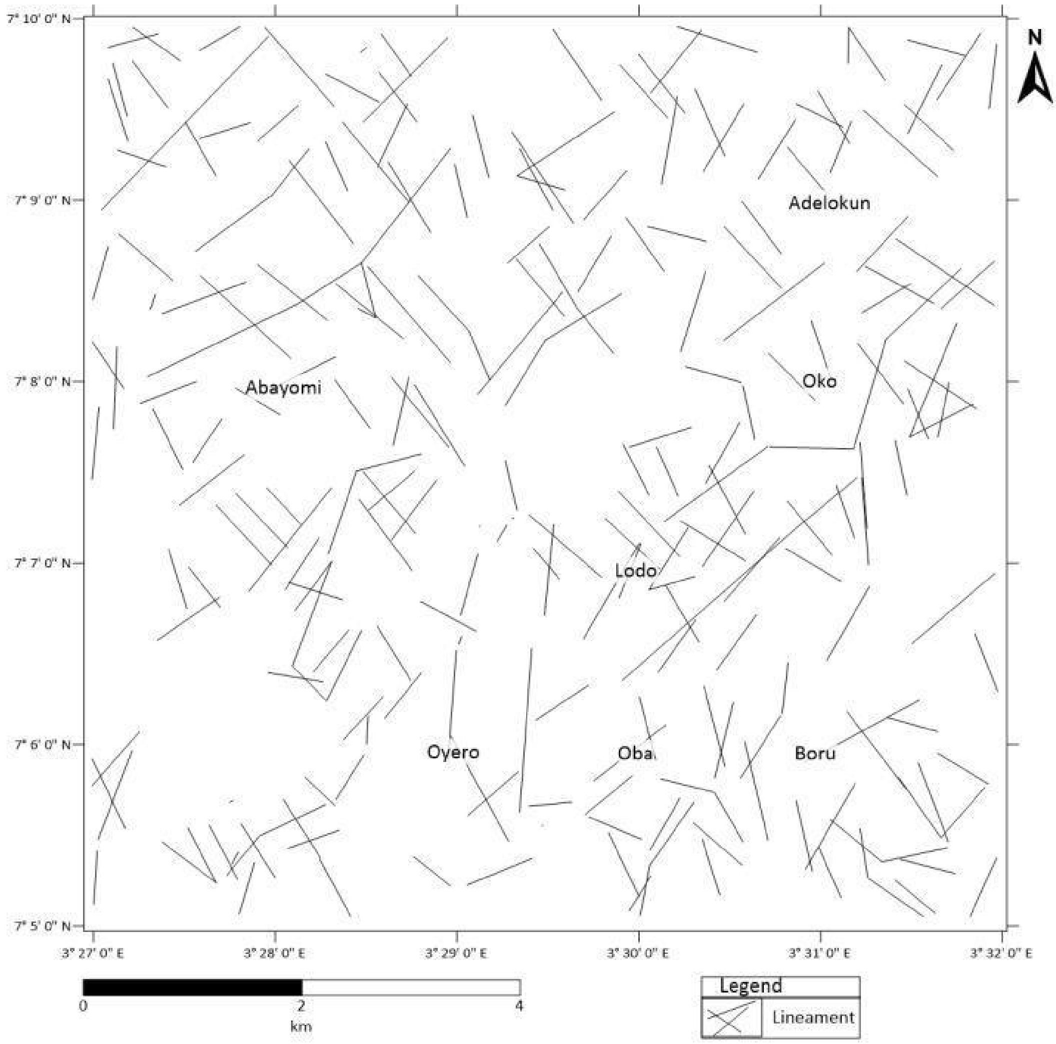

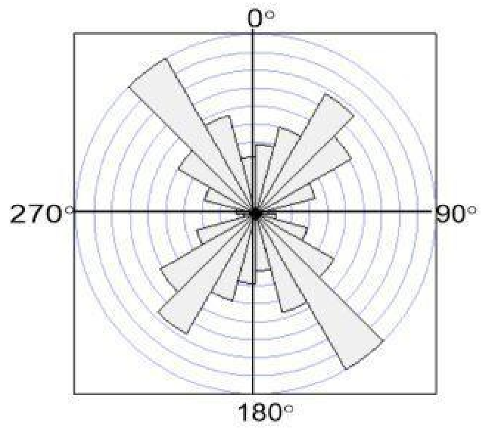

Start Angle	End Angle	Length	Number
0	15	0.101	17
15	30	0.1419	22
30	45	0.24506	34
45	60	0.18945	27
60	75	0.09332	15
75	90	0.01478	3
90	105	0.02858	5
105	120	0.06794	13
120	135	0.14911	22
135	150	0.30048	44
150	165	0.15029	25
165	180	0.08603	14

Figure 4: Structural Orientation of the Study Area

Table 4: Summary of Geophysical Survey data

VES	Resistivity (Ωm)	THICKNESS	DEPTH (m)	LITHOLOGIC DESCRIPTIONS
VES 1	936.2	0.69	0.69	Top soil
	162.1	4.03	4.73	Weathered layer
	1084	33.04	37.77	Partly Fractured basement
	76031	Infinity	Infinity	Crystalline basement
VES 2	691.4	1.02	1.02	Top soil
	312.8	3.50	4.52	Weathered layer
	802.8	20.86	25.38	Partly Fractured basement
	109810	Infinity	Infinity	Crystalline basement
VES 3	453.1	1.31	1.31	Top soil
	13.89	1.04	2.34	Weathered layer
	66.24	4.24	6.59	Fractured layer basement
	29798	Infinity	Infinity	Bed Rock
VES 4	753.3	0.34	0.34	Top soil
	1112	1.51	1.85	Partly fractured basement
	110.7	1.49	3.35	Weathered layer
	3079	Infinity	Infinity	Crystalline basement
VES 5	11047	0.44	0.44	Top soil
	283	6.73	3.99	Weathered layer
	890	7.17	26.10	Partly fractured basement
	12000	Infinity	Infinity	Crystalline basement

Geotechnical Survey

The recovered cores showed textural and colour consistency in all rock types (Figure 5). The colour variation in migmatite-gneiss and granite – gneiss is limited in extent and resulted from physical weathering and not mineral segregation. The rock quality designation (RQD) showed 65%, 64.5% and 54% for porphyroblastic gneiss, granitic gneiss, and migmatite gneiss respectively. These are rated fair (Palmstrom, 1985; Palmstrom, 2005; Arora, 2004).

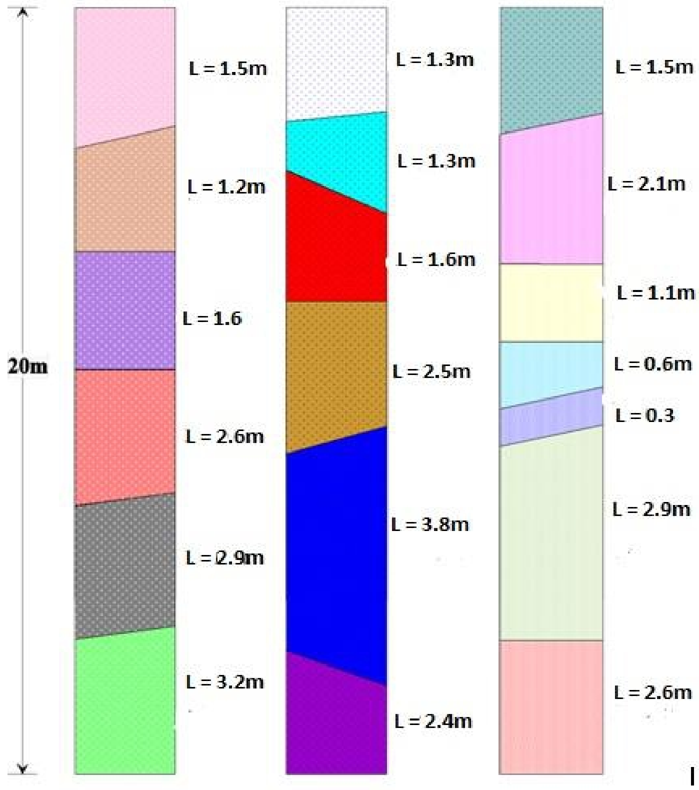

Figure 5: Drilled boreholes showing recovered cores

$$\text{Rock Quality Designation (RQD)} = \frac{\sum \text{of lengths of core pieces} > 10\text{cm in lenght}}{\text{total depth of drilled hole}} \text{x } 100 \quad \ldots (4)$$

$$\text{RQD Borehole 1} = \frac{1.5 + 1.2 + 1.6 + 2.6 + 2.9 + 3.2}{20} \text{x } 100$$

$$= 65\%$$

$$\text{RQD Borehole 2} = \frac{1.3 + 1.3 + 1.6 + 2.5 + 3.8 + 2.4}{20} \text{x } 100$$

$$= 64.5\%$$

$$\text{RQD Borehole 3} = \frac{1.5 + 2.1 + 1.1 + 0.6 + 0.3 + 2.9 + 2.6}{20} \text{x } 100$$

$$= 54\%$$

Geotechnical Test

Geotechnical test results showed that the compressive shear strength (CS) varied between 135 and 248 Mpa (Table 5) and 68 to 90 Mpa (Table 6) for cores and surface samples respectively, with the granitic gneiss recording the highest CS and migmatite gneiss having the least. These values, however, increase with depth. The CS of all samples fall within the ASTM (2005) specified limit for dimension stones. The cores exhibit a very low water absorption (WA) ratio of 0.25 – 1.05% due to low void spaces as indicated by the porosity (P) (0.35 – 0.98%) while the surface samples exhibit higher water retention (1.32 - 2.74%) with high porosity (0.64 – 1.52%). Both WA and P decrease with increasing depth indicating high durability of the rocks (Nasir *et al.,* 2015). These pore spaces are known to significantly affect the

weathering resistance of a natural stone (Ruedrich *et al.,* 2010a).
The densities range from 2.53 – 2.65g/cm^3 and 2.69 – 2.84 g/cm^3 for surface and core samples respectively and showed an increase with depth. The core sample's higher CS, lower WA, and P indicate a compact and durable rock (Nasir *et al.,* 2015), less susceptible to weathering thus, suitable for dimension stones. Although, the surface sample CS is within a limit, the high WA and high P makes it prone to weathering and abrasion thus, unsuitable for dimension stone. From these results, the surface rocks will constitute part of the deleterious materials when quarried and has further shown that surface samples alone should not be used to ascertain the suitability of rocks for dimension stone.

Table 5: Geotechnical Test Results (Core samples)

S/No	SAMPLES	CS (Mpa)	WA (%)	D (g/cm3)	ρ (%)
1	BH1	175	1.05	2.69	0.93
2	BH1	205	0.44	2.84	0.45
3	BH2	145	1.55	2.73	0.65
4	BH2	248	0.25	2.78	0.35
5	BH3	135	1.14	2.71	0.86
6	BH3	159	1.32	2.69	0.98

Table 6: Geotechnical Test Results (Surface samples)

S/No	SAMPLES	CS (Mpa)	WA (%)	D (g/cm3)	P (%)
1	SS2	71	2.59	2.62	1.32
2	SS3	68	2.66	2.65	1.22
3	SS4	90	1.86	2.65	1.52

The various parameters used in assessing the suitability of the rocks for dimension stone was assigned a rating (R) in order of importance from 1-10, and weight (W) from 1 – 5 based on its overall impact on a particular rock for use as dimension stone. The obtain the final rating for dimension stone was obtained using

$$\mathrm{R \times W} = \sum_{i=1}^{n=9} \binom{n}{k} \qquad \ldots (5)$$

Table 7: RATING OF PARAMETERS FOR DIMENSION STONE
Porphyroblastic gneiss

	Rating	Excellent 5	V.Good 4	Good 3	Fair 2	Poor 1	R x W
Rock type	10		√				40
Colour	7			√			21
Texture	2		√				8
Minerology	9			√			27
Joints	5			√			15
Weatherability	8				√		6
RQD	5			√			
Block volume	6				√		12
CS	5				√		10
Ratio of overburden to Basement	4			√			12 (151)

Granitic gneiss

	Rating	Excellent 5	V.Good 4	Good 3	Fair 2	Poor 1	R x W
Rock type	10		√				40
Colour	7			√			21
Texture	2	√					10
Minerology	9		√				36
Joints	5			√			15
Weatherability	8			√			24
RQD	5			√			15
Block volume	6			√			18
CS	5			√			15
Ratio of overburden to Basement	4		√				16 (210)

Migmatite gneiss

	Rating	Excellent 5	V.Good 4	Good 3	Fair 2	Poor 1	R x W
Rock type	10		√				40
Colour	7			√			21
Texture	2				√		4
Minerology	9			√			18
Joints	5				√		10
Weatherability	8				√		6
RQD	5				√		10
Block volume	6					√	6
CS	5				√		10
Ratio of overburden to Basement	4			√			12 (127)

5.0 Conclusion

Geological, geophysical, remote sensing and geotechnical techniques were integrated to ascertain the suitability of rocks in Owode LGA for dimension stones production. The different rock types mapped include porphyroblastic granite, granite gneiss, and migmatite gneiss characterized by low-density deep-seated lineaments and moderate to widely -spaced (0.2 - 1.2m) joints. Thin section analysis revealed the presence of quartz, orthoclase, and plagioclase feldspars in association with biotite and hornblende. Quartz as the dominant mineral is highly resistant to weathering and has the ability to take polish giving dimension stone a shining appearance. VES results revealed thin overburden (2.3 – 4.7m thick) while the partly fractured layer ranges from 4 to 20m. Both the regolith and the fractured layers overlie the highly resistive (803 - 12000 ΩM) fresh basement. The low overburden ratio to the basement implies a low cost of excavation and a low amount of deleterious materials to slabs. Based on an assessment of discontinuities such as joints and fractures, the volumetric joint count revealed a low to moderate degree of jointing dominantly trending in the NE-SW direction. Porphyroblastic and granitic gneisses have the potential to produce blocks one meter square or larger thus, suitable for dimension stone.

The geotechnical properties of the rock samples such as compressive strength, water absorption, porosity, and density meet the ASTM (2005) specification requirements for dimension stone also the RQD was rated fair for all rocks types. These indicate high durability, low susceptibility to abrasion, water retention, and weathering, making the rocks suitable for dimension stones. However, migmatite gneiss recorded the least values in all cases.

The appearance, shallow overburden thickness, and its strength will give the rock an appealing aesthetic, low cost of excavation, and high durability thus, a good rock for dimension stones. Also, integrating the ratings of the different parameters, the rock will yield a high proportion of slabs to aggregates.

References

Arora, K. R. (2004): Soil Mechanics and Foundation Engineering 6th ed. Standard

Publishers Distributors, Delhi.

Arora, K. R. (2004): Soil Mechanics and Foundation Engineering 6th ed. Standard Publishers Distributors, Delhi.

American Society for Testing and Materials ASTM (2005): Standard test methods for specific gravity of soil solids by water pycnometer. Designation D854-00, Philadelphia

Bonnet, E., Bour, O., Odling, N. E., Davy, P., Main, I., Cowie, P. and Berkowitz, B. (2001): Scaling of fracture systems in geological media. Rev Geophys 39(3):347–383.

Bieniawski, Z. T., (1973): Engineering classification of jointed rock masses. Trans. S. African Instn. Civ. Engrs., Vol 15, 12, pp. 335 - 344.

Deere, D. U. (1989): Rock quality designation (RQD) after 20 years. U.S. Army Corps Engrs. Contract Report GL-89-1. Vicksburg, MS: Waterways Experimental Station.

Jing, L. and Stephansson, O. (2007): Fundamentals of discrete element methods for rock engineering: theory and applications, vol 85. 199–232.

Nasir, S., Sankaran, R., El Ghali, M., Hosni, T., Elzebdeh, K. and Al-Rawas, G. (2015): Geotechnical Assessment of Dimension stone Resources in Oman. International Journal of Chemical, Environmental & Biological Sciences Volume 3, Issue 6.

Mah, J., Samson, C., McKinnon, S. D. (2011): 3D -laser imaging for joint orientation analysis. Int Jour Rock Mech Min Sci 48(6):932–941.

Palmstrom, A. (2005): Measurements of and correlations between block size and rock quality designation (RQD). Tunn Undergr Space Technol 20(4):362–377.

Palmstrom, A. (1985): Application of the volumetric joint count as a measure of rock mass jointing. Proceedings international symposium on fundamentals of rock joints. Bjorkliden, p 103–111.

Rahaman, M. A. O. (1989): Review of Basement Geology of SouthWestern Nigeria In: Geology of Nigeria, Kogbe C. A (ed). 2nd ed. Elizabethan Publishing, Lagos, Nigeria. 197

Ruedrich, J., Bartelsen, T., Dohrmann, R. and Siegesmund, S. (2010a): Building sandstone integrity affected by the process of hygric expansion. Environ Earth Sci.

Stuck, H., Siegesmund, S. and Rudrich, J. (2011): Weathering behaviour and construction suitability of dimension stones from the Drei Gleichen area (Thuringia, Germany). Environ Earth Sci 63:1763–1786.

Umar, N.D., Igwe, O. and Idris, I. G. (2019): Evaluation and Characterization of Groundwater of the Maastrichtian Lafia Formation, Central Benue Trough, Nigeria. Journal of Earth System Science. J. Earth Syst. Sci. (2019) 128:168.

Umar, N.D. and Igwe, O. (2019): Geo-electric method applied to groundwater protection of a granular sandstone aquifer Applied Water Science 9:112.

Yarahmadi, R., Bagherpour1, R., Sousa, L. M. O. and Taherian, S. G. (2015): How to determine the appropriate methods to identify the geometry of in situ rock blocks in dimension stones. Environ Earth Sci 74:6779–6790.

Ize and Idris (2022) Nigerian Mining Journal, (20) 34 - 38
© Nigerian Society of Mining Engineers, ISBN 1117 - 4307

Development of Interactive Database for Some Minerals in Nigeria

Ize, U.U. and Idris, M.A.

[1.] *Department of Mining Engineering, Nigerian Institute of Mining and Geosciences, Jos, Nigeria*
[2] *Department of Mining Engineering, Federal University of Technology, Akure, Nigeria*

Abstract
Nigeria is blessed with reserves of mineral resources which are distributed throughout the country. Most of these minerals remain untapped due to inadequate information in terms of location, quantities (reserves) and quality. This research was aimed at developing an interactive offline database for minerals in Nigeria, with emphasis on coal, gold, iron ore and limestone. The database was developed using JavaScript and PHP Frameworks including their estimated reserves and locations. The database would assist in the exploitation of the minerals as it contained most of the information required for investment decisions.

Keywords: Mineral resources, database, JavaScript framework, PHP Framework

1 Introduction

Mineral resources encompass a wide variety of endowments going from mineral fuels to metallic and non-metallic minerals (Butterman and Earle 2005). Some of them are found on the surface while others can only be obtained from beneath the earth through mining. Nigeria is endowed with scores of mineral resources that are widely distributed across the nation, in fact, in all the states of the federation. Some of these mineral resources are of high qualities that meet international standards (Akinrinsola and Adekeye, 1993). The mineral fuel includes coal, lignite, tars and bitumen. The metallic minerals comprise uranium, iron, tin, lead and zinc, etc. while the non-metallic minerals include gemstone, talc, asbestos, marble and limestone (Akinrinsola and Adekeye, 1993). The management of information as regards these minerals can be greatly enhanced by the use of a mineral database where access to relevant information regarding these minerals is made easy.

1.1 Technologies Description

Various computer technologies were used in the creation of the interactive database; all the programs used were the most recent versions at the time of the study.

1.2 Hypertext Markup Language (HTML)

Hypertext Markup Language (HTML) was used to develop a web page browser interactive database, Hypertext markup language is the predominant way to describe web pages for web-browsers to render and display. To publish information for global distribution, one needs a universally understood language, a kind of publishing mother tongue that all computers may potentially understand. The publishing language used by the World Wide Web is HTML.

HTML is written in the form of HTML elements consisting of tags, enclosed in angle brackets (like<html>), within the webpage content HTML tags most commonly come inpairs like<h1>and</h1>, although some tags known as empty elements are unpaired, for example<img>. The first tag in a pair is the start tag, the second tag is the end tag (they are also called opening tags and closing tags). In between these tags web designers can add text, tags, comments and other types of text-based content. The nested nature of HTML can be seen in its domain object model (DOM) tree. (DHTML Utopia: Modern Web Design Using JavaScript & DOM. 2005 Mikko (2012).

1.3 jQuery/JavaScript Framework

jQuery were designed to simplify the client-side scripting of HTML. JavaScript programs made with it are compatible with all major browsers. jQuery's syntax were designed to make it easier to navigate a document, select DOM elements, create animations, handle events, and develop Ajax applications. jQuery also provides capabilities for developers to create plug-ins on top of the JavaScript library.

This enables developers to create abstractions for low-level interaction and animation, advanced effects and high-level theme able widgets. The modular approach to the jQuery library allows the creation of powerful dynamic web pages and Web applications. Without jQuery or a similar Java Script framework, JavaScript developer would have to detect the user's browsers and their versions, keep track of the existing and new unfixed bugs in their JavaScript implementations, and make browser specific functions to work around the bugs (jQuery, 2011).

1.4 CodeIgniter Framework

CodeIgniter is an Application Development Framework for building websites using PHP. It is based on the Model-View-Controller development pattern. CodeIgniter, is loosely based on the model-view-controller architecture pattern. The major difference is that the controller acts as an intermediary between all the other resources (Figure 3). The user interacts with the view, using the HTML and JavaScript controls and functions. The view loads and saves information using the controller's functions. The controller uses the model's functions to load and save information to and from the database. (CodeIgniter 2011, MVC, 2011, MVC, 2012).

1.4.1 Model/View/Controller

The Model/View/Controller approach to programming aims to keep the logic of an application separate from the display logic, splitting the presentation aspect of an application (what the user sees in their browser) and the nuts and bolts that drive that application into three interconnected tiers:

The **Model**, which represents data structures. Classes contained within the Model tier will contain methods that interact with a database.

The **View**, which looks after presentation. A View will normally be a web page, but can also be a page fragment like a header or footer.

The **Controller**, which does most of the hard work, and is an intermediary between the Model, the View, and any other resources needed to run the application.

Separating a project in this manner means each tier does its job extremely efficiently, maintaining its relationship with other tiers yet operating within clearly defined boundaries. It also means multiple Views and Controllers can interface with the same Model, and new or different Views and Controllers can interface with a Model without forcing a change in the Model design (MVC, 2011).

1.5 PHP (*Hypertext Preprocessor*)

PHP is a general-purpose server-side scripting language originally designed for web development to produce dynamic web pages. For this purpose, PHP code is embedded into the HTML source document and interpreted by a web server with a PHP processor module, which generates the web page document. Because PHP code is executed server-side, the client will never see the code generating part or all of the HTML content of a webpage. PHP can also be used for command line scripting and writing desk top applications using PHP- GTK extension (Mikko, 2012; PHP, 2011, PHP, 2012).

1.6 Structured Query Language (SQL)

MySQL is a relational database management system (RDBMS) developed by Oracle that is based on structured query language (SQL). A database is a structured collection of data. It may be anything from a simple shopping list to a picture gallery or a place to hold the vast amounts of information in a corporate network. In particular, a relational database is a digital store collecting data and organizing it according to the relational model. In this model, tables consist of rows and columns, and relationships between data elements all follow a strict logical structure. An RDBMS is simply the set of software tools used to actually implement, manage, and query such a database.

2. Materials and Methods

2.1 Data Collection

Relevant data used include location and current reserves on important mineral sources such as coal, iron ore, gold and limestone in Nigeria, collected from Journals, Internet and Publications. Table 1 shows the records of Iron ore reserves (Ohimain, 2013).

Table 1: Iron ore reserves (Ohimain, 2013)

Locations	State	Iron content, %
Muro Hills	Nasarawa	25- 35
Dakingari	Kebbi	22- 52
Tajimi	Kaduna	22- 52
Ayaba	Kaduna	27.5
Rishi	Bauch	14 – 19
Gamawa	Bauch	40 – 45
Karfa	Borno	34 – 45
Eginija (Egenerga)	Benue	34 – 45
Oko	Anambra	34.4
Gbege	Niger	42.7
Ajase	Oyo	39.0

2.2 System Architecture

The system architecture as shown in Figure 1 is made up of three modules and they are:

- Interfaces Module
- Server-Side Module
- Database Module

The system was developed using HTML, JavaScript, PhP, Codeigniter, and MySQL. The front consist of User login and Administrator login, the user can view the Mineral resources records and their location by querying the server via the user interface. The administrator end consists of login interface to add and edit mineral resources and location.

The server side consists of Mineral Resources Engine, the Mineral Resources location engine and the system configuration web-services. The server side is directly connected to the Mineral Resources database which stores all records.

3. Results and Discussion

The Interactive Database Features and Operations

3.1 The Landing Page

This is the first page, which is displayed upon running the software on a computer and it shows all the available minerals in the database (Figure 3). This interface serves as the landing page of the software there are other links on this page which tell more about the minerals. To have access to any mineral information, the user is expected to click on the mineral to load the database record

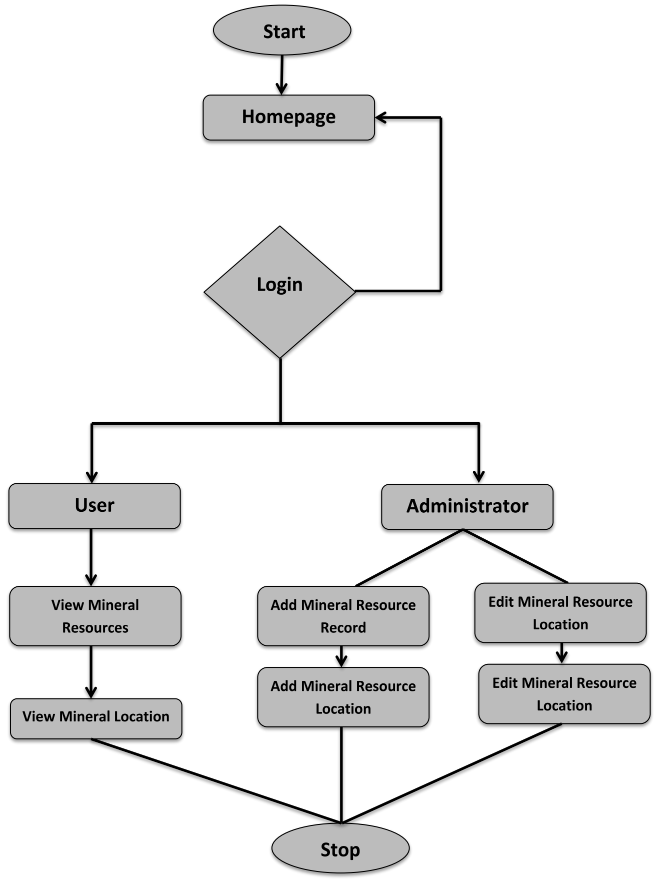

Figure 2: Mineral Database Flowchart

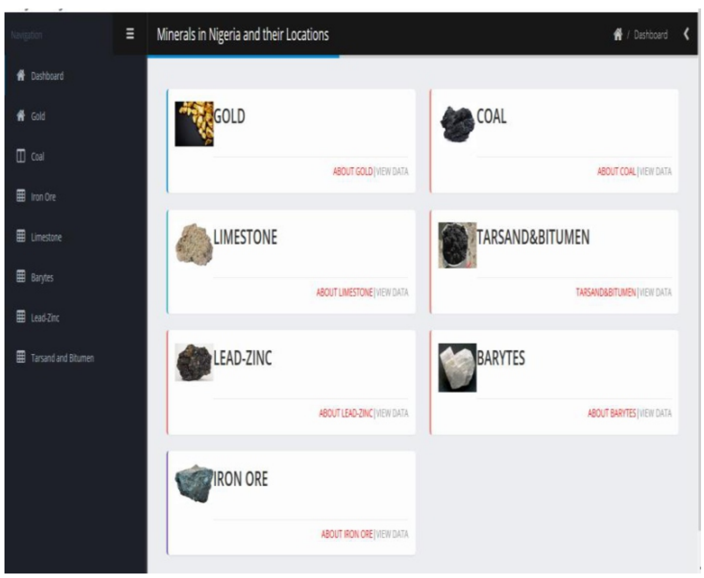

Figure 3: Landing Page for mineral database

3.2 Mineral States Interface

This interface (Figure 4) is shown upon clicking on a specific mineral on the landing page. It displays the states where the mineral can be found. This helps to streamline search query and make it easy to get the exact location of a mineral..

3.2.1 Mineral Location Page

Figure 5 shows the exact locations, estimated

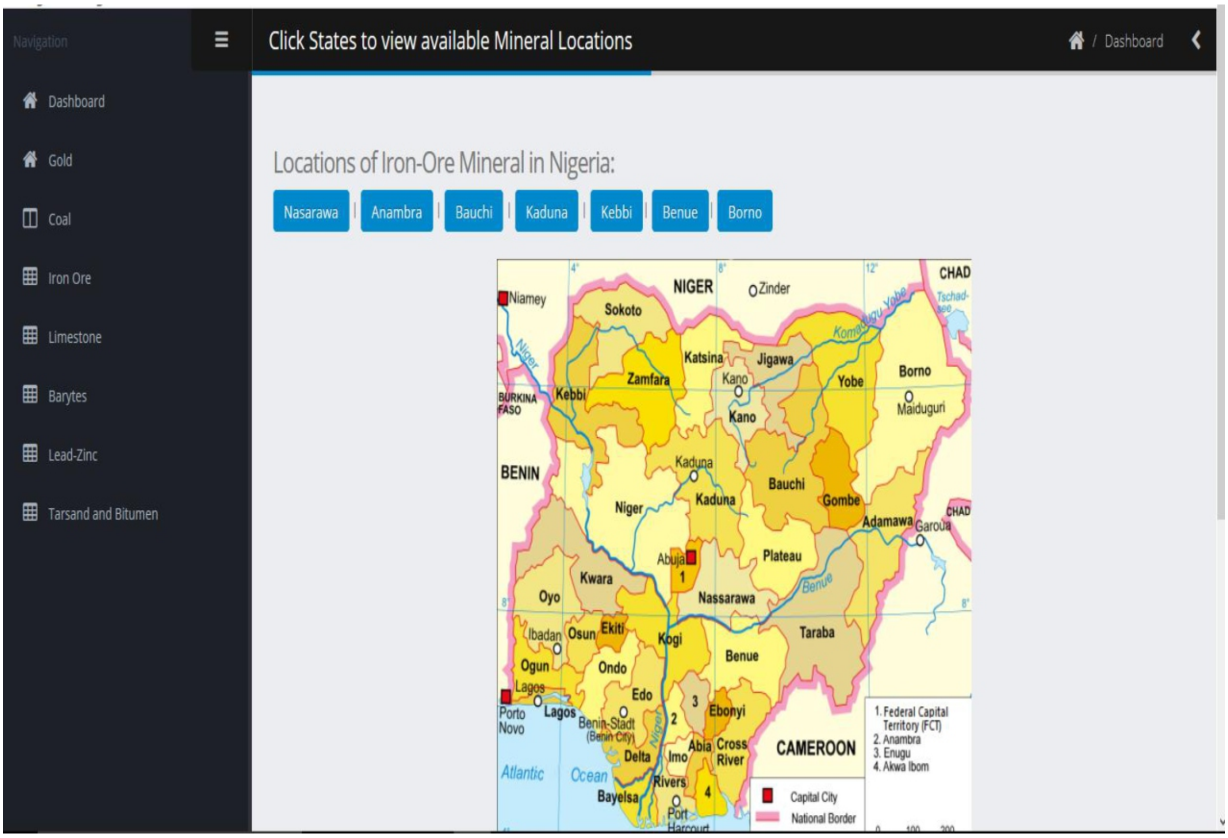

Figure 4: Mineral States Interface

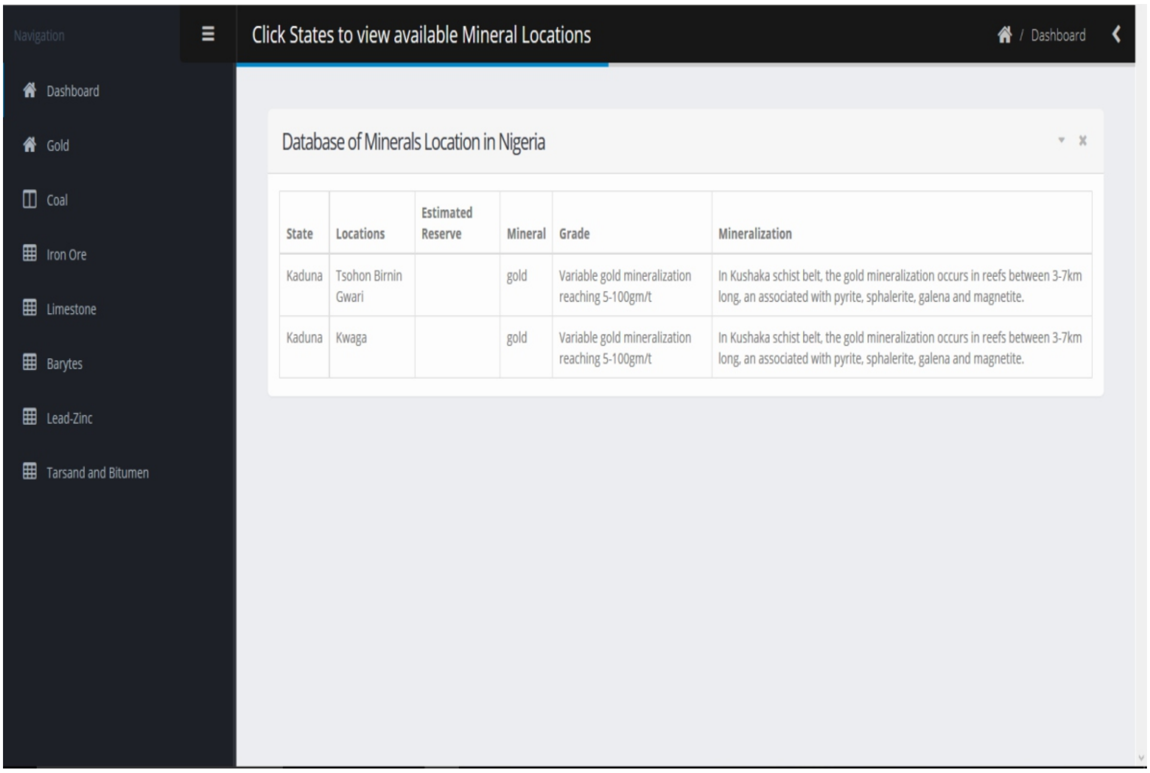

Figure 5: Mineral Location Page

reserve, grade, and mineralization of the mineral. This is shown in tabular format to display the necessary information in one glance.

4. Conclusion

Over the years one of the major reasons for setback in the Nigeria minerals development is due to inadequate information about her potential reserves. It has been demonstrated that an offline software package can be used to create an interactive data base of minerals in Nigeria. This provides a very speedy and reliable tool for quick access to information on minerals in Nigeria. A mineral data base can provide information as regards reserve estimate, location, state etc. about any mineral in Nigeria. In this study an interactive mineral data base has been created using an offline software package to enhance quick search and retrieval of information regarding reserves, states and location of minerals to its user. The vast mineral resources of Nigeria can guarantee sustainable growth and development (economically, socially and environmentally), if properly managed.

References

Akinrinsola, E.O. and Adekeye, J.I.D. (1993). A geostatisical ore reserve estimation of the Itakpe iron ore deposits Okene, Kogi State. *Journal of Mining and Geology* 29 (1): 19 – 25.

Butterman, W.C. and Earle B. A (2005). Mineral Commodity Profiles- Gold. *United States Geological Survey*.

CodeIgniter (2011). Available: http://en.wikipedia.org/wiki/Codeigniter#CodeIgniter (Access PHP. Available: http://*en.wikipedia.org/wiki/PHP*.(Accessed Mar. 2017).

jQuery (2011). Available: *http://en.wikipedia.org/wiki/Jquery*. (Accessed Mar. 2017).

Mikko, L. (2012). Event Pass Generator. Oulu University of Applied Sciences, Finland Bachelor's Thesis Degree

Model View Controller (2011). Available: *http://codeigniter.com/user_guide/overview/mvc.html.* (Accessed Mar. 2017).

Model View Controller (2012). Available:*http://codeigniter.com/wiki/MVC.*(Accessed Mar. 2017).

PHP Manual (2012). Available: http://www.php.net/manual/en/.(Accessed Mar. 2017)

Umar *et al* (2022) Nigerian Mining Journal, (20) 39 - 43

Geochemical Investigation of Gboloko Feldspar, Kwara State North-Central Nigeria for Glass Making and Ceramic Industries.

Umar, A. R.[a], Agbalajobi, S. A. and Jimoh, A.
Department of Minerals and Petroleum Resources Engineering Technology,
Institute of Technology, Kwara State Polytechnic, Ilorin.
[a] Corresponding Author email: umarhnigltd@gmail.com

Abstract
Geochemical analyses of feldspar deposit of Gboloko village of Ifelodun Local Government Area of Kwara State, North–Central, Nigeria were investigated to determine its mineralogical and chemical composition at establishing itspotential usage in glass and ceramic industries with a view to unlock and develop the mineral potential in Nigeria for sustainable economic. The feldspar sample was obtained, prepared and analyzed. The result of the mineralogical analysis using X-Ray Diffraction (XRD), indicate high content of microcline which range from 66.88-69.89 with average value of 69.58%, also, Albite range from 24.55 - 25.10 % with mean value of 24.85% and quartz lies within 5.51-6.27% with average of 5.925%, this depicted that the deposit is potassium – rich feldspar due to the high dominance of microcline/orthoclase, the Albite contents on the other hand represent the plagioclase feldspar. The chemical analysis result using X-Ray Florescence (XRF) shows the basic oxides of the samples mean values: SiO_2(67.60wt %), Al_2O_3 (17.46wt %), Fe_2O_3 (0.13wt%), CaO(0.23wt%),Na_2O(2.57wt%),K_2O(10.95wt%) and loss on ignition is 0.89 wt%. Meanwhile, the percentage chemical constituents of the samples lies within the ranges required bystandard specification for commercial glass and ceramic production. These results proved the Gboloko feldspar sample suitable for ceramic and glass industries.

Keywords: Composition, Ceramic, Chemical, Commercial, Grade, Feldspar, Mineralogical, XRD, XRF

1. Introduction

This Research intends to investigate the feldspar deposit of Gboloko village in Ifelodun Local Government Area of Kwara State, to relate its chemical and mineralogical constituents to facilitate its appropriate usage. The compositional analysis of feldspar is of primary importance, its play an important role to the behavior of the material under various condition and it is the criterion most often used in evaluating the use of feldspar. Feldspars are one of the most abundant groups of minerals in the earth crust and usually make up a large part of the rock. It is a group of closely related rock forming alumino-silicate mineral, which contain varying proportions of potassium, sodium, and calcium (Agbor and Shehu, 2013). Feldspars also tend to crystallize in igneous environments, but are present in many metamorphic rocks (Agbor and Shehu, 2013). They may also be technically defined as alumino-silicates of sodium, potassium, calcium and barium; most commonly, the feldspars are considered as solid solutions of the three limiting compounds; $NaAlSi_3O_8$, $KAlSi_3O_8$ and $CaAl_2Si_3O_8$, which are respectively known as soda feldspar (Albite), potash feldspar (orthoclase) and lime feldspar (Anorthite). Natural deposits of feldspar are generally solid solutions of either the soda and potash feldspars or the soda and lime feldspar (Agbalajobi, *et al.*, 2015).

Feldspar is usually white or nearly white, though they may be clear or light shades of orange or buff they usually have glassy luster. (Agbor and Shehu 2013). Feldspar is most essential raw material mostly for glass and ceramic industries. In the production of glass, feldspar provides alumina, which improves hardness durability and ability of glass to resist chemical corrosion. In the ceramic bodies and glazes as a flux feldspar lowers the vitrifying temperature of a ceramic body during firing, forms a glassy phase in the body (Kauffman and Dyke, 1994).

Feldspar plays a significant role as fluxing agent with formation of liquid during firing but when cooled the liquid forms glaze and brings the grains of clay and silica together. It has also been considered a main constituent in most porcelain and other white bodies (Nelson, 1999). The qualitative assessment prior to industrial application is required in order to reduce the prevalence of substandard products in the nation.

1.1. Study Area

The study area is located in Gboloko in Ifelodun Local Government Area of Kwara State, North central, Nigeria. It lies between longitude 04^{0} 54^{I} 96^{II}E and latitude 08^{0} 31^{I} 76^{II} N. The area is situated on the undifferentiated Precambrian basement complex of igneous and metamorphic origin. Some of these rocks include the migmatite, granites and gneiss. Figure 1 shows the map indicating the location of the study area.

2. Materials and Methods

2.1. Sample Collection and Preparation

Four feldspar samples of 800g were collected at four points at 20m apart from Gboloko deposit, the samples were thoroughly dried in an oven at 31^{0}C for 12 hrs. The dried samples were crushed and ground respectively to powder using jaw crusher and ball mill. The samples were thoroughly mixed and passed through the sieve size 6.3 micronsrespectively in accordance to Wills and Napler (2006), these were carried out at the Department of Minerals and Petroleum Resources Engineering Technology, Kwara State Polytechnic, Ilorin.

2.2. Laboratory Analyses of Gboloko Feldspar Samples.

The chemical analysis and mineralogical analysis were carried out at the Department of Geology Laboratory, Afe Babalola

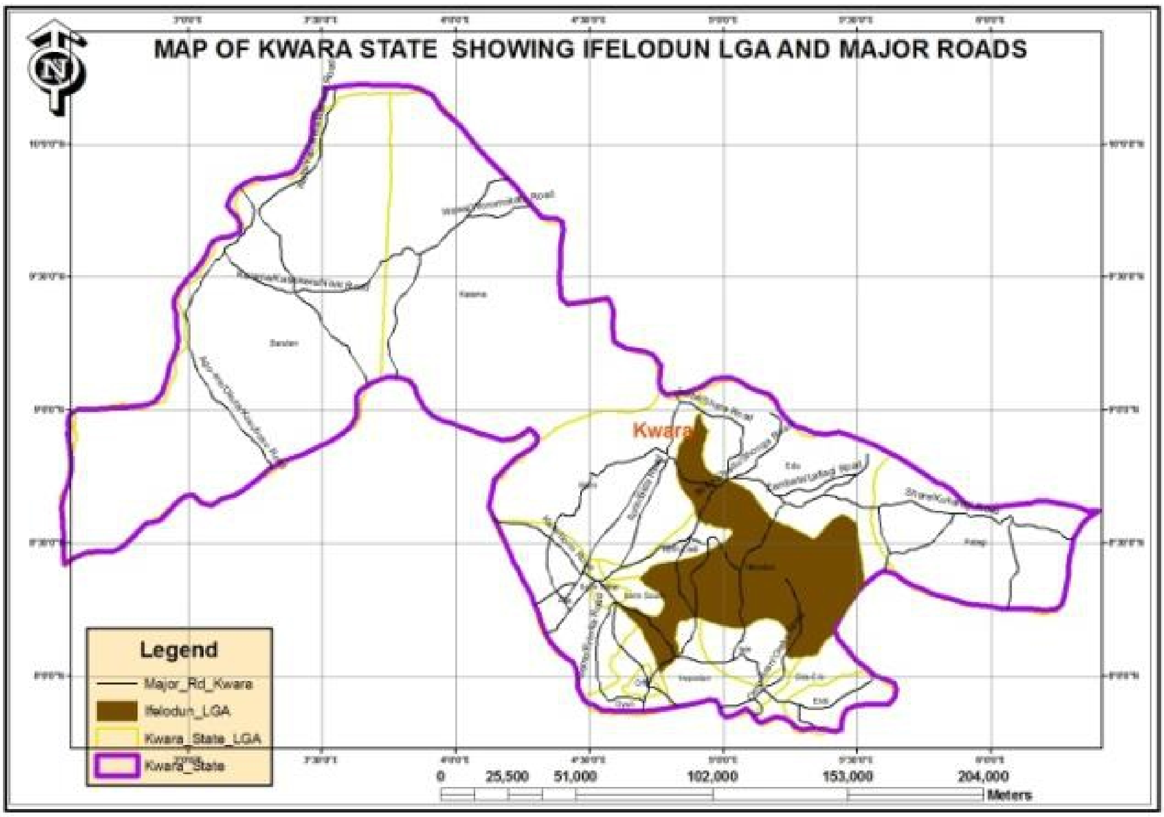

Figure 1: Map Showing the Location of the Deposit (Agbalajobi *et al.,* 2015).

University, Ado-Ekiti, Ekiti State. The results obtained were compared with the standard specifications.

2.3. Chemical Analysis

Energy dispersive X-ray fluorescence (EDXRF) spectrometer of model "mini pal 4" was used for the chemical analyses of the Gboloko feldspar samples.

Each sample was first dried to avoid moisture content; 20g each of the dried samples were weighed into a sample cup. The current used was 14KV for major oxides, 20KV for the trace elements/rare earth metals. Selected filters were "Kapton" for major oxides, Ag/Al-thin for the trace element/rare earth metals. LOI were determined gravimetrically by heating 1g of the powdered samples each in a cleaned weighed crucible at 100^0C.

Table 1: Results of Gboloko Sample (%)

S/N	Basic oxide (%)	Sample 1	Sample 2	Sample 3	Sample 4	Average
1	SiO_2	66.86	68.30	67.80	66.95	67.50
2	Al_2O_3	16.85	18.60	16.68	17.55	17.42
3	Fe_2O_3	0.15	0.10	0.14	0.12	0.13
4	CaO	0.31	0.24	0.15	0.20	0.23
5	MgO	0.03	0.04	0.02	0.05	0.04
6	Na_2O	2.66	2.60	2.41	2.55	2.57
7	K_2O	9.72	11.67	10.63	11.72	10.95
8	SO_3	0.04	0.02	0.02	0.05	0.03
9	MnO	0.04	0.05	0.03	0.06	0.05
10	Pb_2O_5	0.03	0.01	0.02	0.01	0.02
11	LOI	0.78	0.89	0.98	0.88	0.89

2.4. Mineralogical Analysis

X-ray diffraction was used for the identification of percentage mineral compositions of Gboloko feldspar samples. The prepared sampleseach were analyzed using X-ray diffraction spectrometer (2400H X-ray diffractometer equipped with a miniflex 2+goniometer and detector). This worked by the combination of other components like the water chiller which cooled X-ray tube and maintained a uniform temperature. Compressed air also helped in opening and closing of the cabinet door. The prepared samples each using prepared blocks were compressed into flat samples that were later mounted on the sample stage in the XRD cabinet respectively. The sampleswereanalyzed using the emission transmission spinner stage with the theta-theta settings. The intensity of diffracted X-ray was continuously recorded as the sample and detector rotated through their respective angles.

3. Results and Discussion

3.1. Chemical Analysis

The X-ray fluorescence results is shown in Table 1 with their percentage weight composition.

From the above results of the chemical analysis of the Gboloko feldspar samples investigated, the deposit can be classified as potash feldspar (k-feldspar) since the mean percentage of K_2O (10.95wt %) in the samples is higher than that of mean % of Na_2O (2.57 wt %) and CaO (0.23 wt%), respectively, meanwhile the average percentage of (K_2O) is satisfactory for industrial grade glass and ceramic production and this constitute the fluxing property of feldspar according to the literatures. The mean % composition of SiO_2

(67.60wt %) and Al_2O_3 (17. 46 wt %) lies within the required amount in commercial grade glass and ceramic production according to the (BIS, 2007), also, low iron contents (Fe_2O_3) which felt within the acceptable range for commercial ceramic and glass grade production, because, high percentage of iron content affects the quality of the final product and contribute in unwanted variation of color toward gray rather than white. The maximum iron content must not be more than 0.3 wt % as established by (Mazen and Mohamad, 2014)or, not more than 0.5 wt % as classified by (BIS, 2007).

3.2. Mineralogy Analysis Result

The results of percentage minerals composition of Gboloko feldspar samples were given in Table 2.

Table 2: Mineralogical Composition of Gboloko Feldspar Sample

S/No	Mineral composition	Sample 1 (%)	Sample 2 (%)	Sample 3 (%)	Sample 4 (%)	Mean value (%)
1	**Microcline/ orthoclase**	68.88	69.75	69.65	69.89	69.58
2	**Albite**	25.10	24.94	24.55	24.75	24.84
3	**Quartz**	5.90	5.51	6.24	6.01	5.92

The summary of the quantitative XRD analysis results were presented in Table 2. The above results revealed the predominant of microcline at highest weight composition of average value of 69.58wt%, this implies that the deposit is potassium – rich alkali feldspar which formed during slow cooling of orthoclase. The Albite on the other hand represents a plagioclase feldspar with mean value of 24.85 wt%, However, the quartz content is relatively low but constitute a significant amount for silica sand in the feldspar sample based on (Hassan, 2016) citation.

3. Comparisons between the Gboloko Feldspar sample with the Bureau of Indian Standard (BIS, 2007).

The main ingredient affecting the ceramic and glass processing and the product quality are K_2O, Na_2O, Al_2O_3, SiO_3 and Fe_2O_3 contents in the sample as described by (Mazen and Mohammad, 2007). Basically, the two properties which make the feldspar useful for downstream industries are their alkali and alumina content. Therefore, comparing the results of the raw feldspar samples of Gboloko with the Bureau of India Standard (BIS) requirement for different grades as given in the Table 3, indicate that the Gboloko feldspar deposit chemical compositions lie within the ranges to the Bureau of India standard requirements, which make it satisfactory as raw material for ceramic and glass industries.

Grade 1 - potash feldspar suitable for glass industry

Grade 2 - potash feldspar suitable for white ware industry

Grade 3- potash feldspar suitable for pottery industry and other than white ware.

Grade 4 - potash feldspar suitable for soda feldspar (BIS, 2007).

4. Conclusions

Conclusively from the result of mineralogical analysis of Gboloko feldspar samples indicated that the deposit felt between Microcline/orthoclaseand Albite/plagioclase feldspar with predominant of Microcline feldspar, and chemical analysis results obtained shows the deposit suitability as raw material in the glass and ceramic industries.

References

Agbalajobi, S.A., Bello, W.A. and Obaro, R. (2015): Characterization of Egbe Feldspar for raw material in Ceramic Industries;

Table 3: Bureau of Indian standard Requirement of Feldspar for Glass and Ceramics industry

S/No	Basic oxide (%)	Grade 1	Grade 2	Grade 3	Grade 4
1	LOI	0.6	0.6	0.8	1.0
2	SiO_2.	67	67	68	68
3	Al_2O_3	17.20	17.21	17.21	19.22
4	Fe_2O_3	0.20	0.35	0.5	0.20
5	(CaO+ MgO)	0.75	1.0	1.0	4.5
6	K_2O	4.0	4.0	6.0	3.0
7	**Na_2O**	**-**	**-**	**-**	**8.0**

Book of Proceedings of Tin city 2015 Annual General Meeting/ International Conference of Nigeria Society of Mining Engineers, pp.59-64, ISSN 1117 – 4307.

Agbor, A.T and Shehu, O.U. (2013): Geology and Economic Evaluation of Odobola, Ogodo Feldspar Mineral Deposit, Ajaokuta Local Government Area, KOGI state, *Nigeria Earth Science Research*; vol. 2, No.1; ISSN 1927 – 0542 E-ISSN 1927 – 0550

Bureau of Indian Standards (BIS, 2007): Potash Feldspar and Soda Feldspar for Glass and Ceramic Industry-Specification, First Revision, IS 9749.

Hassan, U.J. (2016): Structural Analysis and Surface Morphology of Quartz, .*Bayero Journal of Pure and Applied Sciences* 9 (2): 230 -233, ISSN 2006-6996.

Kauffman R.A and Van Dyke D. (1994): Industrial Minerals Rocks Handbook 6th Edition. P.248

Mazen Amaireh, and Mohammad Aljaradin (2014): Characterization of the Jordanian Feldspar as raw materials for application in the Ceramic and Glass Industries, *International Journal of Mining Engineering and Mineral Processing,* 3(2): 28-31 DOI: 10:5923/J Mining 20140302.02.

Nelson C.G. (1999): Ceramic–A potter's Handbook – Holt Hex Hat wisdom, New York.

Wills B.A. and Napler –Munn, T.J. (2006): Wills Mineral Processing Technology. Introduction to the practical aspect of ore treatment and mineral recovery, (Seventh Edition). Elsevier Science and Technology Books, pp. 225-267.

Assessing Wheel Loader-Truck Productivities in Opencast Operation: A Case of Dangote Coal Mines, Effeche-Akpali, Benue State, Nigeria.

Salati L. K. and Idris I.
Department of Mineral and Petroleum Resources Engineering, Kaduna Polytechnic, Kaduna, Nigeria

Abstract
Wheel loaders are deployed as primary loading machines in surface mines due to their mobility and low operating cost. A study was conducted to assess the productivities of wheel loader-truck at Effeche-Akpali site of Dangote Coal Mine in Benue State. Data collection in this study was done through the review of related literatures, personal interview, field studies and observations. Field values for maneuvering, loading, hauling, dumping, and return time of dump trucks are recorded. From the results of the study, the total cycle time/shift for the Komat'su dump trucks is found to be as follows: RD-01, 46.50 minutes, RD-04, 50.55 minutes, RD-05, 46.58 minutes, RD-22, 46.90 minutes, RD-27, 48.19 minutes, and RD-28, 46.50 minutes respectively. The production per annum for each dump truck was found to be 2,968,560.00 tonnes, 3,227,112.00 tonnes, 2,973,667.20 tonnes, 2,994,096.00 tonnes, 3,076,449.6 tonnes and 2,968,560.00 tonnes respectively. Hence, the wheel loader-truck productivities in the company are considered high and effective. It was recommended that a continuous fleet maintenance be given top priority to minimize equipment downfalls, production disruptions and other avoidable problems. It was also suggested that the number of fleet should be maintained especially the dumpers, to reach the company's production projection.

Keywords: Wheel loaders, trucks, load-haul-dump, productivities, cycle time.

1. Introduction

Materials transportation in an opencast operation requires the engagement of trucks shunting between loaders located in different loading and dumping points. The productivity of fully loaded (full haul) and empty (empty haul) trucks to and from their loading and hauling locations can be determined by loading location, shift availability and loader-truck match. Evaluating the loading and haulage units cost for any given opencast operation is generally dependent on factors such as the best choice of shovel and truck types for the mine conditions, a corresponding choice of optimal grade for the given truck and adequate selection of correct truck fleet size economic range (Nguyen *et al.,* 2014). According to Pasch and Uludag (2018), the load-haul cycle time is defined as the total time to complete a cycle. The critical cycle stages comprise spotting at loading, loading time, hauling-full time, travel empty time and queuing time. Hence, effectively managing these cycle steps optimizes the load-haul opencast operation leading to higher loader-truck productivity.

Fig. 1 Schematic of Haulage in Surface Mines

Dey *et al.* (2018) have mathematically defined the actual cycle time of a dump truck in a typical opencwhere,

$$T = t_{te} + t_{wl} + t_{wd} + t_{md} + t_j + t_d \; ...(1)$$

T is Total cycle time;
t_d is Time for dumping;
t_{te} is Travel time of empty dumper;

t_{wl} is Waiting time of dumper at loading point;
t_{ml} is Maneuver time near shovel for loading;
t_{wd} is Waiting time of dumper at dump point;
t_{md} is Maneuver time at unloading point;
t_l is Loading time;
t_{tl} is Travel time of loaded dumper ast operation as expressed in Equation 1.

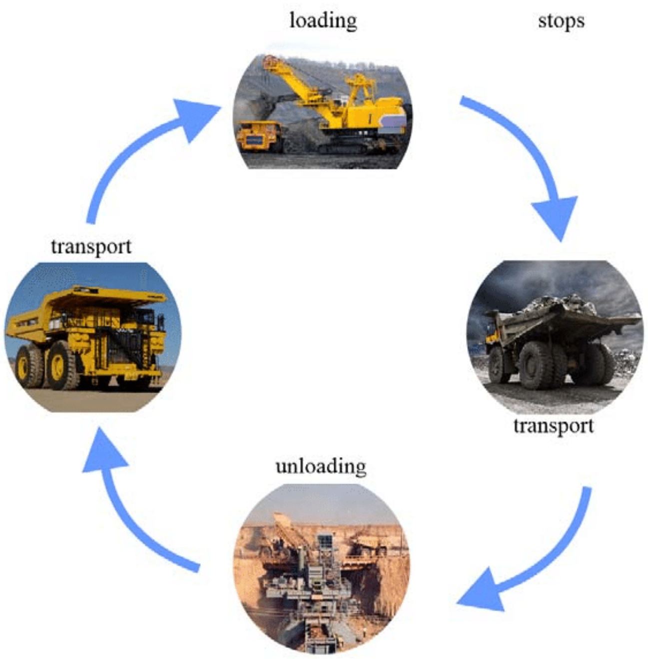

Fig. 2 Truck Cycle in Surface Mining Operation

As a major aspect of opencast operation, haulage is responsible for materials handing within the mine. Adams and Bansah (2016) have described materials handing as involving loading and transporting of blasted materials in the pits from where they are mined to the point of processing with the aid of haulage equipment. Delays and break downs in haulage are traced to unplanned and inadequate fleet operation; however, improving truck-shovel match and allocation, effectively scheduling shift operation and appropriately designing haul roads would eliminate such delays and significantly improve haulage fleet productivity (Nel *et al.*, 2011). In the event of a downtime, scheduled or unscheduled, it is also significantly important for the technical support department to put in adequate plans for prompt maintenance of the machine towards returning it to its reliable state as quickly as possible (Achelpohl, 2018).

Ercelebi and Bascetin (2009) have shown how the optimization of shovel-truck system in surface mining requires careful determination of production over a given time period of interest (typically one shift) which can be calculated by the number of loads that trucks take to the dump:

$$Production = \frac{\text{time period of interes}}{\text{average cycle time}} \times \text{N} \times \text{Truck capacity} \quad (2)$$

Where N is the number of trucks in the system.

Production can also be estimated from:

$$\text{Production} = \text{time period of interest} \times \eta\text{shovel} \times \mu\text{shovel} \times \text{truck capacity} \ldots (3)$$

ŋshovel is shovel utilization and µshovel is shovel loading rate.

Considering all the already highlighted variables for the optimization of load-haul production, therefore, this research seeks assess wheel-loader productivities in opencast operation at Dangote Coal Mine Limited at Efeche-Akpali Site, Benue State. This is with a view to determining the effectiveness of wheel-loader productivities in the mine in spite of occasional occurrences of breakdowns, delay and other operational bottlenecks.

1. Materials and Methods Used

Dangote coal mine is located in Effeche/Akpali community, Okpokwu local government area of Benue State, North-central Nigeria. The study area is on Latitude 7°03'27.60" N and Longitude 8°12'21.60" E. The mining area is 64.5 hectares and can be accessed through Idoba - Otukpa road along Enugu - Otukpo express – way. The 6 km access road was constructed by Dangote coal mine from Idoba to Effeche mining area in 2021. Figure 3 shows the map of Benue showing Okpokwu local government area, while figure 4 shows the Dangote coal mine offices situated within Effeche-Akpali community in Okpokwu.

Fig. 3 Map of Benue State showing the Study Area

Fig. 4 Dangote Coal Mine Offices in the Study Area

was recorded as quickly as the dump truck offloaded before moving, and as quickly as it arrived to the loading point, it was referred to as the return time. The stockpile is about one (1km) kilometer away from the loading point. This completes the cycle, which was repeated several times for another 100t dump truck and six other dump trucks of the same bucket capacity.

2. Results and Discussion

Results from Tables 1 to 6 on the cycle time of Komat'su dump trucks of different capacities used in the study are have shown that, based on the working hours of Dangote Coal Mine Limited, the wheel loader-truck productivity is found to be effective and high. From the Tables, the total cycle time/shift for the Komat'su dump trucks is found to be 46.50 minutes, 50.55 minutes, 46.58 minutes, 46.90 minutes, 48.19 minutes and 46.50 minutes for RD-01, RD-04, RD-05, RD-22, RD-27 and RD-28 respectively. Equivalently, the production per annum for each dump truck was also found to be 2,968,560.00 tonnes, 3,227,112.00 tonnes, 2,973,667.20 tonnes, 2,994,096.00 tonnes, 3,076,449.6 tonnes and 2,968,560.00 tonnes respectively.

Figures 1 to 8, from the analysis of daily, weekly, monthly and annual productivities of the company's dump trucks, have shown differing rate of production for each of the dump truck. With actual production target of coal per day of 5000 tonnes, the company's working regime is run in two shifts per day in which a shift is expected to extract 2500 tonnes of coal, while nine (9) hours per shift has been identified as the working hours of the company. The different productivities recorded by each of the trucks have also been found to be traced to operator's experience, matching of loading equipment and truck and loading and cycle time as suggested by Cheng (2019), Elevli and Elevli (2010) and Dembetembe and Mutambo (2018). Therefore, Komat'su RD-01 has a production rate of 8835.00 tonnes/day, RD-04, 9604.50tonnes/day, RD-05, 8850.20 tonnes/day, RD-22, 8911.00 tonnes/day, RD-27, 9156.10 tonnes/day, and RD-28, 8835.00 tonnes/day. Hence, from Figures 1 to 8, it is indicated that the dump trucks have been able to meet the set production target of the company. Tables 1 to 6 show the cycle time analysis of different Komat'su dump trucks in Dangote Coal Mine Limited, Efeche-Akpali Site, Benue State.

Table 1: The Cycle Time of Dump Truck Komat'su RD-01 of 100t Capacity

No of trips	No of passes	Wait time (Min)	Maneuver (spot) time (Min)	Load time (Min)	Haul time (Min)	Dump time (Min)	Return time (Min)
1	4	0.34	0.25	1.59	4.04	0.26	3.20
2	4	0.23	0.35	2.45	3.45	0.27	3.37
3	4	1.01	0.26	3.02	3.56	0.30	4.01
4	4	0.00	0.34	2.00	3.39	0.24	3.45
5	4	0.59	0.28	2.27	3.59	0.26	3.34
6	4	0.00	0.21	2.50	4.01	0.29	3.40
7	4	0.51	0.45	3.00	3.34	0.24	3.43
Total time	**28**	**2.68**	**2.14**	**16.83**	**25.38**	**1.86**	**24.20**
Average time	**4**	**0.38**	**0.31**	**2.40**	**3.63**	**0.27**	**3.46**

Table 2: The Cycle Time of Dump Truck Komat'su RD-04 of 100t Capacity

No of trips	No of passes	Wait time (Min)	Maneuver (spot) time (Min)	Load time (Min)	Haul time (Min)	Dump time (Min)	Return time (Min)
1	4	0.25	0.24	2.50	3.02	0.20	3.19
2	4	0.26	0.30	2.44	2.37	0.17	3.43
3	4	0.00	0.23	3.48	3.00	0.27	2.59
4	4	0.04	0.31	2.59	3.56	0.22	3.03
5	4	0.22	0.27	2.35	3.52	0.26	3.15
6	4	0.00	0.20	3.07	4.01	0.22	2.49
7	4	0.35	0.38	3.01	3.30	0.28	2.56
Total time	**28**	**1.12**	**1.93**	**19.44**	**22.78**	**1.62**	**20.44**
Average time	**4**	**0.16**	**0.28**	**2.78**	**3.25**	**0.23**	**2.92**

Table 3: The Cycle Time of Dump Truck Komat'su RD-05 of 100t Capacity

No of trips	No of passes	Wait time (Min)	Maneuver (spot) time (Min)	Load time (Min)	Haul time (Min)	Dump time (Min)	Return time (Min)
1	4	0.32	0.17	2.51	4.12	0.15	3.43
2	4	0.07	0.22	3.44	3.57	0.21	3.55
3	4	0.19	0.14	3.42	3.02	0.17	3.24
4	4	0.29	0.30	3.13	3.34	0.20	2.52
5	4	0.02	0.25	3.55	3.18	0.19	3.21
6	4	0.10	0.19	3.28	4.09	0.24	2.57
7	4	0.05	0.31	3.53	3.24	0.25	3.01
Total time	**28**	**1.04**	**1.58**	**22.86**	**24.56**	**1.41**	**21.53**
Average time	**4**	**0.15**	**0.23**	**3.27**	**3.51**	**0.20**	**3.08**

Table 4: The Cycle Time of Dump Truck Komat'su RD-22 of 100t Capacity

No of trips	No of passes	Wait time (Min)	Maneuver (spot) time (Min)	Load time (Min)	Haul time (Min)	Dump time (Min)	Return time (Min)
1	4	1.00	0.16	2.00	3.02	0.26	3.10
2	4	0.17	0.26	3.01	3.44	0.29	3.45
3	4	0.10	0.20	3.33	3.23	0.16	3.22
4	4	0.19	0.32	3.44	3.29	0.32	3.05
5	4	0.24	0.31	3.57	3.55	0.28	2.53
6	4	0.08	0.25	3.24	3.31	0.25	3.59
7	4	0.00	0.27	3.27	3.20	0.31	3.31
Total time	**28**	**1.78**	**1.77**	**21.86**	**23.04**	**1.87**	**22.25**
Average time	**4**	**0.25**	**0.25**	**3.12**	**3.29**	**0.27**	**3.18**

Table 5: The Cycle Time of Dump Truck Komat'su RD-27 of 100t Capacity

No of trips	No of passes	Wait time (Min)	Maneuver (spot) time (Min)	Load time (Min)	Haul time (Min)	Dump time (Min)	Return time (Min)
1	4	0.07	0.37	2.48	3.02	0.21	3.22
2	4	0.21	0.31	2.56	3.55	0.19	3.00
3	4	0.00	0.29	3.01	3.44	0.27	3.40
4	4	0.05	0.20	2.58	3.21	0.23	3.34
5	4	0.26	0.27	2.57	4.06	0.22	3.58
6	4	0.19	0.22	3.05	3.54	0.16	3.46
7	4	0.00	0.36	3.00	3.09	0.33	3.06
Total time	**28**	**0.78**	**2.02**	**19.25**	**23.91**	**1.61**	**23.06**
Average time	**4**	**0.11**	**0.29**	**2.75**	**3.42**	**0.23**	**3.29**

Table 6: The Cycle Time of Dump Truck Komat'su RD-28 of 100t Capacity

No of trips	No of passes	Wait time (Min)	Maneuver (spot) time (Min)	Load time (Min)	Haul time (Min)	Dump time (Min)	Return time (Min)
1	4	0.26	0.21	2.48	4.05	0.24	3.53
2	4	0.13	0.25	3.04	3.56	0.26	3.50
3	4	0.19	0.31	3.34	4.00	0.25	3.44
4	4	0.00	0.24	3.58	3.48	0.22	2.39
5	4	0.41	1.09	3.34	3.57	0.27	3.45
6	4	0.24	0.27	2.50	4.02	0.23	4.00
7	4	0.18	0.22	3.23	3.58	0.25	3.45
Total time	**28**	**1.41**	**1.59**	**18.51**	**26.26**	**1.72**	**23.76**
Average time	**4**	**0.20**	**0.23**	**2.64**	**3.75**	**0.25**	**3.39**

Figures 1 to 8 show the daily, weekly, monthly and annual analysis of the dump trucks productions in the company, while Plates 1 and 2 show Komat'su wheel loader (WL900) of 15m^3 capacity and Volvo (A40F) dump truck of 60t capacity used in Dangote Coal Mine, Effeche/Akpali site Benue State.

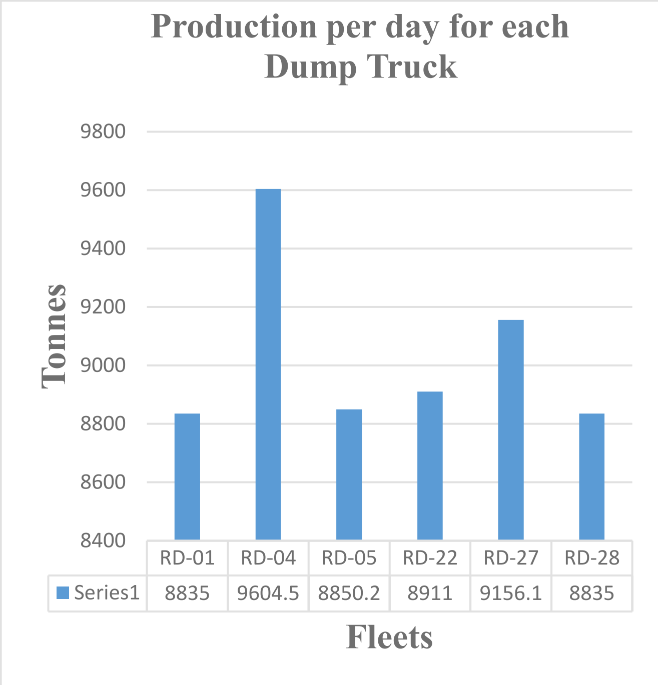

Fig. 5: Production/Day for Each Dump Truck at Dangote Cola Mine, Effeche/Akpali site Benue State

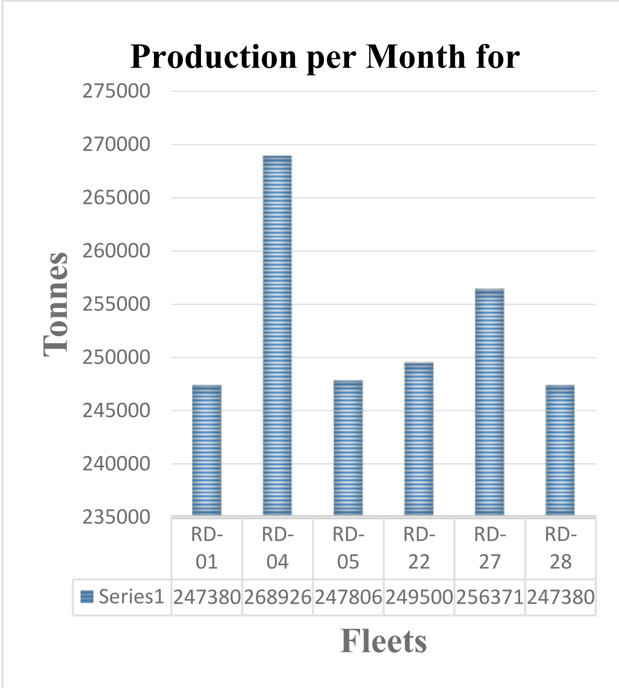

Fig. 6: Monthly Production for each Dump Truck at Dangote Coal Mine, Effeche/Akpali site Benue State

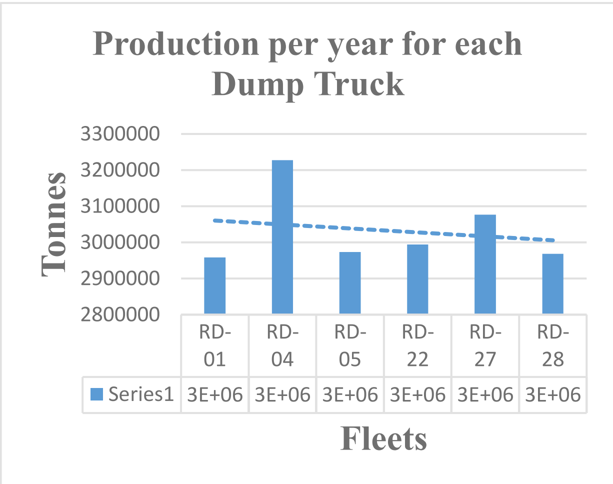

Fig. 7: Annual Production per year for each Dump Truck at Dangote Cola Mine, Effeche/Akpali site Benue State

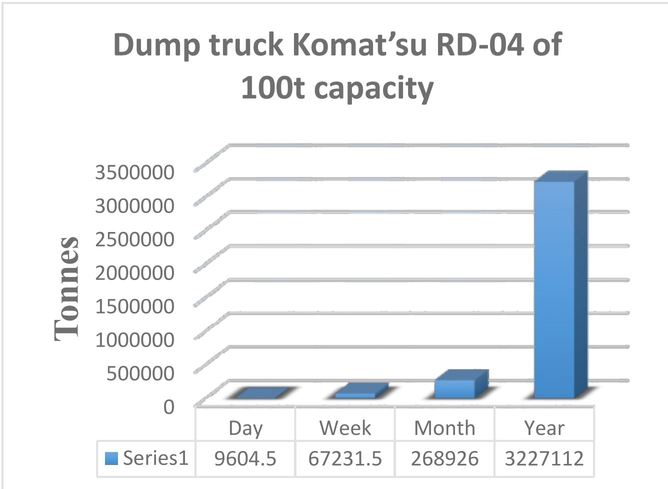

Fig. 8: Productivity of Dump Truck Komat'su RD-04 of 100t capacity

Plate 1: Articulated Wheel loader Komat'su WL900 of 15m^3 Capacity

Plate 2: Articulated Dump Truck Volvo A40F of 60t Capacity

4 Conclusions and Recommendations

From the results of the study, it can be concluded that the wheel loaders and dump trucks used in Dangote Coal mine Limited, Effeche-Akpali Site, Benue State, are in good condition with high efficiency. The mine equipment can be said to be of high capacity which has immensely contributed to meeting the production capacity of the company. The fleets employed in the company are found to be performing optimally with the average production of the six dump trucks being stepped up to 252,894 tonnes. Sustenance of this feat would help the company to continue achieving its production target.

In view of the observations made in this study, the following recommendations are hereby suggested:

i. Prompt fleet maintenance should be given top priority to minimize equipment breakdowns, production interruptions and other avoidable problems;

ii. Constant monitoring of fleet is important apart from maintenance to check sudden anomalies and interruptions that could affect equipment performance;

iii. The haulage way should be improved in other to increase speed of the haulage fleet for quick delivery of materials to the stockpile or crusher; and

iv. The number of fleet should be maintained especially the dumpers, to stand the company's production target.

References

Achelpohl, E.R. (2018). The effect of overloading on reliability of wheel loader structural the effect of overloading on reliability of wheel loader structural components. *Unpublished PhD Thesis,* Missouri University of Science and Technology, 196pp.

Adams, K.K. & Bansah, K.J. (2016). Review of Operational Delays in Shovel-Truck System of Surface Mining Operations. *4th UMaT Biennial International Mining and Mineral Conference,* 60-65.

Cheng, J.E. (2019). Match Factor Determination Of Excavator-Truck Combination In Surface Mining: Case Study Of Merit Pila Coalfield, Sarawak. *Geological Behavior*, 2.(1), 28-29.

Dembetembe, G. & Mutambo, V. (2018). Optimisation of Materials Fleet Performance at Nchanga Open Pit Mine. *Proceedings of the First Zambia National Conference on Geology, Mining, Metallurgy and Groundwater Resources: The Future Mining in Zambia,* Lusaka, 167-192.

Dey, S. Mandal, S. K. & Bhar, C. (2017). Analysis of Factors, Which Influence the Cycle Time of Dumpers of Open Cast Coal Mines to Improve Production. *AMSE JOURNALS-AMSE IIETA publication-2017-Series: Modelling C,* 78(3), 289-30.

Elevli, S. & Elevli, B. (2010). Performance Measurement of Mining Equipments by Utilizing OEE *Acta MontanisticaSlovaca*, 15(2), 95-101.

Erclebi, S.G. & Bascetin, A. (2009). Optimization of Shovel-Truck System for Surface Mining. *The Journal of The Southern African Institute of Mining and Metallurgy*, 109, 433-439.

Nel, S., Kizil, M.S. Knights, P. (2011). Improving Truck-Shovel Matching. *35th APCOM Symposium/Wollongong*, New South Wales, 24 30 September, 381-391.

Nguyen, H., Doan, T.L., Le, T.T.A., Do, N.H. & Pham, V.V. (2014), Determination of Shovel - truck Productivities in Open - pit Mines. Conference Paper, 7.

Pasch, O & Uludag, S. (2018), Optimization of the Load-and-Haul Operation at an Opencast Colliery. *The Journal of the Southern African Institute of Mining and Metallurgy*, 118, 449-456.

Geochemical Analysis of Pesok Mine Tantalite in Ijero Ekiti

Obaro, R. I., Agbalajobi, S. A. and Taiwo, O. J.

Department of Minerals and Petroleum Resources Engineering Technology,
Institute of Technology, Kwara State Polytechnic, Ilorin. Nigeria.
Corresponding Author Email: taiwoolamilekan10@gmial.com

Abstract

Tantalite deposits of IjeroEkiti in Ekiti State were studied in order to assess their geochemical characteristics. The laboratory analysis carried out on the samples A and B include X – Ray diffractometer and X – Ray Fluorescence. Results of X – Ray diffractometer for sample A and B revealed thatmicrocline has the highest peak at (12.28, 24.14, 29.97, 36.00 and 53.01) 2θ values for sample A while sample B was also identified at (8.71, 21.00, 26.48 and 42.43) 2θ values. Ferrotantalite has its peak at (26.29, 41.10 and 59.54) 2θ values for sample A while sample B was also identified at (22.00, 40.38, 59.60) 2θ values. The manganotantalite also has (18.98 and 42.26) 2θ values for sample A while sample B was also identified at (18.98 and 42.26) 2θ values. The X – Ray Fluorescence of Sample A and Sample B are the major oxide and it indicates that the percentage Tantalum oxide (Ta_2O_5) for both samples ranges from 38.61% to 40.71% with an average of 39.66%, Ferric oxide (Fe_2O_3) ranges from 9.15% to 9.35% with an average of 9.25%, Aluminumoxide (Al_2O_3) ranges from 2.00% to 2.02% with an average of 2.01%, Titanium oxide (TiO_2) ranges from 1.59% to 1.66%, with an average of 1.63%, Calcium oxide from 1.23% to 1.36% with an average of 1.30%, Vanadium oxides from 1.10% to 1.12% with an average of 1.11% and Niobium IV oxide ranges from 25.50% to 28.50% with an average of 27% weight percentage composition. However, the mineralogical composition indicates the occurrence of Ferrotantalite and manganotantalite at strong peaks while the chemical composition indicates the occurrence of higher concentration of tantalum oxide which can be used for capacitors and economically valuable for exploration.

Keywords: Ferrotantalite, Manganotantalite, Oxide, Tantalite, XRD, XRF

1 Introduction

Nigeria is blessed with abundant mineral resources. These include vast deposits of coal, cassiterite, columbite, marble, limestone, clay, bitumen and tantalite. Basement complex rock deposits are the most common and today are the main source of ore supply to the industry (Akintola *et al.,* 2011). To simplify this, there are three main types of hard rock deposits: pegmatites, granites and carbonites. Ore bodies are made up of different types of rocks which are made up of various minerals. An example of this is quartz, a mineral which is a major part of granitic rocks. In the case of tantalum, the most common rock formation which hosts the current tantalum ores is called pegmatite. Pegmatite basement rock deposits are the dominant source while carbonites (or alkaline complexes) are rare. The only production of tantalum so far has been from pegmatite and specialty granites. (Akintola *et al.,* 2011).

Large deposit of tantalite exists across the world, namely in Germany, Sweden, Norway, and Nigeria. The major ones in Nigeria can be found in Kaduna (Abia Hill, Tare Naudu, gerti station); Nasarawa State (Wamba, Udege, Akwanga, Kokona-Dengi, Angwa -Doka), Kogi State (Akuta, Ejuku, Takete, Isanlu Isa, Egbe), Kwara State (Oke- Onigbin), Oyo State (Igbeti) and Ekiti (IjeroEkiti) (Adekoya*et al*., 2003).

The principal source of tantalite is an isomorphous series of minerals that contain columbium (niobium), iron, manganese and tantalum oxides. Tantalum and columbium have strong geochemical affinity and are found together in most rocks and minerals in which they occur. Tantalite-columbite (Coltan), which is the major source for tantalum, occurs mainly as accessory minerals disseminated in granitic rocks or in pegmatite associated with granites. The proper name for the mineral is tantalite when tantalum predominates over columbium. When the reverse is true, the proper name is columbite (Hayes and Burge, 2003).

1.2 Geology of the area

Ijero-Ekiti and its environs are endowed with Tantalum-Niobium-Tin and Lithium metals and non-metallic deposits such as feldspar and kaolin hosted by muscovite and lepidolite respectively. It is underlain by the basement complex rocks of Southwest, Nigeria. The local geology consists of the migmatite gneiss, quartzite, schist biotite gneiss, calc-gneiss, epidiorite, biotite schist, amphibole schist, granite and pegmatite. Ijero-Ekiti lies between latitudes 7º46'N and 7º55'N and longitudes 5º00'E and 5º80'E. Rahaman (1988) classified the major rocks into four distinct units namely; the migmatite-gneiss complex, the biotite-hornblende gneiss, the metasediments (schists), and the Older granites. Ijero-Ekiti is located at 42km Northwest of Ado-Ekiti, the Ekiti State capital and about 350km NE of Lagos.

PESOK mine (Figure 1) is located on latitude N07° 49' 813” longitude E005° 03'452” at elevation of 569 meters above sea level, IjeroEkiti, Ekiti State.

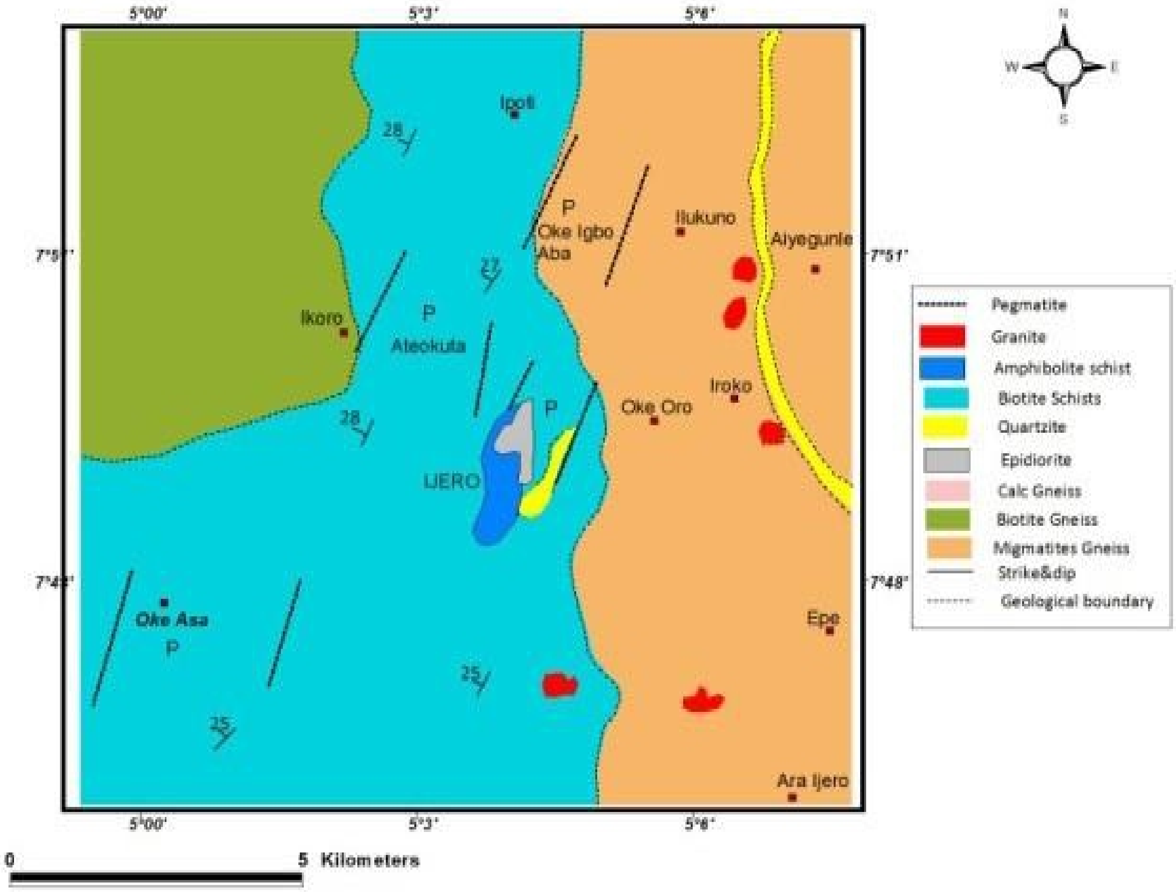

Figure 1: Geological Map of IjeroEkiti (Modified after Okunlola andAkinlola, 2010)

2 Materials and Methods Used

Sample Collection

Fresh representative samples of tantalite tagged sample A and Sample B were collected on the field using global positioning system. The two samples were separated in different sample bags and transported to Afe - Babalola University, Ado - Ekiti State for detailed analysis.

Sample Preparation

Mineral samples of tantalite obtained from the field were brought to Department of Chemical and Petroleum Engineering, Ado – Ekiti, Ekiti State for further analyses. The mineral samples were carefully selected for geochemical analyses. Mineral samples were

pulverized at the same laboratory in preparation for the geochemical analysis.
The samples were tested in the laboratory to determine their chemical composition using X – Ray Diffraction (XRF)

Determination of Chemical Composition
Samples were also tested in the laboratory to determine their chemical composition using X-Ray Fluorescence (XRF)

3 Results and Discussion

Mineralogical composition
Table 1 and figure 3 show the mineral present and the percentage weight composition.

Table 1: Composition Weight of Tantalite for Sample A and B by XRD

S/N	Mineral present	% Composition	
		Sample A	Sample B
1	Microcline	56.3	60.86
2	Manganotantalite	6.65	5.17
3	Ferrotantalite	10.23	9.46
4	Ilmenite	8.43	11.29
5	Muscovite	11.07	4.34
6	Garnet	4.92	2.09
7	Quartz	2.36	5.85
Total		**99.96**	**99.06**

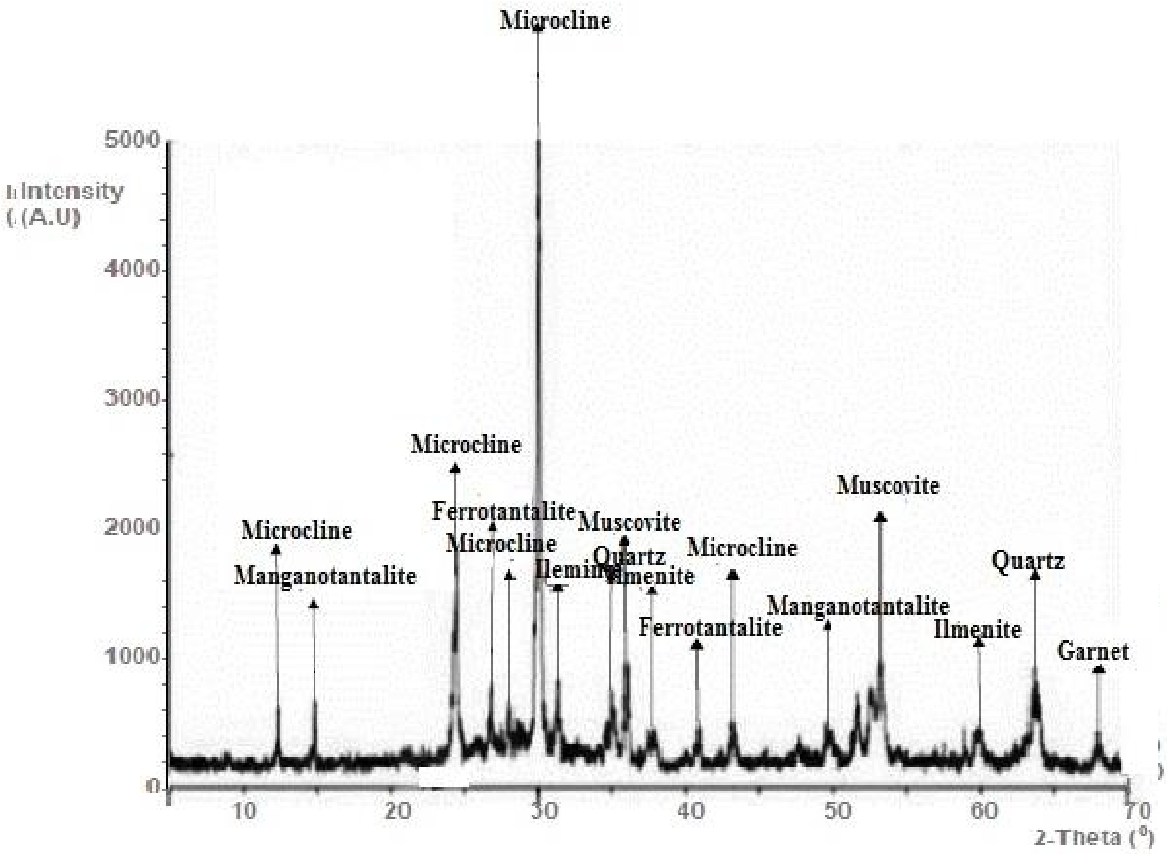

Figure 3: X – Ray Diffractogram of Tantalite Sample B

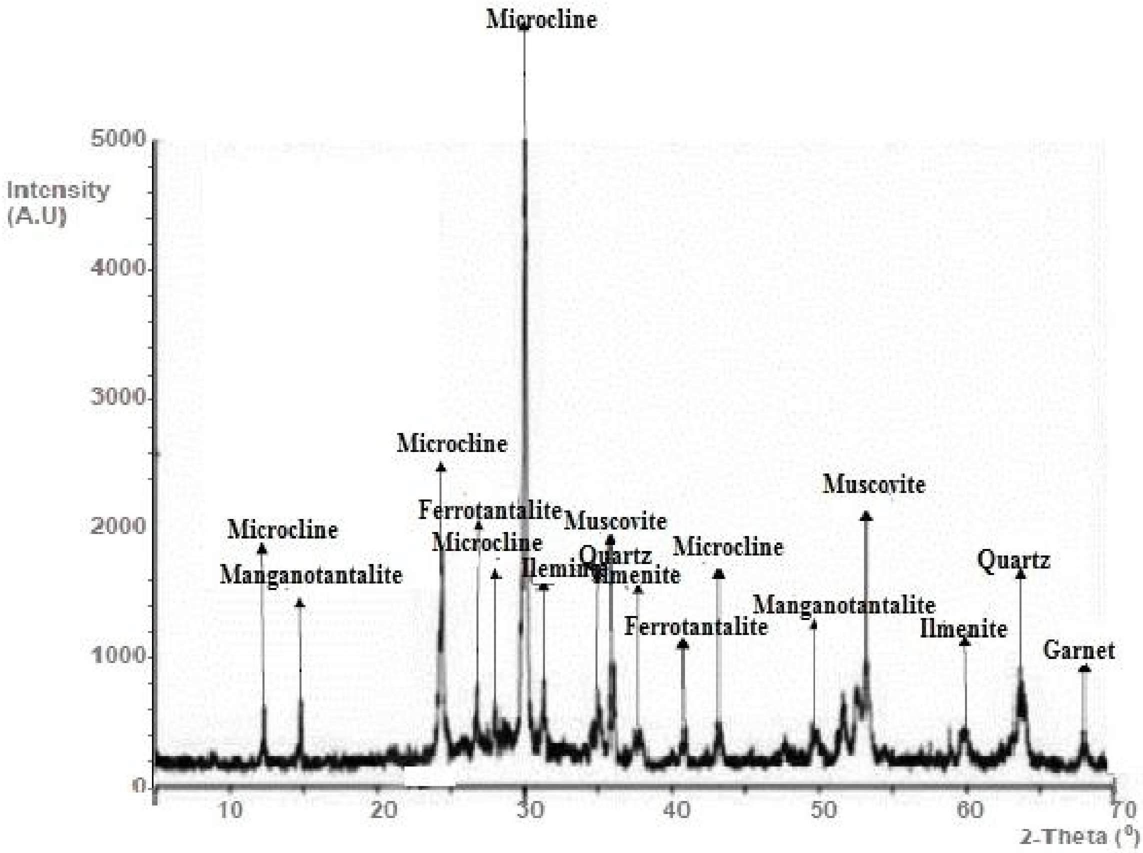

Figure 3: X – Ray Diffractogram of Tantalite Sample B

The XRD patterns for the two Tantalite minerals for Sample A and Sample B are identical with some differences in the intensity of some of the main peaks such as the peak at around 2θ = 29.97° and 26.48° respectively (figure 2). The X – Ray Diffraction patterns indicated a mixture of minerals in all the samples studied. Four major minerals with strong peaks were found, microcline, manganotantalite, ferrotantalite and muscovite, others are ilmenite, garnet and quartz. The highest peaks belong to microcline, ferrotantalite and manganotantalite. The XRD pattern showed that samples contained microcline, as the major component with minor quartz (SiO_2). The best XRD match for the sample minerals was obtained with the microcline, ferrotantalite and manganotantalite mineral patterns. Some nonmatching peaks were found to match with those of ilmenite, garnet and quartz. Interesting enough is that most of the peaks in the sample XRD pattern showed a better match with both the ferrotantalite and manganotantalite mineral XRD patterns, while some other peaks in its XRD spectrum matched with that of muscovite, ilmenite, garnet and quartz.

Chemical composition of Tantalite for Sample A and B.

S/N	Parameters	Formulae	% Weight Composition	
			Sample A	Sample B
1	Silicon Oxide	SiO_2	0.04	0.04
2	Aluminum Oxide	Al_2O_3	2.02	2.00
3	Ferric Oxide	Fe_2O_3	9.35	9.15
4	Calcium Oxide	CaO	1.36	1.23
5	Magnesium Oxide	MgO	0.02	0.02
6	Manganese Oxide	MnO	0.73	0.70
7	Titanium Oxide	TiO_2	1.66	1.59
8	Tantalum(V) Oxide	Ta_2O_5	40.71	38.61
9	Vanadium Oxide	V_2O_5	1.12	1.10
10	Niobium*(V)*Oxide	Nab_2O_5	28.20	25.50
11	Sulphide	SO_3	0.02	0.01
12	Lead Oxide	Pb_2O_5	0.08	0.05
13	Nickel Oxide	NiO	0.01	0.02
14	Zinc Oxide	ZnO	0.07	0.05
15	Chromium Oxide	Cr_2O_3	0.96	0.82
16	Loss on Ignition	LOI	10.09	9.16

The X – Ray Fluorescence of Sample A and Sample B was evaluated for their chemical composition. The major oxide in Table 1and 3 indicates that the percentage Tantalum (Ta_2O_5) for both samples ranges from 38.61% to 40.71% with an average of 39.66%, Ferric oxide (Fe_2O_3) ranges from 9.15% to 9.35% with an average of 9.25%, Aluminum oxide (Al_2O_3) ranges from 2.00% to 2.02% with an average of 2.01%, Titanium oxide (TiO_2) ranges from 1.59% to 1.66%, with an average of 1.63%, Calcium oxide from 1.23% to 1.36% with an average of 1.30%, Vanadium oxides from 1.10% to 1.12% with an average of 1.11% and Niobium iv oxide ranges from 25.50% to 28.50% with an average of 27% weight percentage composition.

There is no universally accepted range for evaluating the percentage of tantalum oxide (Ta_2O_5) of tantalite mineral. However, this evaluation varies as authors reported different percentages of %Ta_2O_5 as rich tantalite mineral. Ruiz *et al*., (2004) reported 10% Ta_2O_5, Funtua (1999a) reported 21 - 30% Ta_2O_5 while Adetunji*et al*. (2005) reported 25% Ta_2O_5. All the percentages indicated above according to the authors can be used for industrial applications particularly capacitors and economically valuable for exploration. It was discovered that the average percentage of niobium iv oxide Nb_2O_5 (27%) in this study was at least higher compared to other samples analyzed. This could be due to high purity tantalite of this area and the variation of the mineral ore from one ore vein to the other (Adetunji*et al.,* 2004). The percentage of ferric oxide (Fe_2O_3) is between 9.15% to 9.35% which indicate the presence of Ilmenite, another valuable mineral. The percentage of titanium oxide (TiO_2) range is between 1.59% to 1.66%. Titanium oxide is used for production of bicycles for cycling because it is light.

According to Alhassan *et al.,* (2010) the loss of ignition displays low volatile matter. Samples A and B ranges from 9.16% to 10.09% with an average of 9.62%, thus a greater percentage of the materials was retained after continuous heating at 1000^{0}C. The average values indicate that the properties of tantalite attained the minimum threshold and can be used for industrial application.

4 Conclusions

The geochemistry of the samples analyzed suggests that the mineralogical composition consist of microcline, ferrotantalite, manganotantalite, ilmenite, muscovite, and quartz. The chemical composition of the samples contains higher concentration of tantalum oxide, niobium oxide Nb_2O_5, ferric oxide (Fe_2O_3), titanium oxide (TiO_2) and loss of ignition which has attained the minimum threshold, economically valuable for exploration and can be used for industrial application such as production of capacitors, super alloys production: Electronics industry, Capacitors, Automobiles

References

Adekoya J. A., Kehinde-Philips, O. and Odukoya, M. (2003): "Geological Distribution of Minerals Resources in Southwest Nigeria". *In Prospects for Investment in Mineral Resources of Southwest Nigeria, Elueze*, A.A. (Edu.). Elsevier, USA., ISBN: 978-36831-0-1 pp 1-13

Adetunji, A., Siyanbola, W., Funtua, I., Olusunke, S., Afonja, A. and Adewoye, O. (2005): "Assessment of Beneficiation Routes of Tantalite Ores from Key Locations in Nigeria"*. J Minerals Mater. Characterization Eng.,* 4(2): 67-73.

Akintola, A., Omosanya, K., Ajibade O., Okunlola, O. and Kehinde-Philips, O. (2011):"Petrographic and Geochemical Evaluations of Rare – Metal (Ta-Nb) Potentials of PrecambrianPegmatite ofAwo Area Southwestern", *NigeriaInternational Journal of Basic & Applied Sciences* Vol: 11 No: 04. pp. 57 – 70

Alhassan Y. Tsafe A.I., Birnin U.A., Okunlola O.J., Yargaamji G.I., and Yebpella (2010): EDXRF Analysis of Tantalite Deposit of Mail-Kabanji North-Western Nigeria, Journal of Environmental Chemistry and Ecotoxicology Vol. 2(7) pp. 117-119

Funtua I. I., (1999a). Analysis of Ta and Nb Ores by Energy Dispersive X - Ray Fluorescence Spectroscopy*.* J. Trace Microprobe Tech., 17(2): 195-197.

Hayes, K. and Burge, R. (2003): "Coltan Mining in the Democratic Republic of Congo":how tantalum-using industries can commit to the reconstruction of the DRC. *Fauna &Flora International*, Cambridge, UK,

Okunlola, O.A. and Akinola, O.O. (2010):"Petrochemical Characteristics of the Precambrian Rare Metal Pegmatite of Oke-Asa area, southwestern Nigeria*":* Implication for Ta-Nb mineralization RMZ-Materials and Geo-environment, vol. 57 (4): 525538,

Rahaman, M.A. (1988): Recent Advances in the study of the Basement Complex of Nigeria in P.O. Oluyide, W.C. Mbonu, A.E. Ogezi, I.G. Egbuniwe, A.C. Ajibade and A.C. Umeji (eds), Precambrian Geology of Nigeria. Geological Survey of Nigeria, Kaduna. 11-44

Ruiz, M., Del, C., Rodriguez, M. and Osina, R. (2004): X-Ray Fluorescence Analytical Methodology for the Determination of Nb, Ta, Fe and Mn Extracted in Hydrometallurgical Processes", Lat. Am. Appl. Res., V34 n.

Adebayo *et al.* (2022) Nigerian Mining Journal, (20) 58 - 75

Mobile App Enabled Gas Monitoring and Control Device for Underground Mines

Adebayo O.E.[1], Damisa E.O.A.[1], Salawu O.M.[1] and Sheshi E.[2]

[1]*Department of Mineral and Petroleum Resources Engineering, Kaduna Polytechnic, Kaduna*

[2]*Department of Mechatronics, Airforce Institute of Technology, Kaduna*

Abstract

Subsurface environments are restricted and natural air flow into them is limited even when the excavation is shallow as in *loto* mines, which are prevalent in Nigeria. Depending on their concentrations, the following gases associated with underground mines can be detrimental to the well-being of underground workers whether immediate or in the long run: Methane (CH_4), Carbon monoxide (CO), hydrogen (H_2), Carbon dioxide (CO_2), Nitrogen (N_2), Methane (CH_4), Carbon monoxide (CO), Oxides of nitrogen (N_2) Hydrogen sulphide (H_2S) and Radon (Rn). To create a thorough safe mining environment underground therefore, accumulation of these hazardous gases must be prevented and prevention must be supported by detection. Thus, the design and construction of a multi-gas monitoring and control device (GMCD). The design utilizes an Arduino Nano and air quality and gas sensor (MQ135 and MQ4) to measure the level of gas concentration in a mine, especially coal mine. It also utilizes *internet of things technology* IoT) to capture the gas data, accessed from a remote location using a mobile application and connected to a specific router with Service Set Identifier (SSID) "Adebayo.Net" with the aid of WI-FI Module (ESP8662) and MIT-App inventor, the device sends information once every 10 seconds to ThingSpeak Server. The trial run of the device was carried out at the ventilation section of the mine services workshop of the Department of Mineral and Petroleum Resources Engineering, Kaduna Polytechnic, which revealed the concentration of four gases; CO (4 ppm), CO_2 (2.8 ppm), H2 (4.3 ppm) and CH_4 (0.8 ppm).

Key words: *Loto* mines, Arduino Nano, MQ135, MQ4, ESP8662, *Internet of Things.*

1.0. Introduction

The primary purpose of detecting and measuring the concentrations of underground mine gases is to ensure that the mine atmosphere provides a safe environment, free from levels of hazardous gases and productivity of mineworkers in mind. When air enters an underground environment, it has a volume composition of approximately 78% nitrogen, 21% oxygen and 1% other gases on a moisture-free basis. However, as the air progresses through the network of underground openings, that composition changes as a result of many factors. It is normally observed that return air from subsurface exhaust shaft is depleted in oxygen content as a result contamination by mine gases. Impurities come from exhalation by men, blasting, underground fires, burning of lights, bacterial action and gases given off from rock strata. It also contains moisture and dust of coal and rock. Depending on their concentrations, the following gases associated with underground mines can be detrimental to the well-being of underground workers whether immediate or in the long run: Methane (CH_4), Carbon monoxide (CO), hydrogen (H_2), Carbon dioxide (CO_2), Nitrogen (N_2), Oxides of nitrogen (N), Hydrogen sulphide (H_2S) and Radon (Rn). To create a safe mining environment underground therefore, accumulation of these hazardous gases must be prevented and prevention must be supported by detection. It is to be noted although the gases that occur most commonly underground have been mentioned, it is more usual that several gaseous pollutants appear together as gas mixtures. Furthermore, the importation of an ever-widening range of materials into underground mines also introduces the risk of additional gases being emitted into the mine environment. Detection of dangerous gases in mines has changed and developed over the years with some techniques becoming traditions ingrained in the mining culture. With advances in technology, the time has come to leverage on technology to modernize the detection of underground mine gases for greater efficiency, reliability and accuracy. In this work, an instrument is developed that is capable of measuring concentrations of more than one gas and incorporates these parameters with real-time sensing and decision-making. This is made by the use of Internet of Things (IoT) (Ashton, 2009). IoT technology supports one or more common ecosystems, and can be controlled via devices associated with that ecosystem, such as smart phones and smart speakers. It is the integration of processes and technology with connectable devices and sensors to enable remote monitoring, detection and control of hazardous gases underground.

1.1 Detection of Mine Gases

Many methods have been used to detect or monitor the presence of gases in underground environments. The oldest detection method was the use of a bird, the canary, which was a symbol for gas testing in mines, along with a testing flame and later flame safety lamps which are still in use today. Some of the old detection methods are based on the on the use of warm-blooded birds like canary as they are affected much earlier than man. The height of the flame reduces progressively with decrease in oxygen content and is extinguished at 16 percent oxygen. However, in a methane-rich atmosphere, the flame may remain lit down to an oxygen concentration of 13%. The use of the flame safety lamp for methane testing has now largely been replaced by **pellistor methanometers** as these are more accurate, reliable and safer. **Pellistor detectors** (filament and catalytic oxidation) are used primarily for the measurement of methane and other gases that will burn in air, for examples, carbon monoxide, hydrogen or the higher gaseous hydrocarbons. In some other cases; detectors are based on the chemical reaction of a gas with certain chemicals resulting in a **change of colour**. Examples are P.S. detectors and stain tubes. The method is based on heat generated on the oxidation of carbon monoxide to carbon dioxide and is called the **Hopcalite detector** which consists of an analyzing cell containing hopcalite, which is a specially prepared mixture of manganese dioxide and copper oxide. Some other detectors depend **colour comparing scale** while some depend on heating an electrical filament to a sufficiently high temperature, then a combustible gas in the surrounding air will burn and, hence, elevate the temperature of the filament even further. (Baker, 1969; Richards, 1970). Acoustic gas detectors rely upon changes in the velocity of sound as the composition of a sample varies. **Interferometers** utilize the refraction of light that occurs when a parallel beam is split, one half passing through the sample and the other through a sealed chamber containing pure air. **The non-dispersive infra-red gas analyzer** is one form of absorption spectrometer that is frequently used for mine gas analysis. (McPherson, 2000). **Laser spectroscopy is another means of air analysis** that has considerable potential for subsurface application. (Holmes and Byers, 1990). The attraction of laser techniques for mine air sampling is that the laser beams may be directed across or along subsurface openings to give continuous mean analyses for large volumes of air. Furthermore, the lasers can also be used to monitor air velocity (McPherson, 2000). Very small concentrations of many gases can be detected by their influence on the output from an electrochemical cell. **In mass spectrometers instruments**, the gas sample passes through a field of free electrons emitted from a filament or other source. A rotation of a magnet is induced as the oxygen content of the sample or atmosphere varies, the movement is amplified optically or electrically for display or recording (McPherson, 2000). **Gas chromatographs** are used widely for the laboratory analysis of sampled mixtures of gases (McPherson, 2000). One of the more recent techniques introduced for gas detection are **semiconductor detectors** which involve passing the sample over the surface of a semi-conducting material maintained at a constant temperature. Adsorption of gas molecules on to the surface of the semiconductor modifies its electrical conductance. Selectivity of the gas to be detected may be achieved by the choice of semi-conductor and the operating temperature (McPherson, 2000).

1.2 Threshold Limit Values of Underground Mine Gases

Threshold limit values (TLVs) of airborne substances refer to those concentrations within which personnel may be exposed without known adverse effects to their health or safety. TLVs are arrived at through a combination of industrial experience and from both animal and human studies. The TLVs adopted in this work are based primarily on recommendations of the American Conference of Governmental Industrial Hygienists, (ACGIH,1989) and the U. S. National Institute for Occupational Safety and Health, (NIOSH, 1987). Three types of threshold limit values identified. The Time-Weighted Average (TWA) is the average concentration to which nearly all workers may be exposed over an 8-hour shift and a 40-hour work week without known adverse effects. However, many substances are sufficiently toxic that short-term exposures at higher concentrations may prove harmful or even fatal. The Short-Term Exposure Limit (STEL) is a time-weighted average concentration occurring over a period of not more than 15 minutes. That is, concentrations above the TWA and up to the STEL should not last for longer than 15 minutes. It is also recommended that such circumstances should not occur more than four times per day nor at intervening intervals of less than one hour. The Ceiling Limit is the concentration that should not be exceeded at any time. This is relevant for the most toxic substances or those that produce an immediate irritant effect (ACGIH,1989).

Table 1: TLV for underground mine gases

Gases	Formula	TLV (TWA)	TLV-STEL (ppm)
Carbon dioxide	CO_2	5000	30000
Carbon monoxide	CO	25	200
Hydrogen sulphide	H_2S	1	5
Sulphur dioxide	SO_2	-	0.25
Nitric oxide	NO	25	-
Nitrogen dioxide	NO_2	0.2	-

(Source: https://researchgate.net>figure>threshold-limit-value)

In any given atmosphere, if there are two or more airborne pollutants (gaseous or particulate) that have adverse effects on the same part of the body, then the threshold limit value should be assessed on the basis of their combined effect. This is calculated as the dimensionless sum.

$$\frac{C_1}{T_1} + \frac{C_2}{T_2} + \frac{C_3}{T_3} + \cdots + \frac{C_n}{T_n} \quad \text{... Equ. 1}$$

Where *C* = measured concentration and *T* = corresponding threshold limit value.

If the sum of the series exceeds unity, then the threshold limit value of the mixture is deemed to be exceeded. (ACGIH, 1989)

2.0 Methodology and Evaluation

The principle of the gas detector is likened to the electrochemical method of detecting gas i.e. (the change in electrical current is proportional to the concentration of gas in the sample/mineral). This work consists of a tin dioxide (SnO_2): a perspective layer inside aluminum oxide micro-tubes (measuring electrodes) and a heating element inside a tubular casing. The end face of the sensor is enclosed by a stainless-steel net and the backside holds the connection terminals. The gases present in the environment are oxidized into acetic acid passing through the heating element. While the gases cascade on the tin dioxide sensing layer, the resistance decreases. By using the external load resistance, the resistance variation is converted into a suitable voltage variation. Once the gas detector senses gas in the environment, it sends the voltage variation reading through the Wi-Fi module via API key (Application Programming Interface) to ThingSpeak (a sever on the web) through a router, the server is a database that reads all the gas voltage variation generated from the detector, interprets and represent the result as graphical model or spreadsheet data and stores them into different fields on the server as parts per million (ppm) or percentage (%). Other platforms can access and read data from the Server, like the Android OS (operating system) which in this case was used to read the generated data on a mobile app that displays the level of each gas in real-time, along with the GPS coordinate of the environment. The schematic of the set-up is shown in Figure 1.

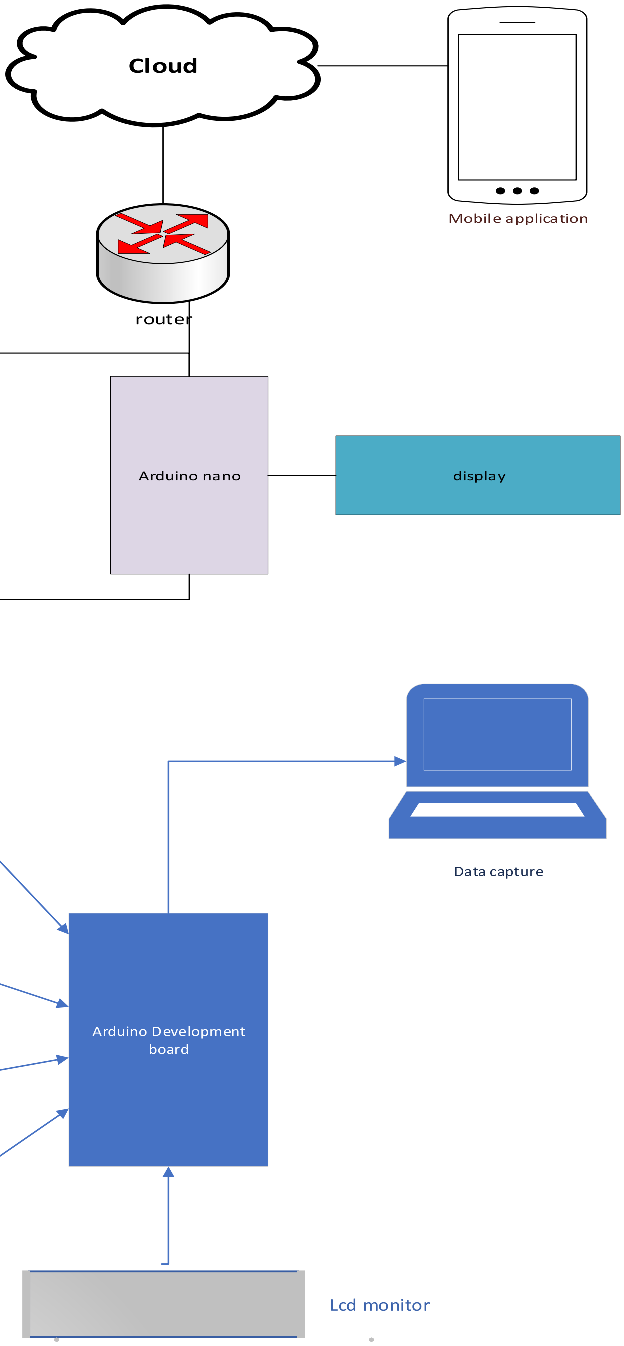

Figure 1: Schematic of the working principle of Underground Mine Multi-Gas Detection System

Software components:

(i) ThingSpeak Server (ii) Massachusetts Institute of Technology Application (MIT App) Inventor (iii) Arduino Integrated Development Environment (IDE)

Hardware components:

(i) Arduino Nano (ii) Esp8662 WIFI module (iii) MQ-135 Air Quality and Gas Sensor (iv) MQ-4 Gas Sensor (v) Buck Converter (vi) Buzzer (vi) RGB Led display.

2.1. The ThingSpeak Web Server

"ThingSpeak" is an open-source Internet of Things (IoT) software and API (Application Programming Interface) which was used storing and downloading information from physical objects using the HTTP protocol over the Internet or through a Local Area Network. ThingSpeak helped to develop Apps for sensor recording, location tracking. ThingSpeak incorporates MathWorks' MATLAB mathematical computation tools which allowed ThingSpeak to evaluate and display downloaded information.

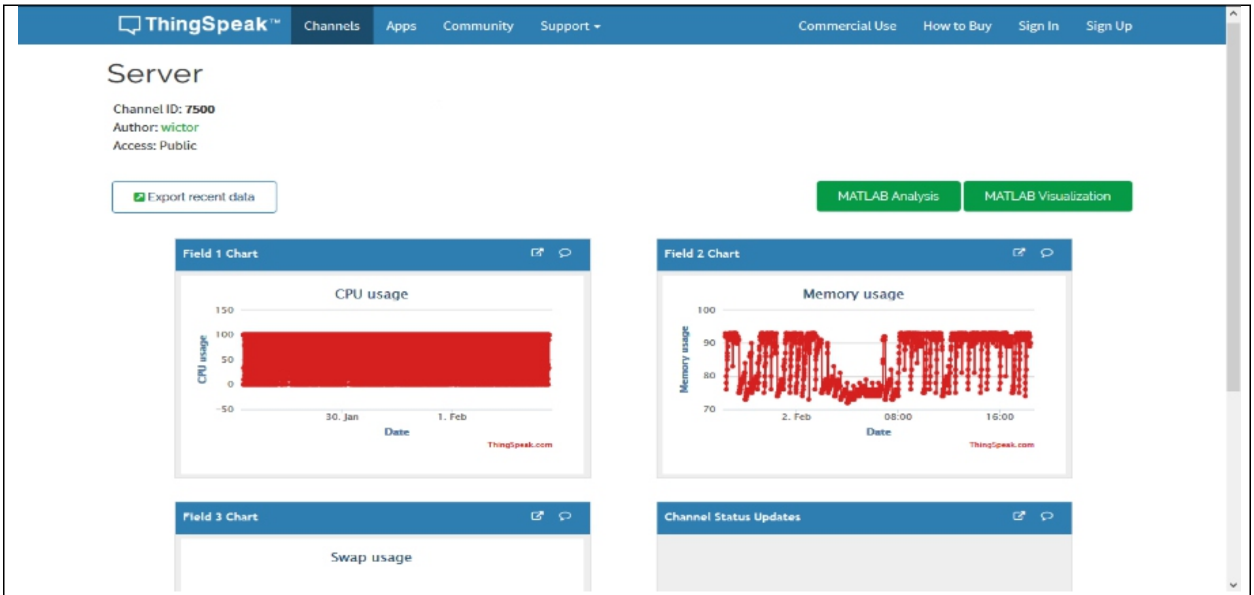

Figure 2: ThingSpeak Web Server Interface

2.2. MIT App Inventor

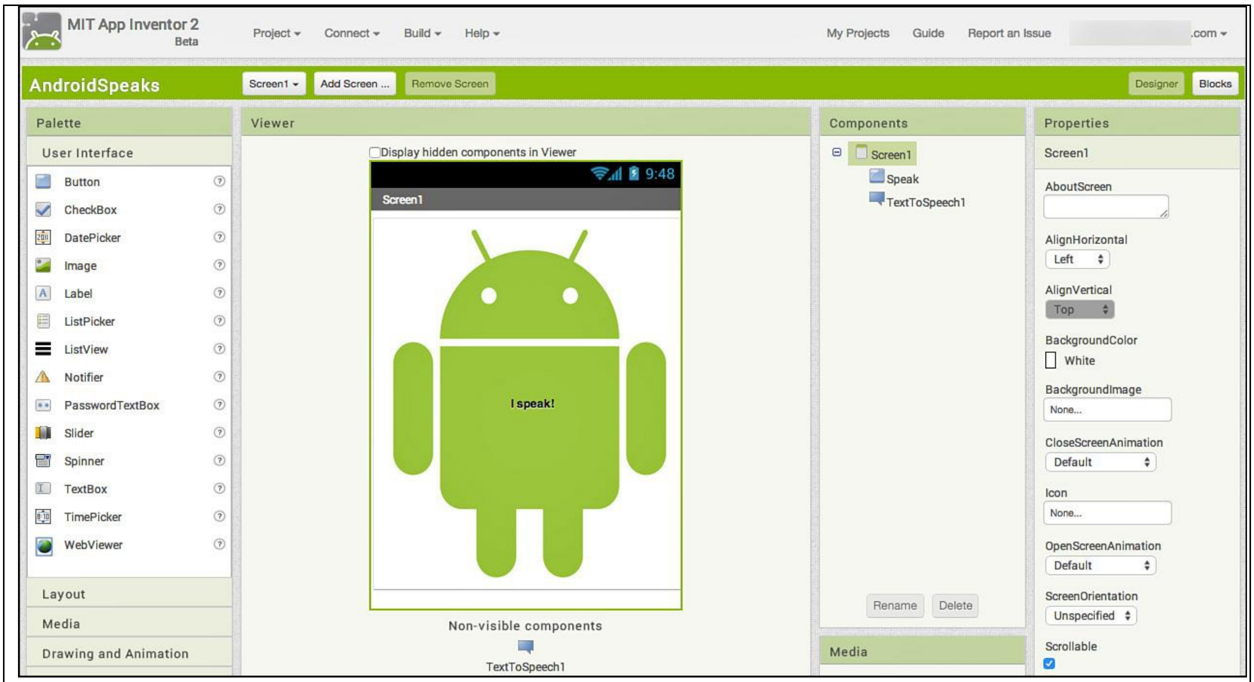

Figure 3: MIT App Inventor Environment

MIT Software Inventor is a user-friendly, visual programming platform that enables the creation of completely functioning applications for smart phones and tablets. (Abelson, 2011)

2.3. Arduino IDE

The Arduino Integrated Development Environment (IDE) or Arduino Software contains a text editor for writing code, a message area, a text console, a toolbar with buttons for common functions and a series of menus. It connects to the Arduino hardware to upload programs and communicate with them (Banzi, 2014).

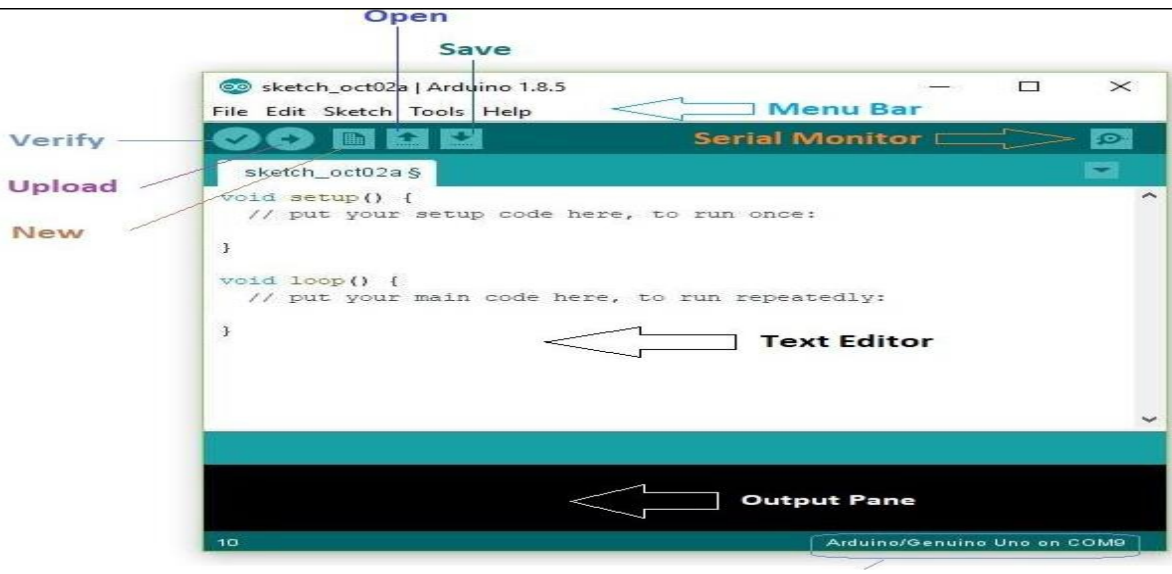

Figure 4: Arduino Integrated Development Environment (IDE)

2.4. Arduino Nano Microcontroller

Arduino is an open-source hardware and software company (2022). The company manufactures single-board microcontrollers and microcontroller kits for building digital devices. The microcontrollers can be programmed with C and C++ programming languages, using a standard API which is also known as the Arduino language, inspired by the Processing language and used with a modified version of the Processing IDE.

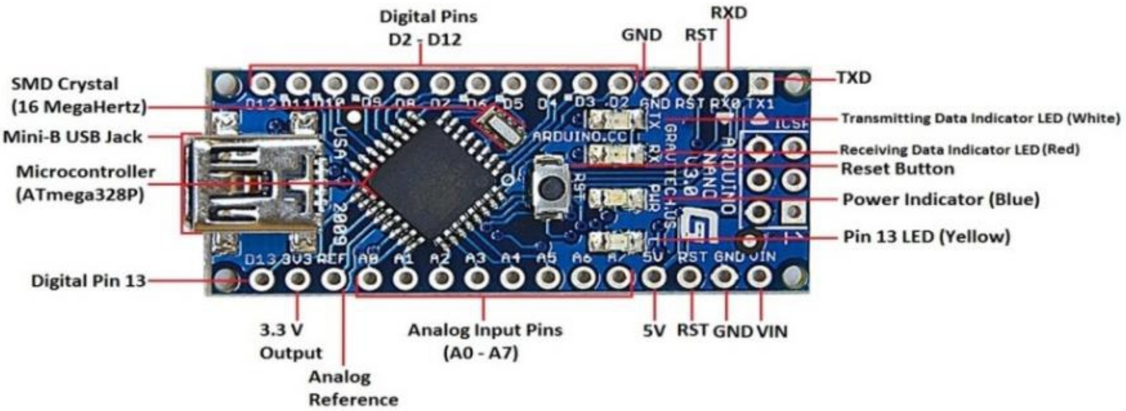

Figure 5: Arduino Microcontroller

2.5 The ESP8266 Wi-Fi Module

The ESP8266 is a user friendly and low-cost device used to provide internet connectivity to a microcontroller-based project (Benchoff, 2014). The unit can function both as a hotspot and a transmitter, so it can quickly capture and upload information to the cloud, making it easy to use the IoT.

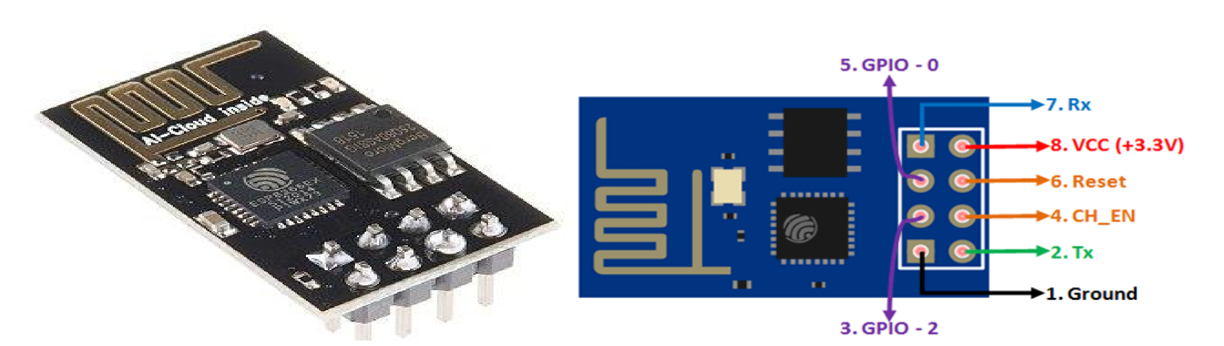

Figure 6: ESP8266 Wi-Fi Module

2.6. MQ-4 Gas Sensor

The **MQ-4** gas **sensor** can detect gases like Methane, LPG, Alcohol, Propane, H_2, CO, CO_2, and NH_3. Using an MQ sensor to detect a gas can be carried out using either the digital pin or the analog pin to accomplish

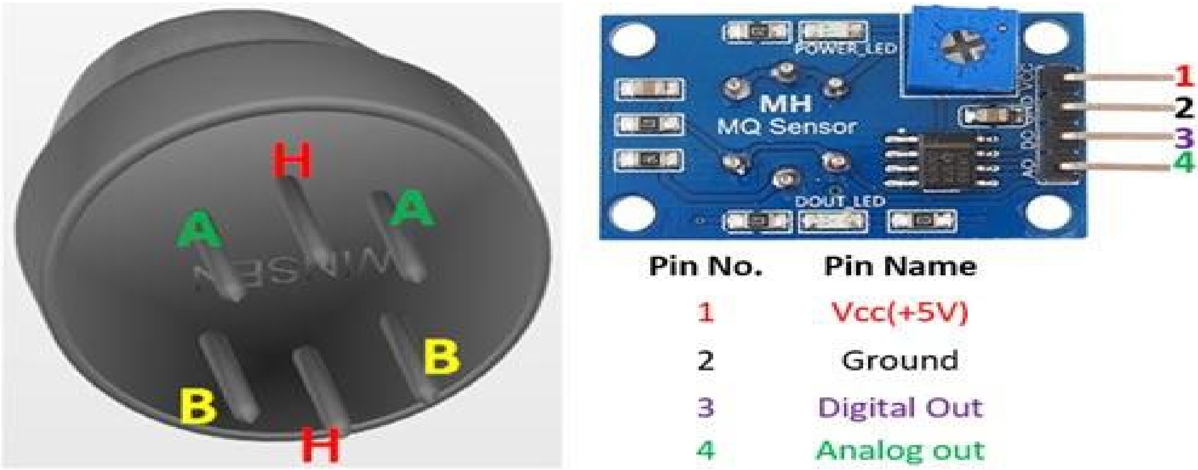

Figure 7:MQ4 Air Quality and GasSensor Module

2.6. MQ-135 Air Quality and Gas Sensor

The **MQ-135 gas sensor** can detect gases like LPG, Alcohol, Propane, Hydrogen, CO, CO_2, Ammonia, Methane, Toluene and Acetone. With MQ sensor, a gas can be detected by using digital pin or the analog pin. This is done by powering the module with 5V battery mentioned above at a specific concentration the digital pin will go high (5V) else will remain low (0V).

Figure 8: MQ135 Air Quality and Gas Sensor Module

Table 2: MQ 135 and MQ 4 Gas Sensor and their different components

S/No	List 0f Gases the Device Can Detect	Sensor Range for Each Gas (PPM)	Threshold Limit Values (PPM)	
1.	Methane	0 to 1012.7	1000	-
2.	Hydrogen	0 to 3000000	1	5
3.	Carbon dioxide	0 to 110.47	5000	30000
4.	Carbon monoxide	0 to 605.18	25	200
5.	Alcohol gas	0 to 6000000	200	400
6.	Liquefied Petroleum Gas (mostly propane)	0 to 3811.9	1000	-
7.	Ammonia	0 to 102.2	25	35
8.	Toluene	0 to 44.947	20	-
9.	Acetone	0 to 34.668	500	750

(Sources: https://nj.gov>documents; https://journals.lww.com>fulltext; https://www.healthline.com>health)

2.6. Buck Converter (LM2596)

A buck converter is a DC-to-DC power converter which decreases voltage from its input (supply) into its output (when less average current is drawn). It is a type of switched-mode power supply (SMPS) that usually consists of a diode and a resistor. Highly powerful buck converters will help convert main (bulk) device supply voltage (substantially 12 volts) to lower voltage, which USB, DRAM and CPUs need (1.8 V or less).

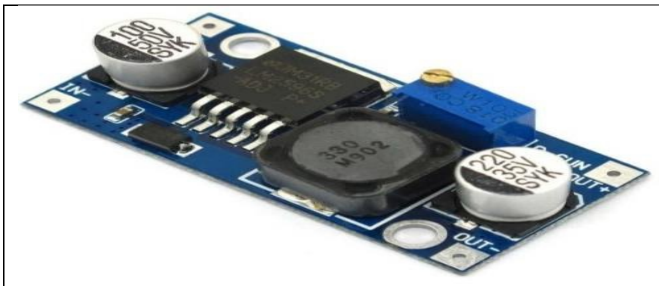

Figure 9: Buck Converter (LM2596)

2.6. Mobile App. Development

The android application was designed with the Massachusetts Institute of Technology Application (MIT App) inventor as shown in Figure10 to Figure 12. Three screens were used for the design. The first screen is the login screen and the next screen displays various levels of gas sensed by the device in parts per million (ppm) and the last screen displays current location of gas in the environment in real time. A responsive approach was taken into consideration for the design. This ensures that the application will run properly and securely on any android device without problems.

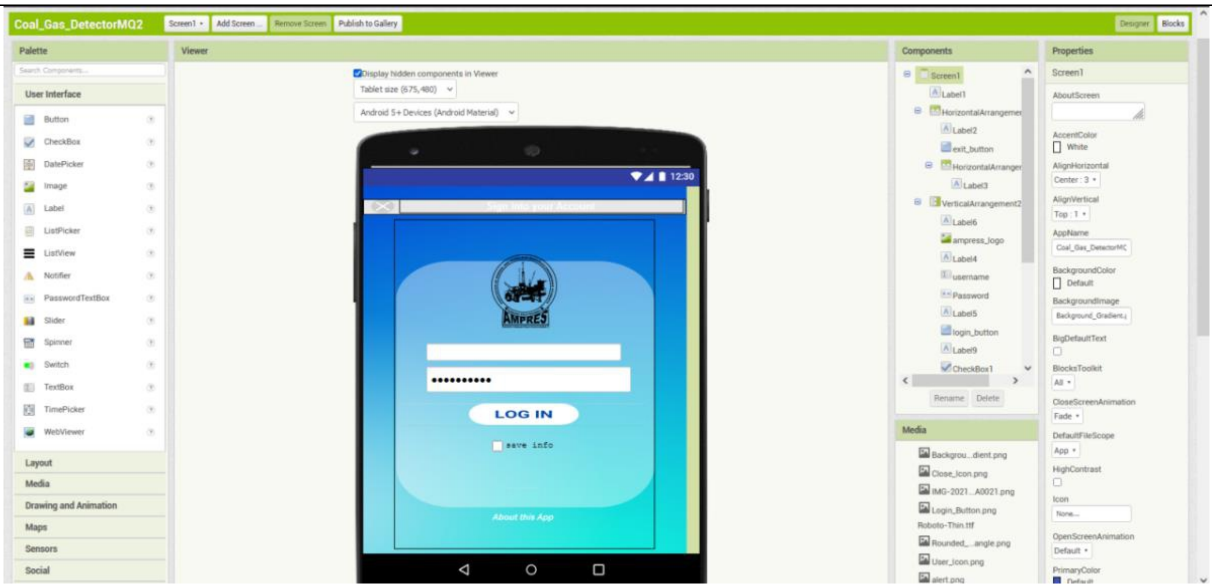

Figure 10: First Screen Displaying User Login Interface

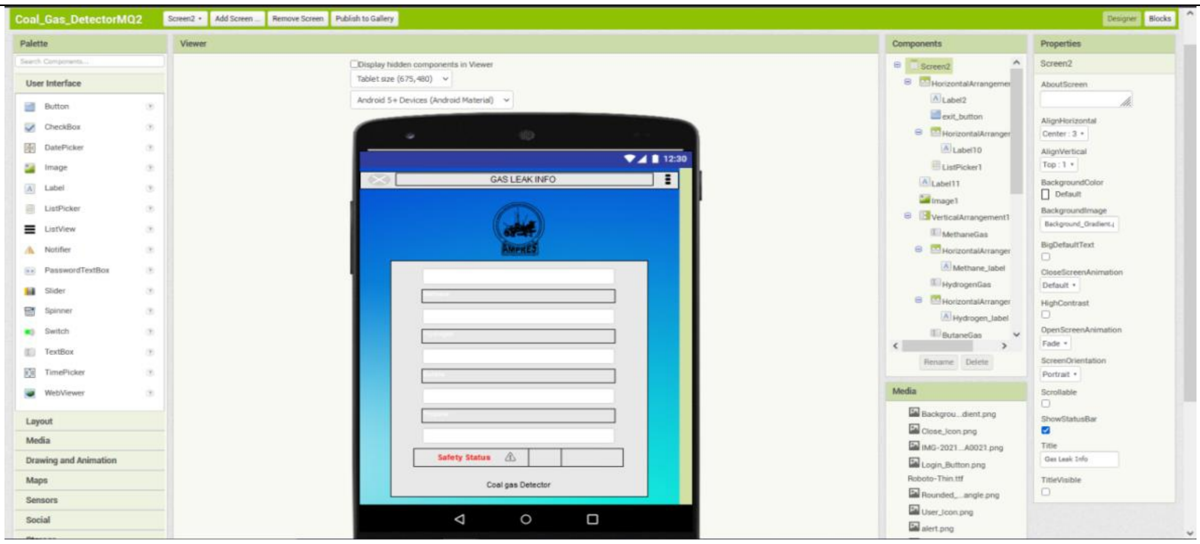

Figure 11: Second Screen Displaying the Percentage of Gases

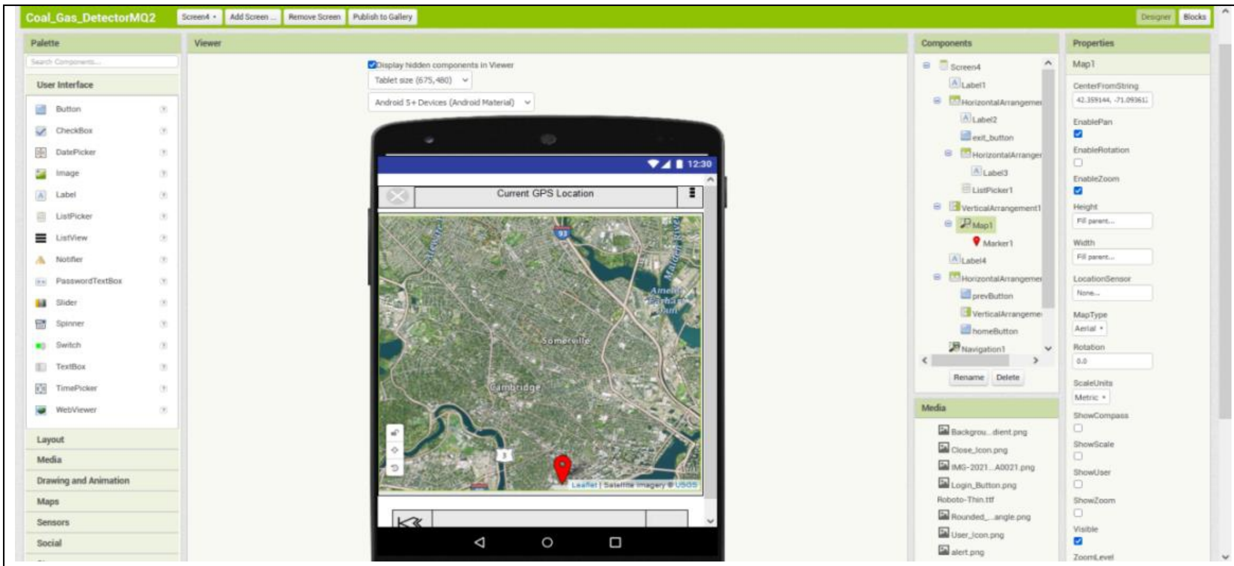

Figure 12: Third Screen Displaying Location of the Gas Device on Aerial Map

As shown in Figures 13 to 19, each field is connected from the code to a channel on the ThingSpeak server. Data sent from the circuit is saved to a particular channel so the mobile application fields simply make a request from its corresponding field.

2.6. The Electrical Circuit and Construction of the Device

The electrical circuitry consists of Esp8662 WI-FI Module which sends the data obtained from the gas sensor to the ThingSpeak Server.

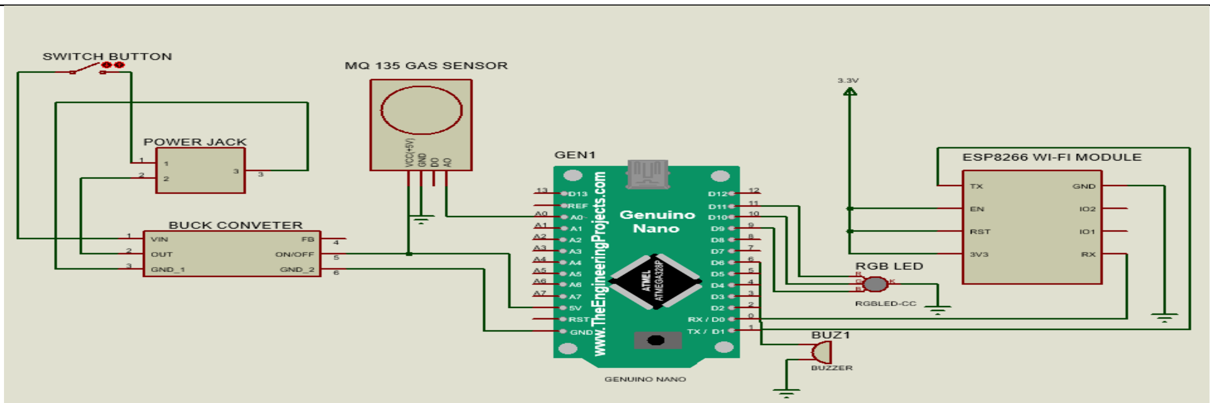

Figure 13: Complete Circuit Design of the Device

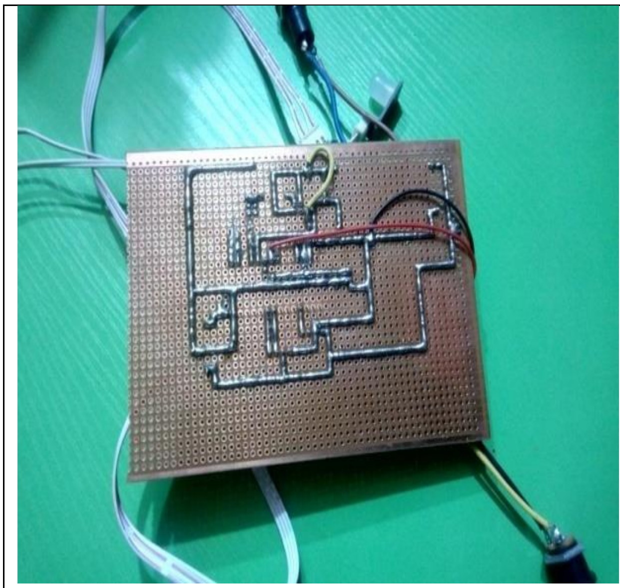

Figure 14a: Soldered Circuit

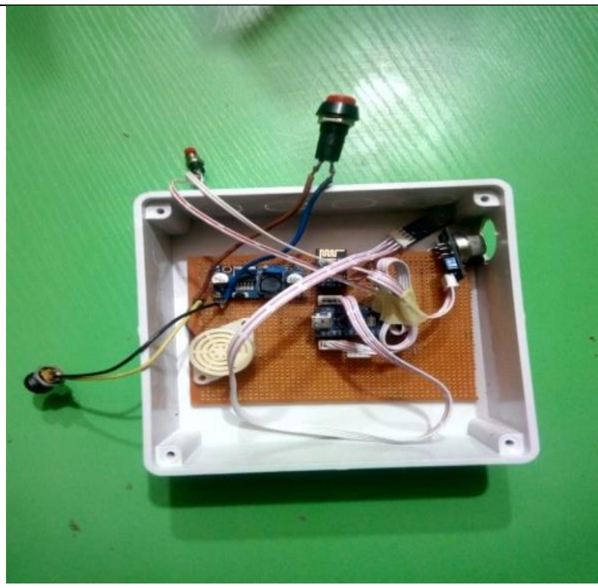

Figure 14b: Soldered Circuit

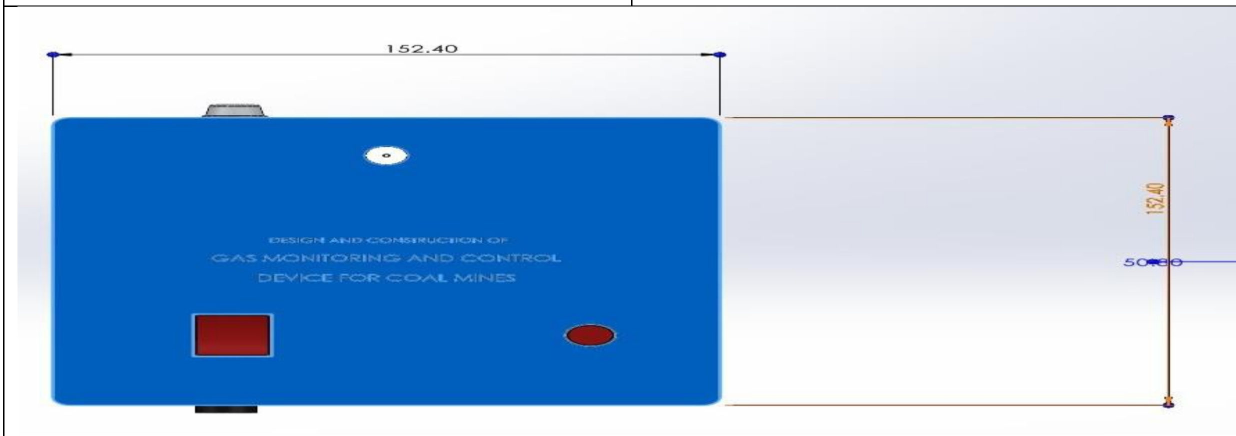

Figure 15: Top Plane 3D Model of the Device

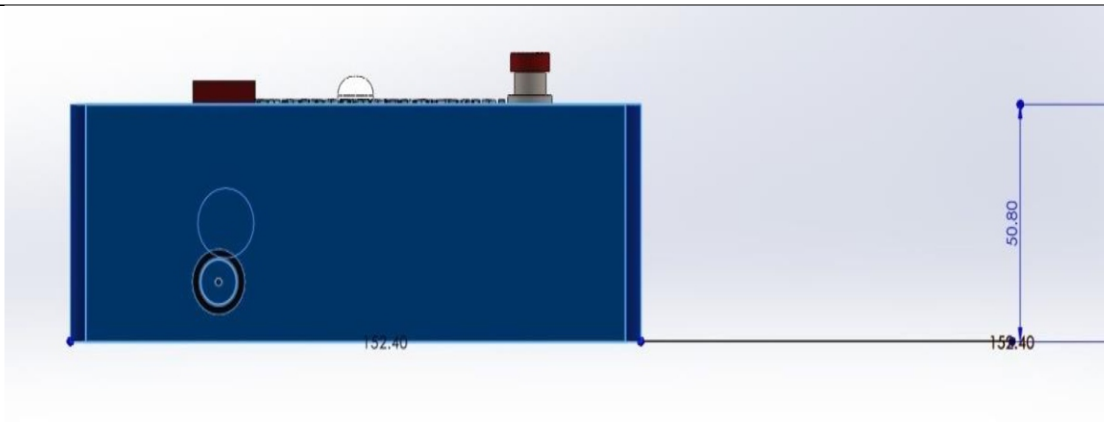

Figure 16: Front Plane 3D Model of the Device

Figure 17: Top Plane Rendered 3D Model of the Device

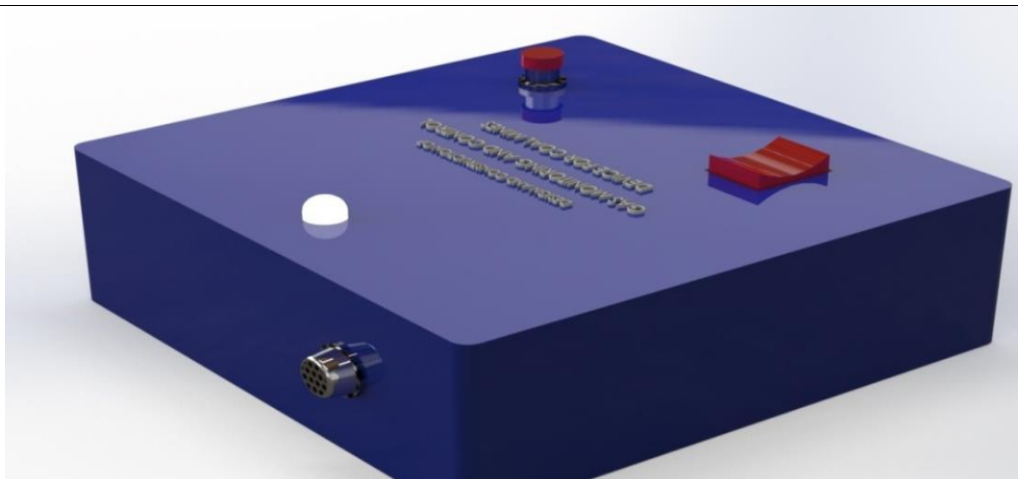

Figure 18: Front and Right Plane Rendered 3D Model of the Device

On Completion of the data capturing section, the design and construction of the Gas Monitoring and Control Device was concluded. The subsequent section discusses the results obtained from the system.

Table 2: Bill of Quantities

S/No	ITEM	NO OF ITEM	PRICE (₦)
1	Arduino Nano	1	10,000
2	Patress Box	1	1,500
3	LED Display Bulb	1	1,000
4	ESP 8226 Wifi Sensor	1	5,000
5	MQ135 Gas Sensor	1	4,000
6	Buck Converter	1	5,000
7	Fero Board	1	500
8	Resistor	5	1,000
9	Buzzer	1	500
10	Power Jack DC	1	500
11	5V DC Adapter	1	1,200
12	Switch Button	1	100
13	Hot Glue Stick	5	750
14	Jumpers/wire connectors	1 pack	500
15	Glue Gun	1	3,500
16	Miscellaneous	-	5950
17	MQ4 Gas Sensor	1	5000
18	LCD	1	5000
	TOTAL	**23**	**50,000**

3.0. RESULT AND DISCUSSION

3.1. Data Presentation

This chapter shows some of the logging results obtained from the mobile application and gas monitoring device; logging information from the ThingSpeak server and general operation of the device. The gas monitoring and control device was tested with mobile networks. The network used for the system was the Smile 4g. This turned out to be slow in some areas as the network strength is not the same everywhere in Kaduna state. When an Airtel router was used it performed much better than the smile 4g network. However, the cellular network that enabled optimal logging was the MTN network in Kaduna state. Once 4g was activated, logging occurred accurately every 10 seconds on the ThingSpeak Server. The table shown below gives an idea of how the logging was stored on the ThingSpeak server. Each field stored each parameter needed to be viewed remotely form the mobile application. The first set of data obtained was taken at the department of Mineral and Petroleum Resources in the equipment laboratory for a period of 1hr. The result(s) are displayed below in form of a graphical model.

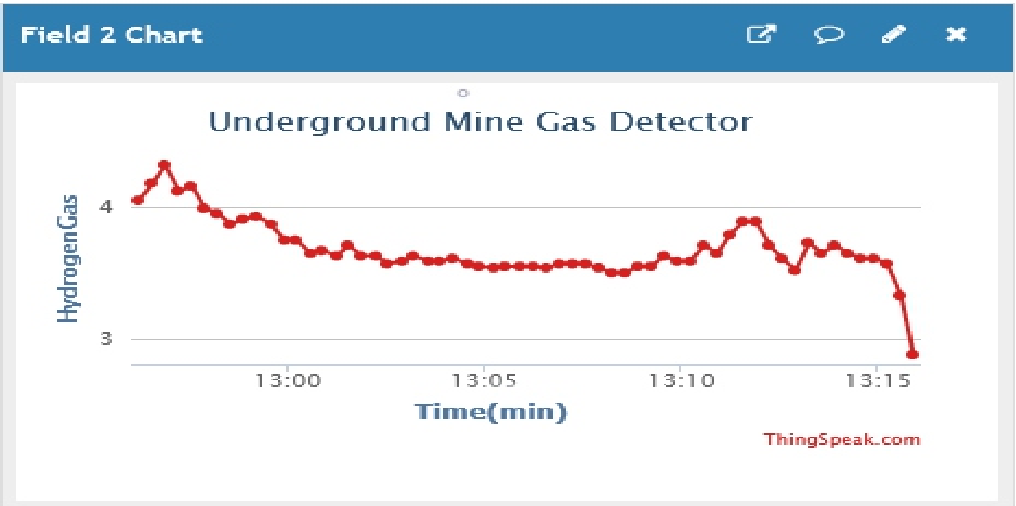

Figure 19: Graphical Model showing Hydrogen gas feed

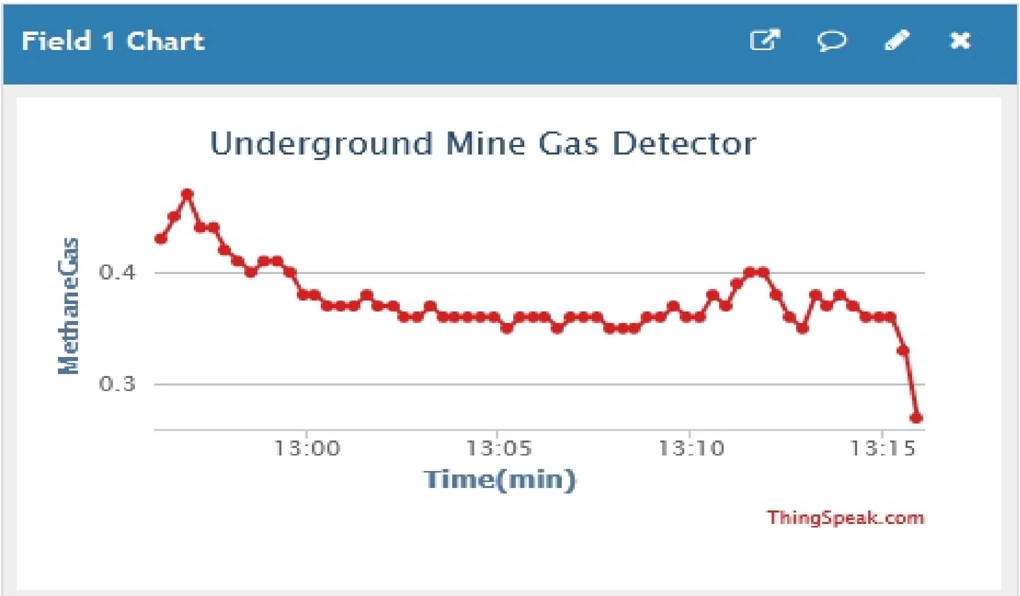

Figure 20: Graphical model showing Methane gas feed

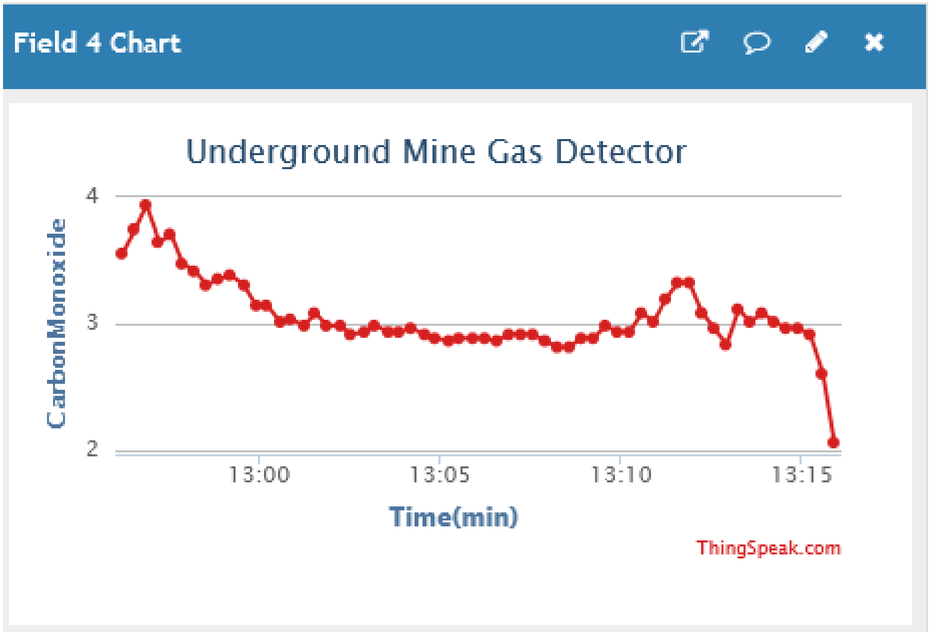

Figure 21: Graphical model showing Carbon Monoxide gas feed

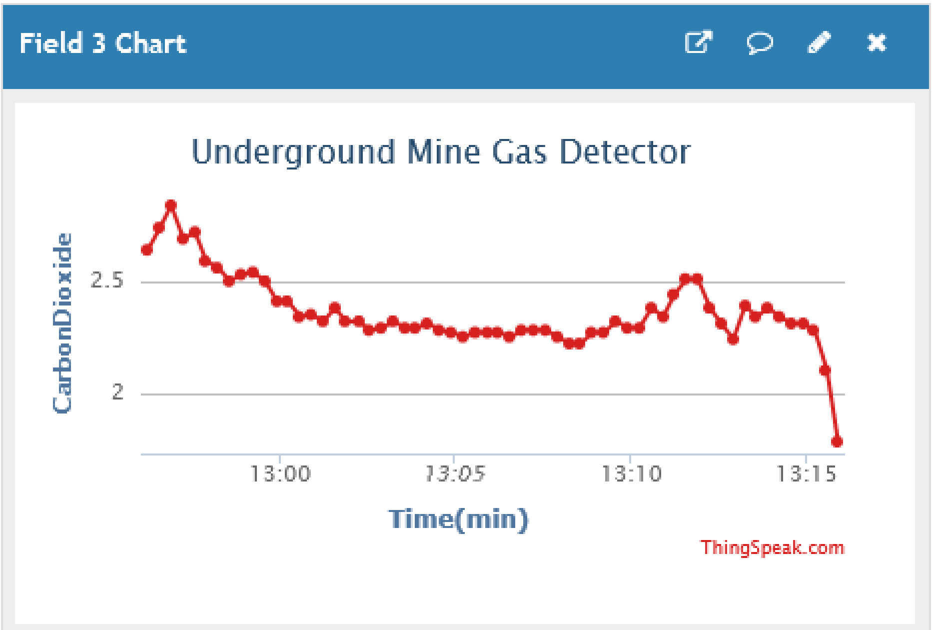

Figure 22: Graphical Model showing Carbon Dioxide gas feed

Reading: CO 4ppm, CO2 2.8ppm, H2 4.3, CH4 0.8ppm

$$\text{TLV (TWA)combined effect from equation 1: } \frac{4}{25} + \frac{2.8}{5000} + \frac{0.8}{1000}$$
$$= 0.16 + 0.0056 + 0.0008 = 0.1664$$

4.0. CONCLUSION AND RECOMMENDATION

4.1. Conclusion

The gas monitoring and control device (GMCD) was tested at the ventilation section of the mine services workshop of the Department of Mineral and Petroleum Resources Engineering, Kaduna Polytechnic and gave the concentration of the following gases; CO (4 ppm), CO_2 (2.8 ppm), H2 (4.3 ppm) and CH_4 (0.8 ppm). The design utilized an Arduino Nano air quality and gas sensor (MQ135 and MQ4) to measure the level of gas concentration in a confined space, especially coal mine. It also utilized internet of things technology IoT) to capture the gas data, accessed from a remote location using a mobile application and connected to a specific router with Service Set Identifier (SSID) “Adebayo.Net” with the aid of WI-FI Module (ESP8662) and MIT-App inventor, the device sent information once every 10 seconds to ThingSpeak Server. The trial run of the device was carried out at the ventilation section of the mine services workshop of the Department of Mineral and Petroleum Resources Engineering, Kaduna Polytechnic, which revealed the concentration of four gases; CO (4 ppm), CO_2 (2.8 ppm), H2 (4.3 ppm) and CH_4 (0.8 ppm).

As a multiple gas detector, the threshold limit value (TLV) for multiple gases to determine the toxicity level by using the TLV(TWA) combined effect equation. Since the sum of the series did not exceed unity, then the threshold limit value of the mixture is deemed not to have been exceeded. Hydrogen is not added in the series calculation because no TLV has been established for hydrogen.

4.2. Recommendation

The present device is limited in the sense that it focused on some of the gases associated with underground mines gases, for example radon, which we hope to include in subsequent update. In the use of the device, when reading less than TLV for a particular gas or the TLV for mixture of gases is greater than unity, palliative measures must be taken by increasing ventilation to dilute further and lower the concentration of the hazardous gases in the underground environment. There is the need to include more sensors to detect the presence of more harmful gases such as MQ6 and DSM501A sensor to accommodate the detection of other gases and tested in the appropriate locations, for instance, loto mines which are predominant in Nigeria. It would also be useful to incorporate solar PV to power the system so that the device is always ON.

In view of the frequent tragedies arising from the use of electric power generators in residences in Nigeria, this device can be installed to detect carbon monoxide fumes in a residence in addition to smoke detectors in residences. Kaduna State Urban Planning and Development Authority (KASUPDA), for instance, can do the same before building approval. Conventional multiple gas detector cost about seven hundred and eighty thousand naira in the market.

Photonics-based gas sensors should be researched into, to support the creation of smaller instruments with equal or higher speed and sensitivity than conventional laboratory-grade gas detectors.

References

Abelson, H; Wolber, D; Spertus, E; Looney, L (2011),App Inventor for Android: Create Your Own Android Apps., O'Reilly.

ACGIH (1989). Threshold limit values and biological exposure indices for 1989-1990. American Conference of

Governmental Industrial Hygienists, Cincinnati, Ohio, USA.

. www.arduino.cc. Retrieved 25 August 2022

Ashton, K. (2009). That ‘Internet of Things’ Thing. Retrieved 25 August 2022

Baker, A. R. and Firth, J. G. (1969). The estimation of firedamp: Applications and limitations of the pellistor. The Mining Engineer, Vol. 128, No. 100, Jan., pp 237-244.

Banzi, Massimo and Shiloh, M (2014): Getting Started with Arduino; 3rd ed.; Make Community; 262 pages.

Benchoff, B (2022) New Chip Alert: The ESP8266 Wi-Fi Module (It’s $5). Hackaday

Benchoff, B (2022) The Current State of ESP8266 Development. Hackaday

McPherson, M.J. (1993) Subsurface Ventilation Engineering. http://www.mvsengineering.com/

NIOSH (1987). Pocket guide to chemical hazards. National Institute for Occupational Safety and Health; US Dept. of Health and Human Services, Washington, D. C. USA.

Oracle. (1995-2022). “What is the Internet of things (IoT)”? Retrieved from https://www.oracle.com//in/internet-of-things/what-is-iot?

Richards, G. O. and Jones, K. (1970). Some recent work on the detection and determination of firedamp. The Mining Engineer, Vol. 130, No. 121, Oct., pp 31-40.